Surfaces and Interfaces 17 (2019) 100340

Contents lists available at ScienceDirect

Surfaces and Interfaces

journal homepage: www.elsevier.com/locate/surfin

Review of superoleophobic surfaces: Evaluation, fabrication methods, and industrial applications

S. Ghaffari, M. Aliofkhazraei*, Gh. Barati Darband, A. Zakeri, E. Ahmadi

Department of Materials Engineering, Tarbiat Modares University, P.O.Box: 14115-143, Tehran, Iran

ARTICLE INFO

Keywords:
Superoleophobic surface
Self-cleaning
Surface energy
Surface roughness

ABSTRACT

Nowadays, superoleophobic surfaces are considered as an innovative solution in many industries due to their various applications and numerous ways of fabrications, all of which have their own advantages. These surfaces are of great importance for a various range of applications including self-cleaning, stain-free clothing, oil/water separation, and drag reduction. Lately, major improvements have been made in order to understand the essential conditions for the creation of superoleophobic surfaces. The lack of a comprehensive review of superoleophobic surfaces has prompted us to gather a wide-ranging article covering most of the issues relating to the surfaces' oleophobicity which can be used in educational and industrial fields. Although many advancements have been achieved in this section, but there are still numbers of fundamental issues in reaching the highest rate of superoleophobicity and also eco-friendly approaches. Therefore, in this review paper, existence of superoleophobicity in nature both on plants and animals, the fundamental requirements for the fabrication of superoleophobic surfaces, the basic and advance oleophobicity and superoleophobicity evaluation methods and also various approaches for superoleophobic surfaces fabrication such as sol-gel, etching, lithography, electrodeposition of conductive polymers, electrospinning, layer by layer assembly, solution-immersion, hydrothermal, anodizing, and spray coating were reviewed. Eventually, recent progress in the applications of superoleophobic surfaces and latest environmental issues were discussed.

1. Introduction

In the past few years, international scientific and industrial societies have become aware of omniphobic surfaces with specific water and oil repelling features. Social media also had an important role in informing common peoples with non-dirt able boots or non-wet able surfaces. In this review, initial concepts of superoleophobicity and also the latest progress and developments related to coating fabrication and various range of practices has been discussed. Since these surfaces have changed liquid-surface interactions, and we recognize the world as the world of water, this technology is going to give a new concept to our surrounding environment. A series of underwater superoleophobic Ni/NiO surfaces have been reported by Zhang et al. equipped with controlled oil adhesion through combining electrodeposition and heating systems [1]. Also, tunable adhesive underwater superoleophobic surfaces were developed by Cheng et al. exercising self-assembled monolayer method in order to transform nanostructured copper substrates [2]. Nevertheless, these developed approaches are tough to curb, and the suggested underwater superoleophobic surfaces display enhanced oil wettability, substantially restricting their use to underwater gadgets, for example, oil-repellent military underwater crafts and amphibious military plane and tanks, which additionally require optical stealth.

This article also reviews oleophobic and superoleophobic surfaces founded in nature as important clues to fabricate industrial and synthetic oleophobic and superoleophobic surfaces. Benchmarking nature is the simplest way to produce omniphobic surfaces [3–5].

We have also revived recent achievement on eco-friendly superoleophobic surfaces. the progress, challenges, and perspectives of the alternative methods for the fabrication in which have less risk of the used materials and the methods to achieve oleophobic properties on the surface is presented. These processes require using risk-free and non-flammable solvents, short-chain fluorinated complexes (C6 or fewer) or substitute materials free of fluorine atoms [6,7].

Although many techniques have been developed to evaluate superoleophobic surfaces in the past decade, advancement of technology still create new opportunity to produce more developed omniphobic surfaces with various range of capabilities such as high corrosion resistivity, great durability in more sophisticated shapes and etc. which in some cases leads to feel the need of newborn surface evaluation techniques. Calvimontes evaluated a technique for the study and

* Corresponding author.
E-mail addresses: maliofkh@gmail.com, khazraei@modares.ac.ir (M. Aliofkhazraei).

https://doi.org/10.1016/j.surfin.2019.100340
Received 21 November 2018; Received in revised form 25 May 2019; Accepted 12 June 2019
Available online 23 July 2019

measurement of the interfacial energies of solid-liquid-gas systems using a laboratory drop tower the presented model based on the thermodynamic equilibrium of the interfaces and not on the balance of bi-dimensional tensors on the contour line [8].

In this review, we tried to gather a comprehensive guide in scientific and also industrial fields. Omniphobic evaluation techniques, superoleophobicity in nature, fabrication methods of superoleophobic surfaces and laboratory and industrial usages of these surface have been discussed in this article focusing on recent changes. In the end, one of the most worldwide concerns, environment compatibility of these surfaces have been reviewed and new eco-friendlier methods are proposed.

1.1. Wettability

Wettability of solid surfaces contacted to liquids is an essential feature of materials science and surface chemistry, which has many real-world uses in daily life, agriculture, and manufacturing. Idyllically, when a drop is positioned down on a superficial part, it either takes a spherical shape or moistures the surface totally. These phenomena are titled "anti-wetting" and "super wetting", respectively [9]. Usually, in wettability studies, measurement of the contact angle has great importance. This data indicates the degree of wetting when a solid and liquid are in interaction. Consider a liquid drop which is placed down on a horizontal surface (Fig. 1). The intersection of the liquid-solid and the liquid-vapor interfaces form a geometrical angle, which we know as the contact angle. Fig. 1 displays a minor contact angle which is formed after the drop extents on the surface, but a great contact angle is formed once the liquid and the solid have a lower interface with one another [10].

1.2. Models of wetting

In order to get a better understanding of superoleophobic surfaces, various models and theories of wetting have been presented in this section based on their evolution trends. The first model was described by Young in 1805 [11–13]. For a liquid drop on a perfectly flat surface (Fig. 2a), wetting is scribed via the interfacial free energy of solid, that is indicated in Young's equation.

$$\cos\theta = \frac{\gamma_{SV} - \gamma_{SL}}{\gamma_{LV}} \tag{1}$$

where γ is the surface stress that characterizes energy per unit area. As known from the formula, there is a connection among the interfacial energy and the contact angle. It can be concluded that Young's angle is formed because of a thermodynamical balance of interfacial energy, in the solid-liquid-vapor boundary area.

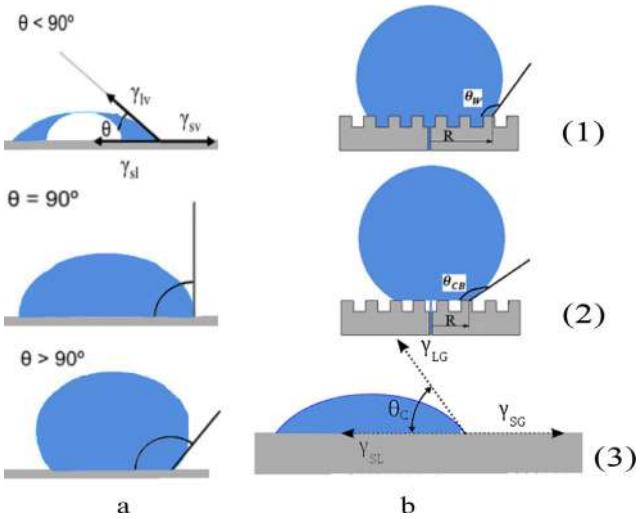

Fig. 1. (a) Illustration of contact angles formed between a liquid and a horizontal solid surface, (b) Wetting state of an oil droplet on different surfaces: (1) Young's equation (2) Wenzel model, (3) Cassie and Baxter model.

Since surface conditions of real surfaces (not ideal) usually have is different in practice, and surface roughness acts as an important factor in the solid surfaces wettability, therefore it's not feasible to the contact angle states with Young's equation.

In 1936, Wenzel introduced an equation in which interfacial roughness and energy are related to the contact angle, as of the following equation [14]:

$$r(\gamma_{SV} - \gamma_{SL}) = \gamma_{LV}\cos\theta_w^* \tag{2}$$

where θ_w^* represents Wenzel's contact angle and is affected by the surface roughness, shown with r (roughness factor). Modified Wenzel's equation is defined by the following equation:

$$\cos\theta_w^* = r\cos\theta \tag{3}$$

In Wenzel's formula, it is presumed that liquid penetrates into the hollows, which are a consequence of surface roughness (Fig. 1(b.2)). Thus a homogeneous wetting regime is typically defined by the Wenzel's equation [15]. From Wenzel's equation, it can be concluded that roughness can increase both wetting and anti-wetting, reliant on the flat surface features. Thereby, if the smooth surface contact angle is bigger than 90°, surface roughness would increase the contact angle and if the contact angle is less than 90°, increased roughness would result in a lower contact angle [16].

Wenzel's model is only applicable to the homogeneous interfaces, and cannot be used for heterogeneous surfaces. Therefore, Cassie and Baxter introduced another model for heterogeneous surfaces in 1944 (Fig. 1(b.3)). This model involves two parts: the initial part includes θ_1 and f_1; where θ_1 is the contact angle for component 1 with area fraction of f_1. The second part includes θ_2 and f_2; where θ_2 is the contact angle for component 2 with the area fraction of f_2 [17]. Accordingly, the contact angle is defined by the Cassie-Baxter equation as following:

$$\cos\theta = f_1\cos\theta_1 + f_2\cos\theta_2 \tag{4}$$

where θ represents the Cassie-Baxter angle, f_i is the area portion of the surface with the contact angle of θ_i ($f_1 + f_2 = 1$).

In Cassie-Baxter's model, assuming the drop and the solid are in contact only at the tip of the picks and small air pockets are stocked underneath the liquid. under the circumstances, it can be considered that the fraction of surface area, in which the air pockets are trapped, doesn't wet by means of the drop. If only air exists between solid and liquid, θ_2 would be equal to 180°. Thereby, Cassie-Baxter's equation could be written as below:

$$\cos\theta_{CB} = f_s(\cos\theta_s + 1) - 1 \tag{5}$$

where f_s represents area fraction of the solid surface with the contact angle of θ_s. It should be noted, Cassie-Baxter's model is not always valid for all kind of surfaces, for example, if a surface owns hydrophilic property then the droplet may immerse into the gap structure. In addition to the mentioned models, there are more advanced models to predict specific states of wetting, which are mentioned in the references section [18–23].

2. Superhydrophobicity and superoleophobicity in nature

Up to now, most of human discoveries and inventions were inspired by nature itself. Thus in order to study and evaluate omniphobic surfaces, we must start from nature itself. In the past decades, the existence of superhydrophobic and superoleophobic surfaces have been proved [24]. The simplest and most reliable method of manufacturing superoleophobic materials is to impersonate nature's behavior. Definitely, numerous plants, insects, and animals which has been produced in nature are capable of preventing water molecules from penetration in addition to low interfacial stress liquids including oils. In this section,

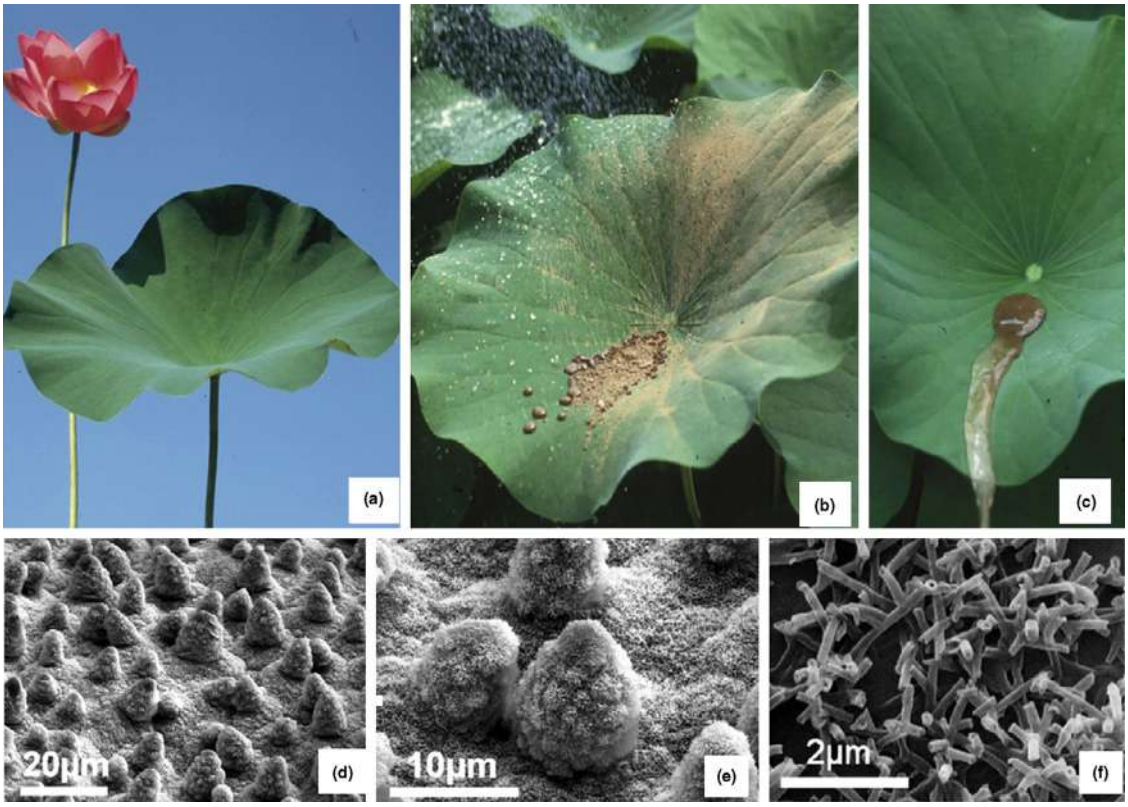

Fig. 2. Pictures of a superhydrophobic lotus greeneries with self-cleaning features at diverse magnifications [27].

we are going to discuss that species which are able to repel liquids with low surface tension.

2.1. Superoleophobicity among plants

Generally, many superhydrophobic surfaces like Lotus plant can be found in nature and by taking inspiration from nature, various approaches have been introduced to produce superhydrophobic surfaces [4,25–27]. Though, there are not so many superoleophobic surfaces in nature. The reason being that could be because of oil's surface energy and its compounds, whereas oil's surface tension is about 20 mNm^{-1} to 35 mNm^{-1}, being less than water's surface tension which generally, makes harder to repel oil droplets from the surfaces.

As is mentioned Lotus (Nelumbo nucifera) is one of the most famous superhydrophobic plants which has shown superoleophobicity for various oil compounds [24]. The value of Θ_w of Lotus leaves is more than 150° which shows ultra-low water adhesion and it also has shown self-cleaning properties [27] (Fig. 2). It can be perceived from Fig. 2b,c that leaves self-cleaning properties which are resultant of the Cassie–-Baxter state help the plant to remove dust from the surface. This feature is the effect of a twofold (micro/nano) surface structure (Fig. 2d. The convex cell papilla is determined from the microscale scanning electron microscopic (SEM) images (Fig. 2e). while at the nanoscale (Fig. 2f) lipids are observed. Pedersen et al. disclosed that Melilotus Siculus, a plant species with superhydrophobic greeneries, is capable of the underwater photosynthesis until three days due to gas treatment on leaves surfaces. because of the gas tramping ability which can physically part the seawater from the leaf, This plant also can survive in saline water [26,27].

Undoubtedly, fabrication of superhydrophobic materials can be by means of essentially hydrophilic materials similar to the fabrication of superoleophobic materials from essentially oleophilic materials [3].

2.2. Superoleophobicity among animals

The discovery of superoleophobic properties in nature led to tremendously exciting innovation in substituting perfluorinated compounds with other materials which can be produced naturally. Due to the problematic process of fabrication that superoleophobic surfaces require, finding examples of them in nature is challenging. Although, some references have referred to the superoleophobic property of several species of insects, such as Insecta, Hemiptera, and Cicadellidae [28].

Sun et al. examined the wings of fifteen species of cicada [29] (Fig. 3). This team detected variances in the similarity of the nanodomes and also dissimilarities in diameter, height, and spacing. The maximum water contact angle ($\Theta w \approx 160°$) were obtained for Terpnosia jinpingensis. Moreover, the possibility of multiple features including anti-reflective and anti-fogging features is reported among structures with an extremely high level of orders at both the micro and the nanoscale. An example is shown in Fig. 4 (a.1–4) [3] that hexagonal facets within eyes (ommatidia) containing periodic arrays of protuberances with a diameter of 200 nm and a height of 70–80 nm. These features are tremendously significant for solar cells uses.

The superoleophobic properties of leafhoppers (the family Cicadellidae of the insect order Hemiptera) is reported by Gorb and Rokitov [28]. There are special structures found on their body surface. These insects secrete intricately structured granules, called Brochosome, which these granules uniformly cover all of their body surfaces. These structures are shown in Fig. 4. As seen in the figures, these granules have a hollow spherical structure, with diameters of about 200–700 n, plus a honeycomb-like shape. These structures have a special morphology named "re-entrant curvatures", which this special morphology results in the creation of superoleophobic property [30,31].

Also, the Werner group had conducted an investigation which led to the determination of one of the most significant species which have

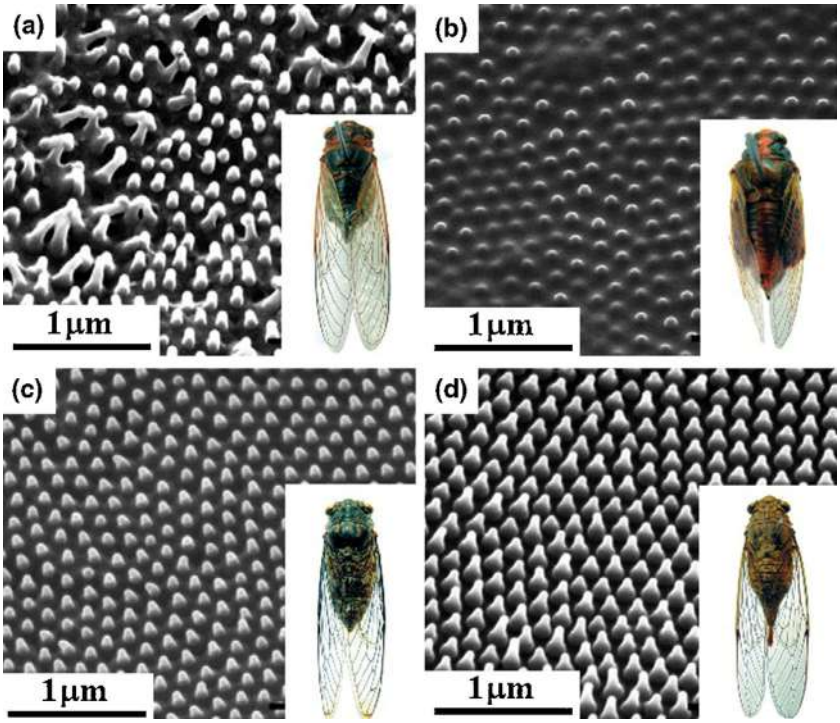

Fig. 3. Images of the nanostructures existent of various species of a specific fly [29].

super oil repellent properties [33]. The team evaluated the cuticle micro/nano structures of forty dissimilar kinds of Collembola (springtails) (Fig. 5). Species of Collembola are usually fewer than 6 mm (0.24 in) long, have six or less intestinal parts and have a tube-shaped appendage (the collophore or ventral tube) with reversible adhesive vesicles, projecting ventrally from the primary intestinal part. The Poduromorpha and Entomobryomorpha have a stretched figure, however, the Symphypleona and Neelipleona have a round figure. Collembola deficient a tracheal breathing structure, which compels them to inhale by means of a permeable cuticle, to the notable exclusion of Sminthuridae which show a rudimentary, while completely efficient, tracheal structure. Because of the negative outcrop in the sketch of the ridges and granules, including robust pinning of the three-phase contact line of a liquid dropped on the surface (even minor interfacial stress liquids), superoleophobic properties are enhanced. As a result, an enormously great energy wall (reliant on the liquid interfacial stress) is shaped to steady the Cassie–Baxter state. The shape of the cavities plays an important rule on the intensity of this energy. The main structural component of arthropod cuticle is chitin a long-chain polymer of N-acetylglucosamine, is derived from glucose. It is a major section of cell surrounding in fungi, the exoskeletons of arthropods, for instance, crustaceans (e.g., crayfish, shrimp, krill, woodlice,) and insects, the radulae of molluscs, cephalopod beaks, and the scales of fish and lissamphibians. The building of chitin is like another polysaccharide - cellulose, forming crystalline nanofibrils or whiskers. Functionally, it might be compared to the protein keratin. Chitin has demonstrated beneficial for numerous therapeutic, manufacturing and bio-high-tech applications [34].

In general, if we want to classify superoleophobic surfaces that are found in nature, we can refer to several types including Snail shell that has a self-cleaning property and helps keep the snail's body surface clean. The main reason for this property (self-cleaning) is because of its superoleophobicity and by taking inspiration from its structure, many other superoleophobic surfaces have been fabricated [35]. Another superoleophobic surface that is found in nature is fish scale [36]. Also by taking inspiration from its structure, many other self-cleaning surfaces have been fabricated. Shark skin can also be classified as the superoleophobic surfaces that are found in nature [37]. Studying these surfaces has led to various approaches to fabricate superoleophobic surfaces, which will be discussed in the following sections. These discoveries have opened new doors to advance superoleophobic surfaces without fluorinated materials.

3. Evaluation methods of wettability

3.1. Static and dynamic contact angle and surface tension measurement

3.1.1. Direct optical method

One of the most commonly used methods of contact angle evaluation using the uninterrupted measurement of the tangent angle at the three-phase contact point on a sessile drop profile. Ramé-hart instrument manufactured the first commercial contact angle goniometer using Bigelow et al. [38] setups and W.A. Zisman design (Fig. 6.a). As is shown, the equipment main parts are at horizontal stage, a micrometer pipette, a lighting origin and a telescope fortified with a protractor eyepiece. Over the years, modifications of the equipment such as using a camera to take photographs of the drop profile [39] or high magnification instrument in order to enhance precision [40] and etc. have been made.

Currently, the optical and hydrophobic transmittance features of the applied silica particles have been studied by Yilbas et al. [41] on the glass surface before and after the transmission of films made of graphene and graphene oxide on the surface. In addition, they applied the Kyowa contact angle goniometer to carry out the wetting experiment. Furthermore, an experiment was performed by Lai et al. [42] on tailor-made thin film nanocomposite membrane combined with graphene, where static contact angle (CA) measurement was carried out with DataPhysics OCA 15Pro contact angle goniometer with the use of Milipore RO water as probe liquid to estimate the surface wetting features of membranes made of composite.

3.1.2. Captive bubble method

We can form an air bubble under the solid sample engrossed in the experimental liquid in order to be used as a substitute for creating a

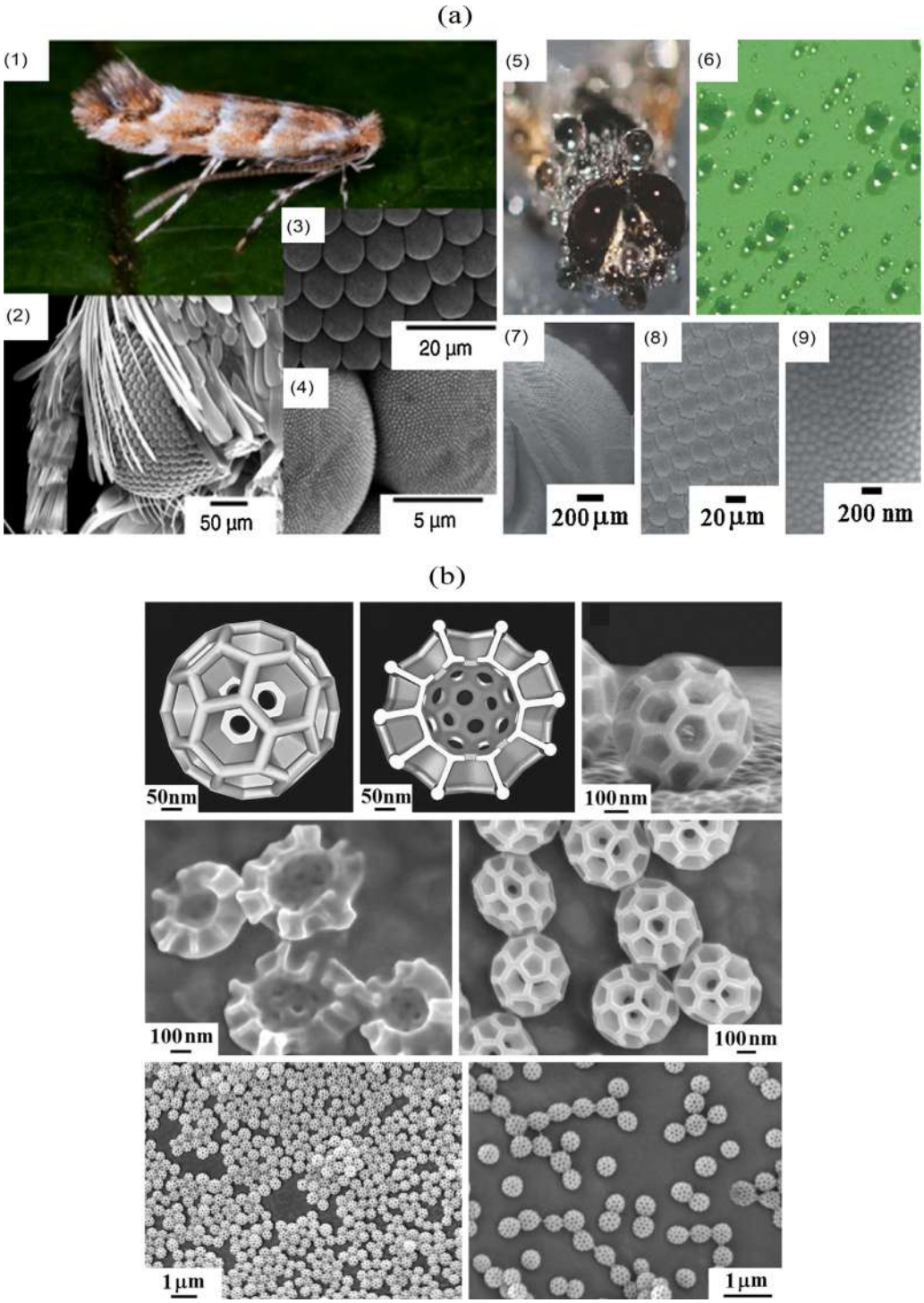

Fig. 4. (a) image at a different magnification of (1–4) antireflective moth-eye [3] and (5–9) anti-fogging fly eye [32], (b) Images at various magnifications of superoleophobic bronchosomes present at the surface of leafhoppers.

liquid sessile drop above the solid sample. Moreover, we can directly calculate the contact angle that is created in the liquid by the air bubble. This technique, which is broadly recognized as the "captive bubble method" today, was designed by Taggart et al. [43] (Fig. 6.b). In this method, we inject a small quantity of air (approximately 0.05 ml) into the desired liquid so that an air bubble is created below the solid surface. As observed in the sessile drop method, it is important to keep the needle in the bubble in order not to interrupt the advancing angle's balance, preventing the slow movement of the bubble from the solid surface if there is no seamlessly horizontal plate.

A new nuclear magnetic resonance (NMR)-based technique was exploited by Sun et al. [44] to assess the coals' water and CO_2 wettability. We applied the current common techniques (e.g., captive-bubble and pendant drop tilting plate) to estimate the angles of water and CO_2 contact.

3.1.3. Tilting plate method

Adam and Jessop introduced the tilting plate method where a solid plate that is tightly grasped above the liquid from an end is revolved toward the surface of the liquid so that the plate's end is engrossed in

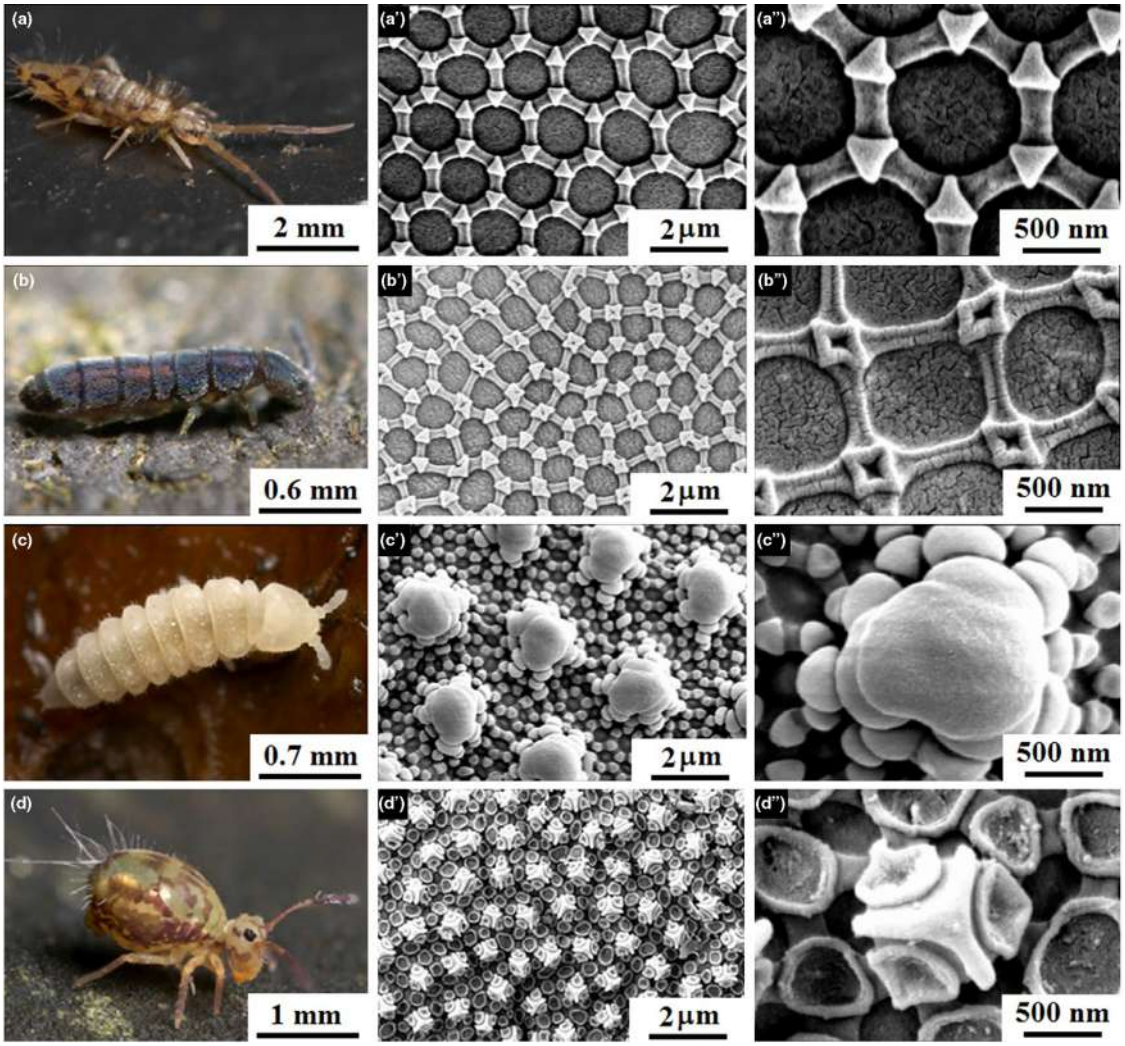

Fig. 5. Image at different magnification of various species of superoleophobic springtails [3].

the liquid. This leads to the formation of a meniscus on the plate's both sides. Following that, the meniscus is made horizontal on a plate's side by slow tilting of the plate (Fig. 6.c).

To enhance the method's precision, Fowkes and Harkins [45] applied glass barriers and a film balance to wipe the surface and recognize the contaminations on the liquid surface, respectively. To make sure that the solid-liquid intersection's edge is placed on the rotation axis, these scholars applied a microscope with an eyepiece. Intending to precisely estimate the angle of contact, Smedley and Coles [46] applied a scanning laser beam with the tilting plate technique to evaluate the moving contact line. This method has a high potential and precision to automatically define the dynamic contact angles' velocity dependence.

Remer et al. [47], conducted an experiment measuring the dynamic water contact angle during the initial phases of the droplet. The results of this investigation show lower accuracy of traditional static quasi-static measurements (sessile drop, tilting plate, or Wilhelmy plate methods) in comparison with fluid flow method which reflects physio-chemical properties of surface impingement.

3.1.4. Wilhelmy balance method

Wilhelmy introduced the generally indirect method that can be used to estimate the angle of contact on a solid sample. The alternations in the weight of a vertical plate are found by a balance when a liquid is contacted with a shrill, vertical and even plate. The force alteration identified on the equilibrium is formed by a mixture of the wetting force and buoyancy (the force of gravity is not changed). In Fig. 6.d, we explained the wetting force f:

$$F = \gamma lv\, p \cos\theta \tag{6}$$

In this equation, θ is the contact angle, γLV is the tension of liquid surface, and P is the contact line's perimeter, which is similar to the perimeter of the cross-section of the solid sample.

Thus, the entire force alteration F detected on the equilibrium is:

$$F = \gamma lv\, p \cos\theta - V\Delta\rho g \tag{7}$$

In this equation, g is gravity acceleration, $\Delta\rho$ represent the alteration in thickness among the air and liquid (or an additional liquid) and V is the displaced liquid's volume.

Therefore, we can easily estimate the value of the contact angle as long as the solid perimeter and tension of the liquid surface are recognized. Princen [48] designed a technique that can be used to achieve a zero angle of contact so that the tension of the liquid surface could be calculated with the use of the Wilhelmy balance method. A receding or advancing contact angle can be formed by pulling out or pushing in the solid sample in the liquid, respectively. The whole process is shown in Fig. 6.d. It is notable that the method of Wilhelmy balance is a force technique that is indirect.

3.1.5. Capillary rise at a vertical plate

In confined liquid films, capillary flows ascend in many contexts, such as spreading and wetting of liquids on asymmetrical surfaces,

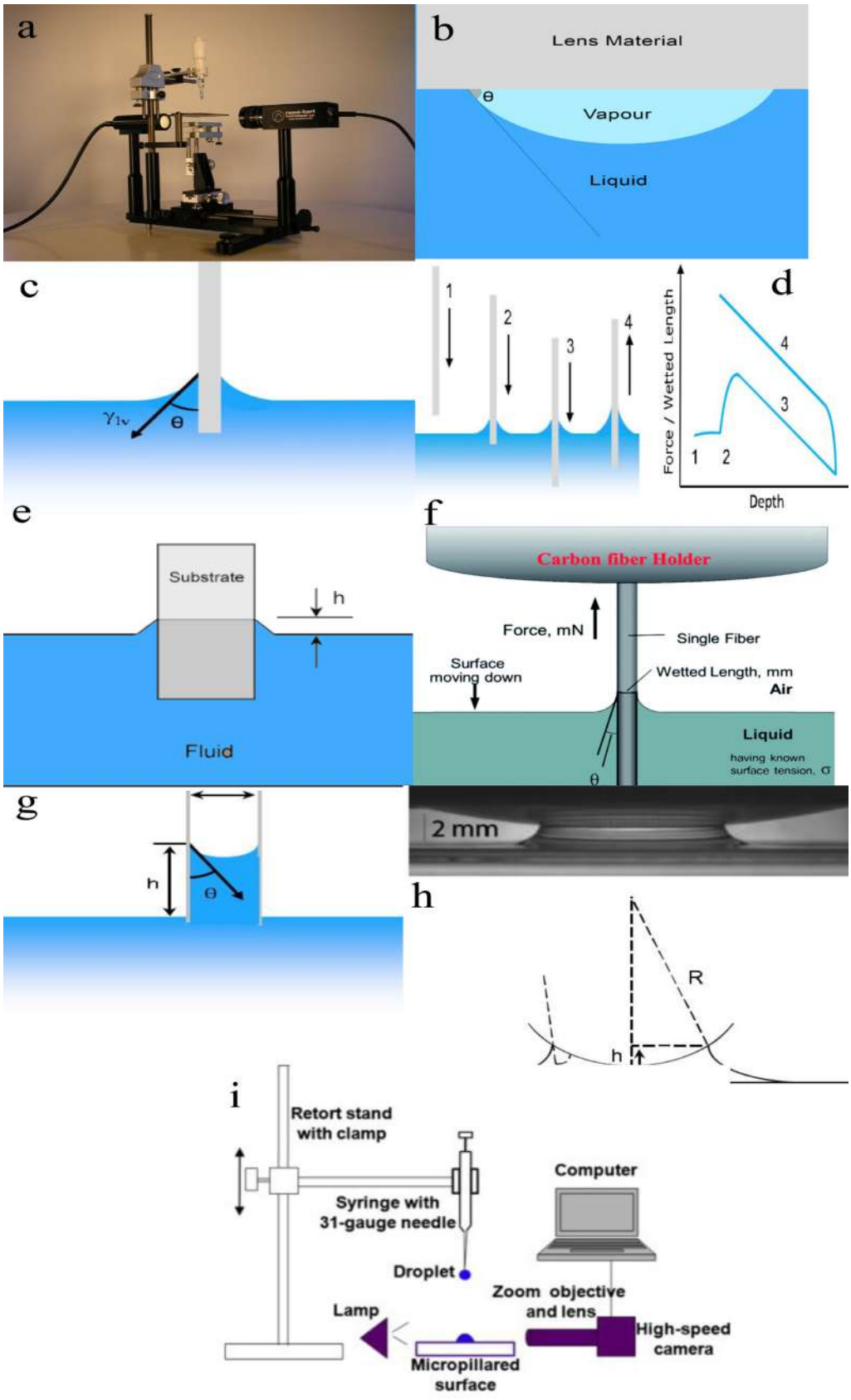

Fig. 6. (a) A reme-hart contact angle telescope-goniometer, (b) captive bubble method, (c) tilting plate method, (d) a submersion cycle for the Wilhelmy balance evaluation: (1) The sample approaches the liquid, and the force/length is zero. (2) The sample is in contact with the liquid surface, forming a contact angle $\theta < 90°$; the liquid rises up, causing a positive wetting force. (3) The sample is immersed further, and the increase of buoyancy causes a decrease in the force detected on the balance; the force is measured for the advancing angle. (4) The sample is pulled out of the liquid after having reached the desired depth; the force is measured for the receding angle. (e) Capillary Rise at a Vertical Plate (f) Individual Fiber method (g) Capillary tube method (h) capillary bridge method (i) Drop shape analysis.

microfluidics, porous media, and management of fluid in environments that have a low gravity. In this regard, you can refer to Kistler [49] and Steen [50]. To satisfy the contact angle, the local curvature of the liquid surface is elevated to improve the capillary impacts by interior corners in a container or channel's solid wall that is partly filled with a wetting liquid. In 1712, there was a report on the equilibrium meniscus's shape in the space between two plates placed in a vertical form that made a small angle. In this report, Taylor [51] and Hauksbee [52] introduced the equilibrium contact line as a hyperbola. Mason and Marror [53], and Concus and Finn [54], have evaluated the static menisci at interior corners. Fig. 6.e. contains the capillary tube method's common schematic.

Oscillating heat pipe (OHP) applications is investigated by Smith and his colleagues using the sessile drop method and capillary rise at a vertical plate [50]. Which indicates the usability of these methods, although because of the development of various high tech, more precise techniques, the application of this method has been reduced.

3.1.6. Individual fiber

Schwartz and co-workers [55] dedicated efforts to the direct estimation of contact angles on fibers. In this regard, an individual fiber was horizontally suspended in a microscope's field and a goniometer eyepiece was applied to calculate the drops' contact angles placed on the fiber. Accordingly, the approximate receding and advancing angles of contact were generated by the rotation of the fiber along its longitudinal axis. This technique was enhanced by Bascom and Romans [56] through situating a small ring made of platinum so that the liquid drop could be held, and vertically passing a glass filament along the drop's center. As the filament was dragged through the static drop, we estimated the receding and advancing angles in contact point.

3.1.7. Capillary tube method

When the same material is used to produce the inner and outer surfaces of the capillary tube, we can apply the Wilhelmy balance method to estimate the angle of contact. The total amount of the outer and inner perimeters is the capillary tube's perimeter p. Generally, we can exploit the Wilhelmy balance method in many objects, including tubes, plates, wires, capillaries, and rods 6.g).

When a vertical capillary has an adequately slender circular cross-section, we might regard the meniscus as a spiral. In addition, Jurin's law describes the capillary rise recognized as h.

$$h = \frac{2\gamma_{lv} cos\theta}{\Delta pgr} \tag{8}$$

In this equation, g is the gravitational acceleration, $\Delta\rho$ is the dissimilarity in density between the vapor and liquid, and r is the radius of the capillary.

3.1.8. Capillary bridge method

A technique that can measure the contact angle with high accuracy has been designed by Restagno et al. [52].' [57]. In this method, a large liquid bath is contacted by a spherical solid surface (e.g., a watch glass).

On the solid surface, the wetted area is defined by the formation of a meniscus or "capillary bridge" caused by the capillary effects. To provide a systematically changeable wetted region, the solid is gradually moved up or down, causing a modification in the form of the "capillary bridge" created between the liquid and the solid surface. We can quantitatively determine the dynamic angles of contact with a simplified approximated relation or by numerical resolution of the Young-Laplace equation if we oversee the alternations in the distance passed by the solid surface and the wetted area.

$$A = 2\,\pi R(k^{-1}\sqrt{2(1 + cos\theta)} - h \tag{9}$$

In this equation, h is the distance between the liquid bath surface the solid surface, A is the wetted area, and k^{-1} stands for the capillary length, identified for each certain liquid. The empirically established A(h) curve is applied to deduce the θ contact angle.

3.1.9. Drop shape analysis

In the past, the θ /2 method was broadly applied throughout the primary period of contact angle estimation in order to assess a sessile drop's profile. This examination regards the liquid droplet as a section of a sphere. From a geometrical point of view, measuring the apex's height and diameter of the droplet is carried out to estimate the angle of contact (Fig. 6.i):

$$\frac{\theta}{2} = tan^{-1}\left(\frac{h}{d}\right) \tag{10}$$

Rational findings can be obtained by this method if there is a significantly small liquid droplet. Nevertheless, in the case of having a sufficiently large drop that can be affected by gravity, we cannot apply the spherical shape assumption.

The form of droplet profiles was first assessed by Bashforth and Adams using the Laplace equation. Based on various values of curvature radius and tension of surface at the drop apex, these scholars manually made a collection of sessile drop profiles. As a result, the task used to determine the tension of the surface turned into the easy insertion from tables of these researchers, whose significant influence resulted in the thriving of this field. The Bashforth and Adams tables were enhanced by Tawde and Parvatikar [58] and Blaisdell [59]. In addition, the same tables were created by Fordham [60] and Mills for pendant drops. Several novel techniques have been introduced and there has been a great enhancement in the shape of the drop since the revolution in the use of digital computers [61–63].

There have been considerable enhancements in computational technology and design of hardware, causing a significant improvement in the analysis of drop shape for the science of surface. Designed by Rotenberg et al. [64] and enhanced by Cheng et al. [63], Kalantarian et al. [65]., Spelt et al. [61], and Río [66], the technique of axisymmetric drop shape analysis (ADSA) is assumed to be among the most precise methods for significantly accurate measuring the angle of contact. This method has a ± 0.2° reproducibility and compared to the direct tangent measurements that have the same rate of reproducibility, this technique can enhance the precision of estimation of the contact angle through basically an order of magnitude.

Finding the most efficient theoretic profile which complies with the

Table 1
The evaluations of axisymmetric drop shape analysis-profile (ADSA-P) method.

Writer	Contribution in ADSA-P method advancement
Rotenberg et al. [64]	In this method, an objective function is defined as the sum of the squares of the normal distances between experimental profile points and corresponding theoretical profile points.
Cheng et al. [67]	The first generation ADSA-P method by implementing a computer-based edge operator
Dodel [68]	Extracting the drop interface profiles automatically
Rio and Neumann [66]	Developing the second-generation ADSA-P method by integrating more efficient algorithms. Overcoming the apex limitation using the curvature at the apex instead of the radius of curvature at the apex as a parameter.
F.K. Skinner and E. Moy [67]' [69]	Developing the axisymmetric drop shape analysis-diameter (ADSA-D)
Cabezas et al. [70]	Introducing A new drop shape analysis method called theoretical image fitting analysis (TIFA)

drop profile obtained from an empirical image that is used to estimate the drop volume, the angle of contact, as well as surface tension and area is the ADSA technique's fundamental principle. The two major hypotheses involved in the ADSA method include having a Laplacian and axisymmetric empirical drop and presence of gravity as the independent outer force. Applied as a parameter that can be adjusted, surface tension is searched by the algorithm to find the precise level of surface tension requires for production of the most efficient theoretical profile, which matches the empirical drop profile. Table 1 contains information about the assessment of the axisymmetric drop form analysis-profile (ADSA-P) method.

3.1.10. Contact angle measurement of ultra-small droplets

Despite the significant assessments performed on the wetting phenomenon at the macroscale (ml), there is a lack of research on the wetting attitude at the nano- or microscale (nano- or micrometers) and a lot of issues are yet to be resolved. Wetting theories can be assessed at the nanoscale level by evaluating the ultra-small droplets on solid surfaces. In this condition, the wetting attitude is considerably affected by evaporation of liquid and tension of life (both being typically insignificant in macroscale research). Studies conducted in this area are related to several industrial uses, including wastewater treatment [71], friction in microelectromechanical systems (MEMS) devices [72], and flotation in mineral recovery.

Different dimensions of ultra-small liquid droplets (e.g., creation and results of wetting evaluations) have been investigated by Mendes-Vilas et al. [73]. Emulsion drops, condensation in environmental chambers by heterogeneous nucleation, electrospray, and spraying are among the most conventional techniques to create ultra-small droplets. Since atomic force microscopy (AFM) has a nanometer-scale resolution and can be operated in ambient air or any type of monitored fluid (whether being liquid or gaseous) atmosphere, it is regarded as the most proper method for imaging liquid droplets and films of micrometer and sub-micrometer dimensions on flat substrates [74].

In terms of AFM's time resolution, it seems that we need 15–30 min to take sturdy liquid images. Use of AFM to image small volatile liquid droplets is delayed by this inefficient time resolution since these droplets evaporate before we get a chance to take an image. In addition, the mentioned time resolution causes difficulties in completing dynamic wetting studies (estimation of receding and advancing contact angles or following of dewetting processes). Therefore, the best method for these [75] purposes is video-rate AFMs. The AFM scanning speeds are quickly moved toward [76] achieving video-rates by recent developments.

The non-evaporating phenomenon involves the presence of the droplets for long hours to keep constant contact [77] areas, volume, and angle. However, this event has still not been applied along with microscopic droplets. While one of the suggested methods for overcoming the evaporation issue is environmental scanning electron microscope (ESEM), its shortage is that it can be employed on a micrometer instead of a nanometer-scale. Moreover, the high price of this technique causes a delay in its overall accessibility in laboratories of surface science. More explanations about this topic are provided in the ESEM section.

3.2. Bouncing characteristic

Over the last century, researchers have focused on the impingement of droplets on dry or wetted surfaces, which is pervasive in natural and industrial processes. Several mechanisms are involved in the mentioned phenomenon that is accountable for an extensive range of results. Fig. 7 contains a conventional bouncing test setup with sections of a flat specimen, a gauge needle, a white LED lamp serving as a source of the backlight, and high-speed visualization devices.

While there is a great number of studies on this phenomenon, it is still not fully covered and its several interesting dimensions are investigated by scholars. According to Couder et al. [78], droplet

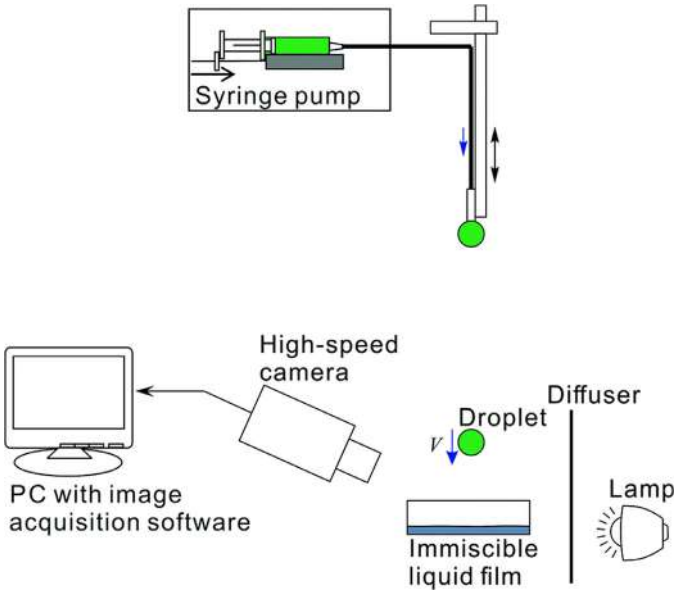

Fig. 7. Schematic diagram of the experimental setup for the impact of droplets on immiscible liquid films.

bouncing that is mediated by air on a vibrating bath, which contains similar fluids, is among the fascinating uses of this phenomenon. A behavior that was formerly known to be only related to the quantum mechanics' world is displayed by the droplet, piloted and directed by its own field of the wave (Bush [79]).

Significant impact of surrounding gas on droplet's behavior has been suggested by this phenomenon when accompanied by others, including the droplet bouncing a soap film and multiple bouncing of droplet on a bath prior to enduring partial coalescence (Chen and Mandre, [80], Bach et al. [76], Charles and Mason, [75]). Regarding the effect of a droplet on the solid surface, the shaping of a bubble at the droplet's center has been assessed by several researchers, specifically and thoroughly evaluated by Josserand and Thoroddsen [77].

Bubble formation involves the entrapment of air by forming of a dimple at the droplet's bottom caused by rising of pressure as the substrate is approached by the droplet, reported by Chandra and Avedisian [79]. On the other hand, Pumphrey and Elmore [81] conducted empirical studies and provided logical descriptions of the phenomenon. In this regard, they have reported similar entertainment of air if the droplet has an effect on the water pool. Details have been provided on the pressure in the phase of gas and droplet deformation prior to surface wetting by performing of several studies on impingement of droplet on a solid surface by Mehdi-Nejad et al. [82].

Bubble entrainment at the droplet's center is approved by their numerical findings as well. For the first time, Mandre et al. [83] hypothesized the probability of spreading droplets on a layer of thin air with no direct contact between the solid surface and droplet. Kolinski et al. [84] evaluated this hypothesis as well, marking the rebound of the droplets from super hydrophilic surfaces with no contact with the solid due to the existence of an air film layer at the nanometer-scale level.

Moreover, Ruiter et al. [85] conducted detailed empirical assessments of the phenomenon, demonstrating the bouncing off of the droplets, which have velocities at a low impact, with no contact with solid. The technique of dual wavelength reflection interference microscopy (Ruiter et al. [86]) was applied by these researchers to estimate the air layer's density and obtain thorough data about the air's behavior under the droplet during the whole process of bouncing. De Ruiter et al., [85] reported the formation of a kind at the droplet's edge spread outward simultaneously with maintaining a still position by the dimple's center. On the other hand, a reduction is observed in the density of film in the presence of higher impact velocities. This decrease continued until the

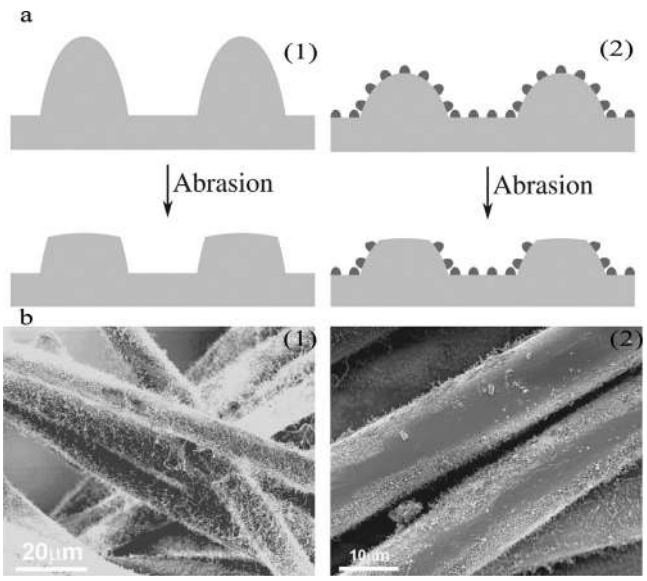

Fig. 8. (a) The effect of wear on surfaces with topography in one or two length scales. (1) The only microroughness is present. Abrasion causes the bumps to wear off, making the Cassie state no longer stable. (2) The pattern consists of shallow, mechanically stable micro bumps with a nanoroughness on them. Most of the nanoroughness is unaffected by wear and the Cassie state remains stable. (b) PET fabric coated with nanofilaments before and after a wear test that simulates skin contact. Reproduced with permission [90].

formation of a contact between the solid and liquid, which leads to the wetting of the surface by droplet depending on the surface's wettability features.

3.3. Durability

Required for superhydrophobicity, the delicateness of the microscopic roughness structures impede the enhancement of surfaces that are both durable and non-wetting. To guarantee that the Cassie state will be kept stable after the removal of some surface characteristics, several studies [87,88,21,89] have applied roughness at two length scales. In order to protect a more delicate roughness at nanoscale level superimposed on the larger pattern, robust microscale bumps are included in such morphology. Generally, microscale characteristics require a large aspect ratio in the absence of nanostructures. However, no such thing is needed when the Cassie state is significantly alleviated due to the existence of two scales of roughness. Therefore, it could be concluded that while non-wettability is ensured by the nano-roughness, there can be optimizations in the microroughness through mechanical steadiness in mind. This topic is shown in Fig. 8.a.

A layer of superhydrophobic silicone nanofilament was grown by Zimmermann et al. [87] on textile fibers so that a hierarchically rough superhydrophobic fabric, which is presented in Fig. 8.b., could be obtained. Applying a force of 5 N, the coated textile maintained its superhydrophobic feature following lengthy wear with simulated skin contact despite the fact that this type of nanofilaments are significantly delicate and can be readily destroyed. Using of the water shedding angle that is regarded as the title angle and experiences drops of water at the upper side by the surface after being fell from a predetermined height, is associated with the quantification of the wear's impact.

Making the surface more adhesive toward water by the abrasion is illustrated when 1450 cycles of wear result in the elevation in the angle of shedding from 2° to 25°. According to the SEM image (Fig. 9), while the nanofilaments were removed from the surfaces of contact, they were kept unchanged in another place. In this respect, Xiu et al., [88] provided another demonstration of the concept by preparing two-tier roughness on silicon (Fig. 9) through creating microscale pyramids via KOH-involved etching at first, followed by the application of Au nanoparticle catalyzed HF/H_2O_2 etching so that nanostructures could be generated on the pyramids. This was accompanied by a rendering of the hydrophilic or hydrophobic silicon surface via a fluorination treatment.

Drawing of the sample on a Technicloth wipe under a 3.5 kPa load was used to examine the surface characteristics' durability. The non-wetting of the surface is maintained in spite of the upsurge in the contact angle hysteresis, which indicated the protection of the nanoscale characteristics on the pyramids' walls by the microscale pyramids (Fig. 9). Nevertheless, the water droplets rattled down the surface and the abrasion left the trace.

4. Fabrication of superoleophobic surfaces

As mentioned, fabricating superoleophobic surfaces is much more complicated than the fabrication of superhydrophobic surfaces, due to the low levels of oil's surface tension. Most of the approaches of fabrication of superoleophobic interfaces are complex and expensive therefore, these approaches are restricted to specific substrates. In this section, first, we will review basic chemical compounds and physical conditions in order to fabricate a superoleophobic surface then we review the various approaches to fabricate superoleophobic surfaces and their advantages and disadvantages. In principle, there are two different approaches to fabricate superoleophobic surfaces, by altering surface chemistry and/or altering the surface texture. These two approaches will be discussed in the next section.

4.1. Surface chemistry in fabrication of superoleophobic surfaces

As mentioned, the surface tension of the oil and organic liquids is lower than the water surface tension, therefore to fabricate a superoleophobic surface, solid surface energy needs to be lower than the oil surface energy. The primary and most significant stage to manufacture a superoleophobic surface is the correct choice of the materials to use. The important materials that are used in the fabrication of superoleophobic surfaces typically include fluorocarbon-based materials. It has been disclosed that the nethermost energy groups in monolayer films are as follows: $CH_3 > CF_2 > CF_2H > CF_3$ [48,91–93]. Flouropolymers are one of the most widely used materials in order to lower the interfacial energy, because of the presence of CF_3 and CF_2 groups [94]. Different types of fluorocarbons can be found as polymers, surfactants, and lubricants, which are used in the fabrication of superoleophobic surfaces. Flourocarbon-based materials are involved in many industrial applications, due to the favorable properties (good thermal and chemical stability, low surface energy and etc.) they have [95]. Another group of materials that are used in the fabrication of surfaces which exhibit superoleophobic property is called Flourinated Salines [7, 96–98]. In this section, properties and the mechanisms of these materials will be explained.

4.1.1. Perfluorocarbons (PFC) compounds

Fluorine as the most electronegative element has high atomic polarization which also is small in size [99]. Their atypical physicochemical features lead to exciting and valued applications in many fields, for instance, surfactants in supercritical solvents, alternatives for chlorinated solvents, environmental probes to regulate the conversion between the atmosphere and natural waters, anticorrosive and antifriction ingredients, noncombustible, oil and water repellents [100]. Low polarizability of the fluorine atoms can lead to low levels of energy which will result in low intermolecular force between fluorocarbon molecules. The low levels of energy cause the fluorocarbon-based tissues to be both oleophobic and hydrophobic. It has been disclosed that CF_3 has the lowermost levels of surface energy [101]. One of the most important superoleophobic surfaces are the polyelectrolyte/fluorinated surfactant complexes [102,103], which were studied for the first time in 1996 [104]. Preparation of these kinds of complexes is done by the

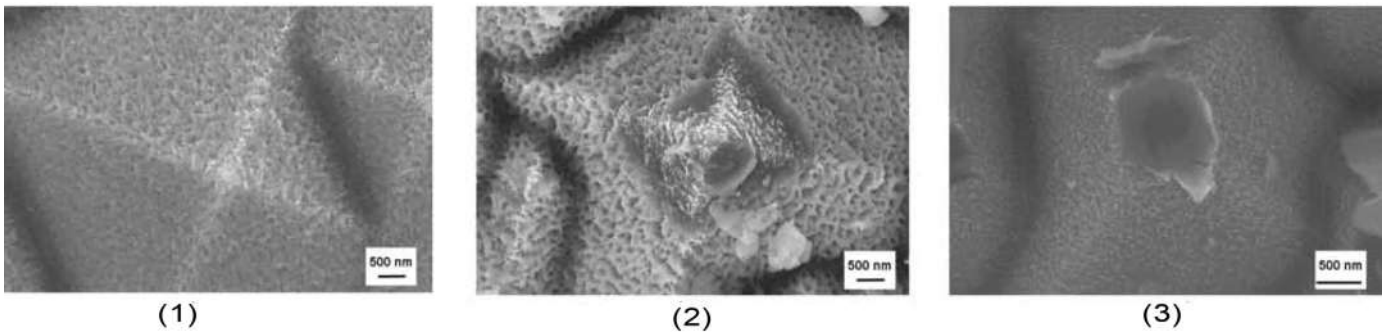

Fig. 9. (1) A hierarchically rough wet etched silicon surface (2) after rubbing with a Technicloth wipe and (3) after sand abrasion [88].

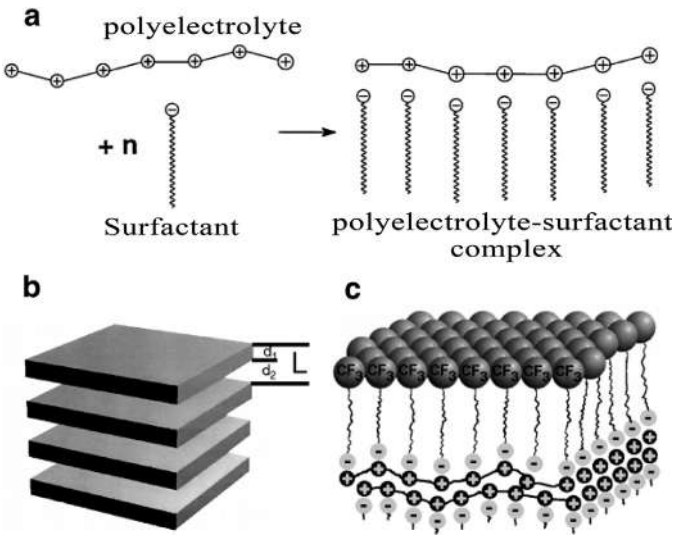

Fig. 10. (a) Formation of a PEFA compound by an accommodating zipper mechanism among a polyelectrolyte chain and oppositely charged fluorinated amphiphile molecules. (b) A faultless lamellar mesomorphous multifaceted structure with a duplication unit length L containing fluoroalkyl-containing sheets with thickness d1 (dark shaded) and ionic sheets containing polyelectrolytes with thickness d2 (not shown). This multi-lamellar structure is typical of numerous fluorinated PEFA materials. (c) The molecular arrangement at the complex interface – air is dominated by the enrichment of CF3 groups. The amphiphiles are strongly linked to the polyelectrolyte chains which lie about 1 nm beyond the CF3 layer [103].

precipitation from an aqueous solution and as a result of cooperative zipper mechanism between polyelectrolyte and surfactants with an opposite charge, the stoichiometry of 1:1 will be formed [105–107]. It has also observed that the PEFA can be prepared through organic solutions and also aqueous dispersion. Examples of fluorinated surfactants include fluorinated sulphonates, perfluorinated carboxylates and fluorinated phosphates [108]. Formation of a single-chain is schematically shown in Fig. 10(a). It can be seen that the formation of a nanostructured polymer requires two building blocks. The main phase morphology of the bulk materials exhibiting lamellar architecture is ideally shown in Fig. 10(b). As seen from the Fig. 10, CF_3 groups are present at the PEFA-air interface which leads to the lower levels of the surface energy of these complexes (Fig. 10(c)). Fluorinated alkyl chains at the solid-air interface form a periodic array with a period of 5 nm [103].

One of the important surfaces that has both oleophobic and hydrophilic properties is the polyelectrolyte-surfactant complexes which their structure had described in the previous sections. Structure of these complexes causes the concentration of the polyelectrolyte's hydrophilic parts to the subsurface region by the electrostatic absorption [102–105]. This leads to changing from hydrophobicity to hydrophilicity as the water reaches to the surface and penetrates to the hydrophilic subsurface [109]. It should be mentioned that the large oil molecules cannot penetrate to the subsurface through defects which leads to the surficial oleophobicity. One of the important parameters of these surfaces is the period of changing from hydrophobicity to hydrophilicity, which is a limiting factor in many industries. The long period required for water penetration is the reason why the primary polyelectrolyte-surfactant complex oleophobic/hydrophilic surfaces were initially hydrophobic and also had limited application due to the weak oleophobic properties [110]. Other two-step methods were introduced in order to improve these properties however; the two-step method is not suitable for use in massive industrial applications.

Meng et al. [100] have studied the effect of a Perfluorocarbon chain on the oil/water mixture. They proposed that perfluorooctane sulfonate (PFOS) is able to emulsify oil-water combination just in the company of air, totally diverse to hydrocarbon surfactants. The perfluorocarbon chain prevents hydrophobic complexes and its oleophobicity rises with reducing the polarity of organic solvents. Fig. 11 shows how a Perfluorocarbon compound can separate oil and water from each other.

Making great contact angle by liquids with minor interfacial energy, like oil, is much harder only via lowering the surface energy. However; oftentimes perfluoro polymers which have long $[CF_3(CF_2)_xCH_2CH_2COO]$ (x = 4–7) chains are used to overcome this problem [111–115]. One of the parameters in the optimization and improvement of oleophobicity is the chain length of the fluorocarbon. It

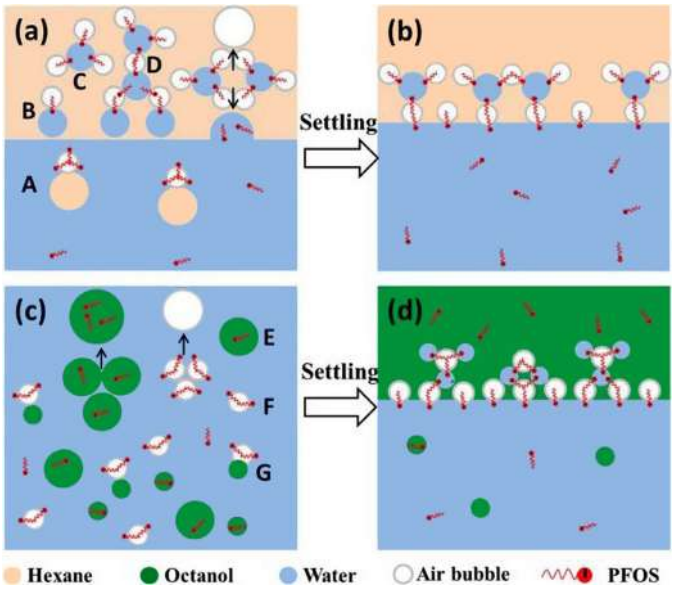

Fig. 11. Schematic diagram for PFOS distribution in hexane-water (a) after shaking, (b) after settling, and octanol-water (c) after shaking, (d) after settling mixture in the presence of an air bubble.

has been reported that by increasing the number of -CF_2- groups in the chain, oleophobic and hydrophobic properties will improve which leads to lowering the surface energy of the polymer [116–119]. Cansoy and Cengiz. [120] investigated the effect of perfluoroalkyl weight percentage and hydrocarbon chain length on the oleophobic features of perfluoroethyl alkyl methacrylate-methyl methacrylate copolymer, with oils which had different surface energies. They have concluded that by increasing the hydrocarbon chain length, the contact angle of the copolymer's flat film will increase. Also, it has been found that the hysteresis angle is affected by the hydrocarbon chain length of the liquids and increases with the increase of the hydrocarbon chain length while using oils with low surface energy. Whereas changes in the hydrocarbon chain length did not have any perceptible effect on the hysteresis angle while using oils with high surface tension.

4.1.2. Fluorinated polyhedral oligomeric silsesquioxanes (POSS)

Fluorinated poly hedraloligomeric silsesquioxanes (POSS) molecule has the lowest surface energy (9.3 *mN/m*) among all other solid crystals. This molecule contains a silicon-oxygen cage which is included with eight 1H,1H,2H,2H- heptadecafluorodecyl chains [121–124]. POSS molecules can be functionally controlled, be easily synthesized, their size is in nanoscale and is commercially available. In addition, POSS compounds may have high biocompatibility with polymers [125]. So far, many nonwettable surfaces have been fabricated by this material [126–129]. Oftentimes F-POSS is utilized as an independent compound. This can lead to the limited dissolution of this compound in ordinary solvents and also limited mechanical strength and resistance to wear of the surfaces containing F-POSS. Ramirez et al. [130] synthesized moderately compressed long-chain F-POSS along with silanol via a three-step reaction, in order to overcome the recent problem. This will result in the synthesis of new material with low surface energy and strength. Fig. 12 displays the three-step reaction. This research showed that the new structure displays excellent wetting behavior, similar to the primary F-POSS compound.

Recently a group of researches has developed a superomniphobic film using a polyhedral oligomeric silsesquioxane (POSS) based diblock polymer (P) and polyethylene glycol (PEG) in selective solvents [131]. The outcomes presented that the water contact angle raised along with the PEG content inside a definite range and the surface roughness was improved after the addition of AC. This shows cooperative applications of POSS compounds.

4.1.3. Fluorinated silanes

Another group that is used for the creation of superoleophobicity, is fluorinated silanes. Due to the strong chemical absorption on hydrophilic surfaces (glass, quartz, and oxides) and hydrophobic surfaces (plastics), recently thin films of silane have being used in order to control physicochemical characteristics of various solid surfaces through adjusting the wetting properties [132–134]. Malaga and Mueller. [135] have employed fluorinated silanes on the surface of concrete and stone for anti-graffiti uses. In comparison with the mentioned systems, fluorinated silanes or silsesquioxanes are supreme as a coating for these spongy surfaces with minor pores. The reason is that these coatings cause the transfer of water vapor which will maintain the adhesion of these coatings to the substrate, even in moist and jungle conditions (these conditions will cause the gradual disbanding of the normal coatings). Furthermore, the aforementioned materials display decent transparency though; porosity affects the cleaning capacity of the surface. As a result, in some cases, paint pigments get trapped in the pores and getting them out can be challenging.

Recently, Wang et al. [136] have developed metamorphic superomniphobic (MorphS) surfaces that alter their morphology in retort to heat. They manufactured the mushroom-like pillars of the thermos-responsive shape memory polymer by means of blending photolithography and reactive ion etching (see Fig. 13). Afterward, they improved the surface chemistry by means of a fluorinated silane to impart low solid interfacial energy.

4.1.4. Surface structure in fabrication of superoleophobic surfaces

As mentioned, fabrication of a liquid-repellent surface requires lower surface energy and also the surface structure should be I a proper condition for this purpose. Various approaches have developed in order to fabricate superhydrophobic surfaces by altering the surface structure, these methods can be also used to fabricate oleophobic and even superoleophobic surfaces. In this section, initial requirements of fabricating superoleophobic surfaces are presented then various approaches to prepare the surface structure in order to fabricate superoleophobic surfaces are explained.

4.1.5. Surface structure requirements for the creation of superoleophobicity

By using various nanostructured techniques, a wide range of surface topologies can be fabricated [137,138]. Structures with oleophobic properties mostly include overhang and re-entrant geometries [139–141]. The overhang structure was initially introduced for the fabrication of superhydrophobic structures [142,143]. The overhang structure prevents liquids from penetrating into the bulges due to the capillary force [144]. Kumar et al. [145] fabricated SiNG overhang nanostructure at the apexes of silicon nanograss via controlling etching parameters of Si wafers and showed that this structure improves oleophobicity and hydrophobicity of the surface. It has been observed that after the fabrication of this structure, the wetting angle for water and benzyl alcohol was 165 and 152, respectively. Fig. 14 shows different views of the samples with different overhang diameters. As can be seen, by fabricating the overhang structures at the apexes of the SiNG rods, wetting contact angle of benzyl alcohol increases by an increase of silicon oxide top layer thickness from 0 nm to 400 nm. It can be found that the overhang structure prevents liquids from penetrating into the space between the rods which leads to improving the oleophobic property of the surface. According to the modified Cassie-Baxter equation for the spherical-top pillar structures [146], by increasing the pillar diameters and/or increasing the sphere diameters of the pillar surfaces, wetting angle decreases. Recently, Xu has [147] invented new

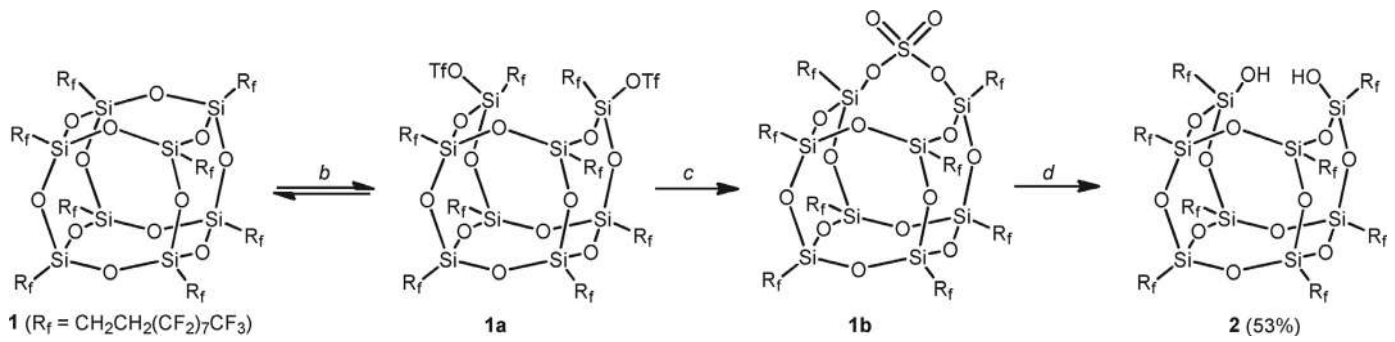

Fig. 12. Synthesis of incompletely condensed Fluoroalkyl Silsesquioxane [130].

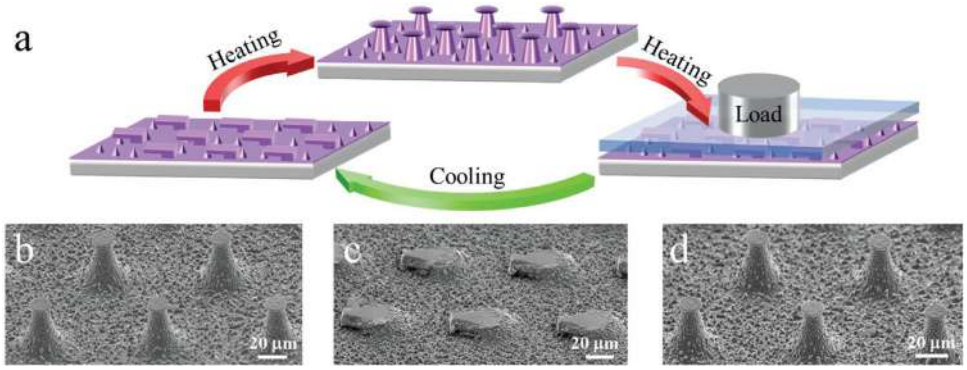

Fig. 13. (a) Schematic depicting the reversible morphology transformation between the mushroom-like pillar texture and the collapsed pillar texture. (b–d) SEM images showing the as-prepared mushroom-like pillar texture, the collapsed pillar texture, and the recovered mushroom-like pillar texture, respectively [136].

molding-based fabrication method for manufacturing re-entrant surface. This method has overcome previous problems by first making the main microstructures upside down by using a mold and the substrate while the initial substrate used during the molding process is removed.

Christian Aulin et al. [92] have fabricated a superoleophobic surface by the formation of an overhang structure on the silicon, which has an oleophilic nature. In this study, overhang structures were formed via the plasma-etching process. After the formation of the cellular structure on the surface and getting covered by the fluorinated trichlorosilanes, the fabricated surface displayed superoleophobic property.

Formation of the overhang structure results in a stable state of nonwetting Cassie-Baxter which leads to the superoleophobicity and superhydrophobicity of the surfaces [148]. Fig. 15 shows the overhang structure formed on the FOTS surface. Also wetting angle for oil and water is presented. As can be seen, the overhang structure leads to the superoleophobic and superhydrophobic properties on the surface.

As mentioned, in general, in order to fabricate a surface which has liquid repellency property, surface roughness should be incorporated and also surface energy should be decreased. In many cases, first, a rough structure is fabricated on the surface then the surface energy of this rough structure will decrease. But the important point in the fabrication of the superoleophobic surfaces is that, incorporation of the surface roughness for the creation of superoleophobicity is more complicated and challenging than the incorporation of the surface roughness for the superhydrophobic surfaces We illustrated a schematic of the liquids' states in contact with rough surfaces in Fig. 16 to better grasp the intricacy of the elements required to generate the superoleophobic surfaces. In the mentioned figure, θ is the liquid's equilibrium angle and $\varnothing_{structure}$ is the local geometric angle of the rough surfaces found between the horizontal line and structure's side walls.

In case of the establishment of $\varnothing_{structure} < \theta_{liquid}$, we have an upward resultant force F on the liquid-air interface and a convex liquid-air boundary area in the rough structure's grooves. This results in a delay in the wetting of the surface by the liquids inside the rough structure and the development of a composite sold-liquid-air interface in the Cassie-Baxter state. However, in case of the establishment of $\varnothing_{structure} > \theta_{liquid}$, we have an inward resultant force on the liquid-air interface, which causes a full surface wetting by the liquids inside the rough structures [150].

Water's contact angle is within the range of 90°−120° for the

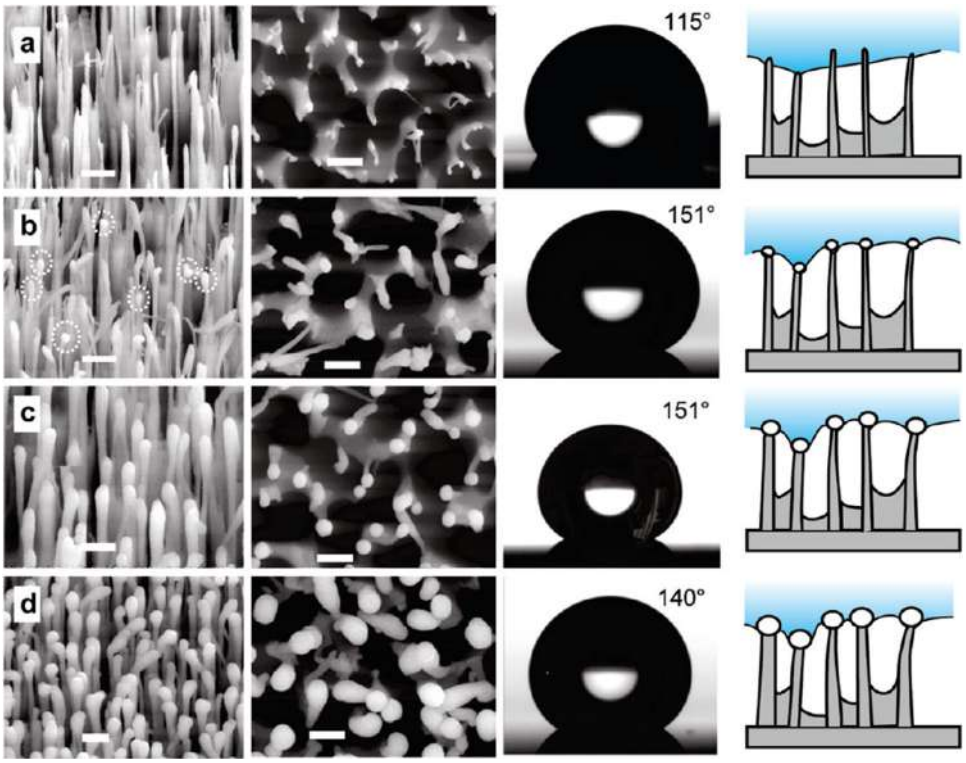

Fig. 14. Tilted view, top view, contact angle image of benzyl alcohol, and cross-section illustration of liquid covered SiNG surface (a) with 0 nm, (b) 100 nm, (c) 200 nm and (d) 400 nm thick silicon oxide on top. The scale bars are 1 μm. The contact angle changes from 115 to 151° by depositing overhanging oxide structures to the Si tips, which also cause the nanowires to widen [145].

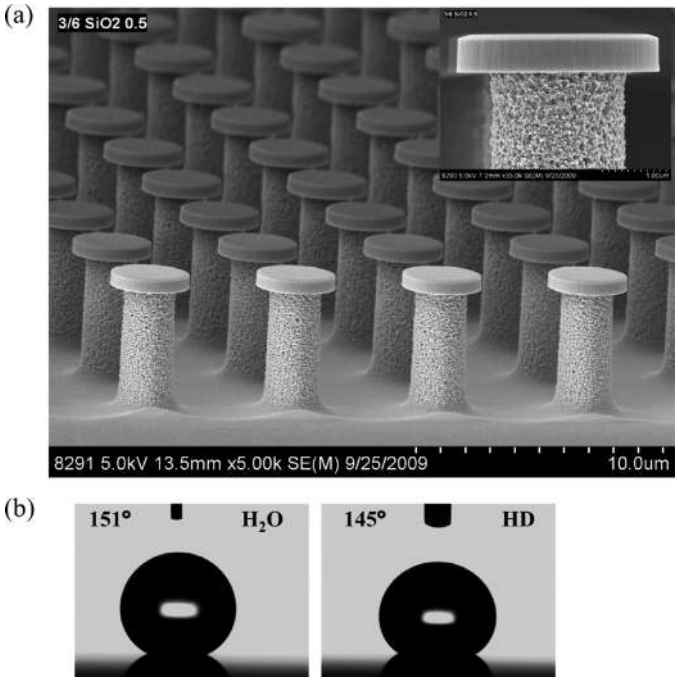

Fig. 15. (a) SEM micrograph of the textured FOTS surface with an overhang pillar structure on Si-wafer (inset: higher magnification micrograph showing details of the pillar structure) and (b) static contact angles for water and hexadecane on the textured surface in panel a [149].

majority of materials that have low surface energy levels. Therefore, it could be inferred that the majority of rough surfaces with $\varnothing_{structure}$ below 120° can be applied to generate a superhydrophobic exterior area in the Cassie-Baxter state (Fig. 16(a–c)).

Meanwhile, the oil's contact angle on the surface materials that have been altered and have a low surface energy level is below 90°, meaning that just a rough surface that has a $\varnothing_{structure}$ below 90° can be exploited to generate superoleophobic surfaces in the Cassie-Baxter state

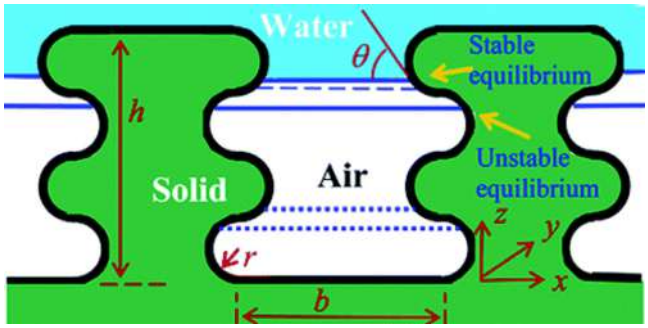

Fig. 17. Two-dimensional pillars with semicircular bumps/grooves. (a) Schematic of the structure. The bumps may pin the triple line because of an advancing LA interface results in a decrease in the contact angle ($\theta < \theta_0$), making the equilibrium stable. Grooves provide equilibrium positions that satisfy the Young equation; however, the equilibrium is unstable because an advancing LA interface results in an increase in the contact angle ($\theta > \theta_0$) [152].

(Fig. 16(d–f)). As such, more difficulties are involved in the generation of superoleophobic surfaces by the rough surface, compared to superhydrophobic surfaces. In addition, the superoleophobic surface can only be formed by the re-entrant structures ($\varphi_{structure} < \theta_{oil} < 90°$) [151].

The re-entrant structure is a two-dimensional hierarchical structure in which a composite solid-liquid-air interface is formed. At first, this structure was used for the creation of superhydrophobicity [152,153]. The superhydrophobic property on most of the trees' leaves is due to the re-entrant surface texture on them [142,144,148,154]. The re-entrant structure is schematically shown in Fig. 17. According to the small distance between the pillars, compared to the capillary length, the effect of gravity is insignificant and the liquid-air interface can be considered as a flat plane, which its position is determined by the vertical coordinate z [152]. Fabrication of the liquid-repellent surfaces by using the concept of the re-entrant surface structure has been the subject of many investigations [155–157].

Structures that were introduced for the fabrication of superoleophobic surfaces have limitations such as surface contamination after several uses, high intricacy and also high cost. In order to

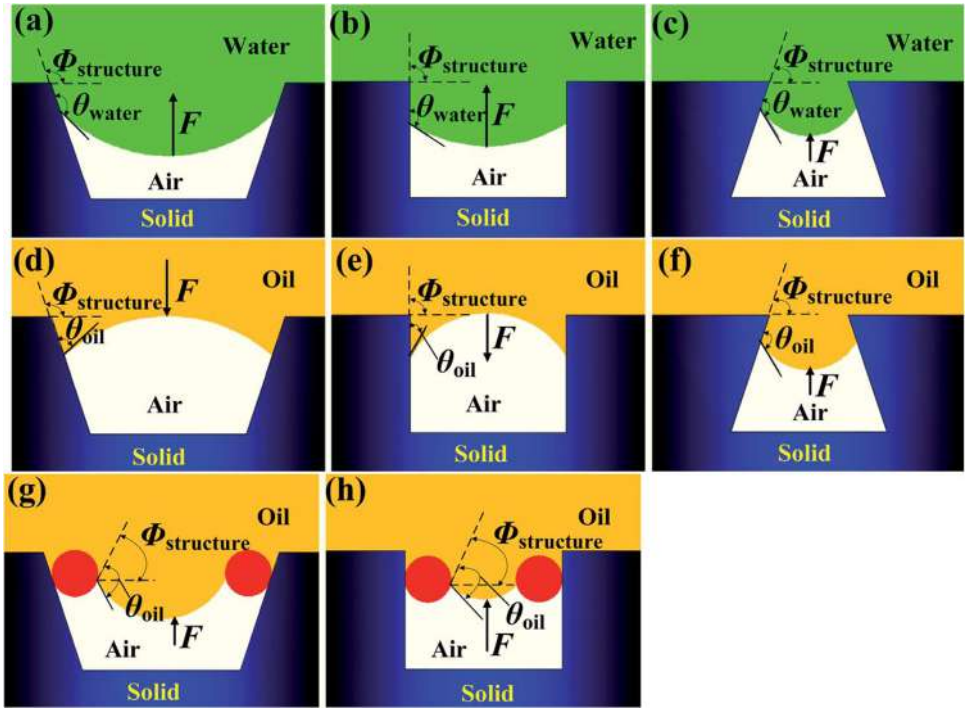

Fig. 16. Schematics of water (a–c) and oil (d–h) in contact with the rough structures with different values of $\varnothing_{structure}$ [151].

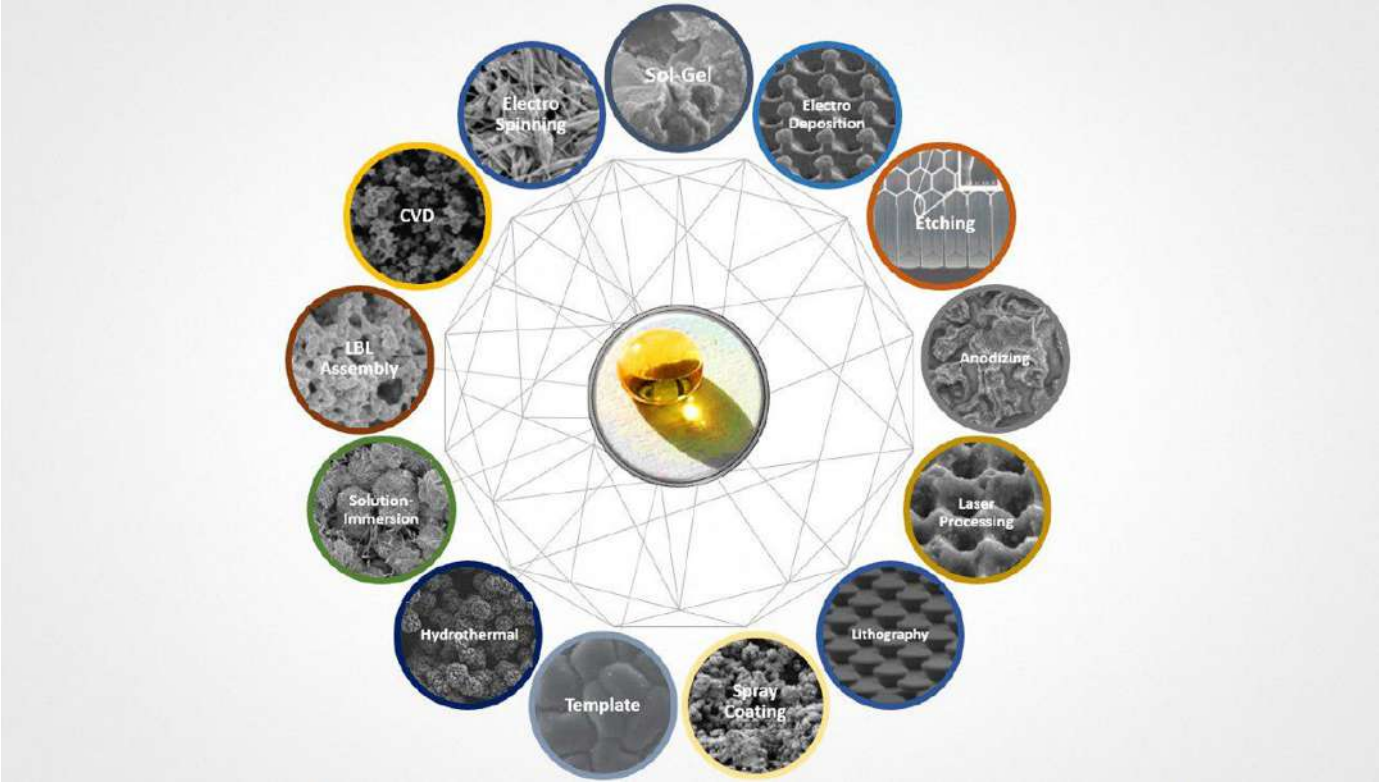

Fig. 18. Schematic of various approaches to fabricate superoleophobic surfaces.

overcome these limitations, another structure is used to make surfaces superoleophobic, called mushroom-like structure. Fabrication of this structure is inspired by gecko toe pad [158–160]. Kang et al. [161] fabricated a polymeric superomniphobic surface by a simple micro modeling and fluorocarbon surface treatment. The presented model was inexpensive and did not have the previous model's limitations. Also, the fabricated surface showed high durability.

4.2. Various approaches to fabricate superoleophobic surfaces

In this section, various approaches toward the fabrication of superoleophobic surfaces will be described and discussed. First, each method is explained and then some examples of them are brought. These methods are shown schematically in Fig. 18.

4.2.1. Sol-Gel

Sol-Gel method is a cost-effective, efficient method and it is low pressure and low-temperature process. Rough surfaces can be fabricated on various oxides, using this method however; the problem with this method is that it is an extremely slow process and it may take several hours or several days [162]. In addition, superhydrophobic surfaces can be fabricated via Sol-Gel, based on Cassie-Baxter theory [163–165]. Superoleophobic surfaces have also been fabricated via Sol-Gel method [166–172]. Xia et al. [173] have prepared a robust CuO/TiO2 Superamphiphobic Steel Surface through Chemical Deposition and Sol-Gel method using two-step immersing method which led to the formation of CuO/TiO2 micro/nano structure on the surface as is shown in Fig. 19. This film showed a contact angle of about 150 ° and sliding angle of fewer than 10°.

Regarding the generation of coatings with significant mechanical sustainability, which contains superoleophobic and superhydrophobic features in the mentioned studies, Wu et al. [174] applied both high and low SiO_2 nanoparticles' surface energy to fabricate these types of coatings using the Sol-Gel technique. The coating's mechanical stability was assessed using the cross-cut tape adhesion test, Posttest Pull-Off adhesion test, pencil scratch test, and nano-indentation. Moreover, the superoleophobic and superhydrophobic features of the coating were evaluated applying different liquid droplets with various surface energies. Furthermore, the molar ratio of SiO_2 nanoparticles with surface energies at a high and low rate was monitored in order to tune the surface topology. According to the results, the coating exhibits the most efficient mechanical and superoleophobic features when the molar ratio is at 2:4 between the SiO_2 nanoparticles' low and high surface energy.

4.2.2. Etching

The etching is a simple process and cost efficient which can be used for the creation of surfaces with various roughness's and this process is being used widely for the fabrication of superoleophobic surfaces [175–177]. As mentioned, re-entrant and overhang surface texture is necessary in order to have superoleophobicity on the surface. It should be stated that the creation of these structures can readily be done, using the etching method. The etching process can be classified as wet etching and dry etching, whether it uses a solution or not. Generally, wet etching is being used for simple species and controlling the surface topology is complicated, however; dimensional control is simpler in wet etching and the required equipment for dry etching is more complicated and also more expensive. Anyhow, fabricated surfaces using both methods are fragile, as they get bitten from the primary etching substrate. Fabrication of the superoleophobic surfaces via etching method has been the subject of many studies [151,178–181]. One of the main challenges that are concerned in the fabrication of superhydrophobic and superoleophobic coatings, is the mechanical stability of these coatings. Due to the fact that fabricating most of these coatings require incorporation of the rough surfaces, the created surface roughness can be removed by mechanical forces and as a result of that, the hydrophobic or oleophobic efficiency of these surfaces decreases. Aluminum and its alloys are an important part of engineering materials and have applications in most of the industries due to the unique properties [182]. Therefore, fabricating both superoleophobic and superhydrophobic surfaces on the aluminum to improve its unique

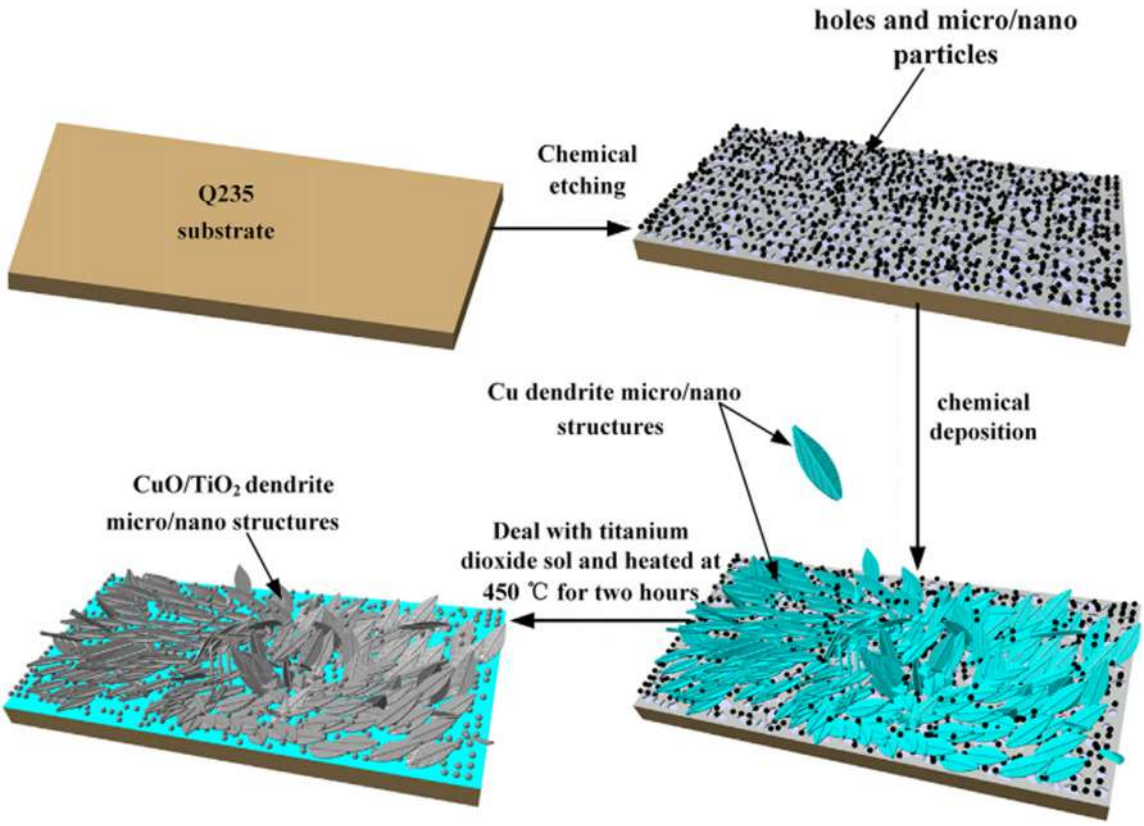

Fig. 19. The scheme of the preparation of superamphiphobic CuO/TiO2 dendrite micro/nanostructures on the Q235 steel surface [193].

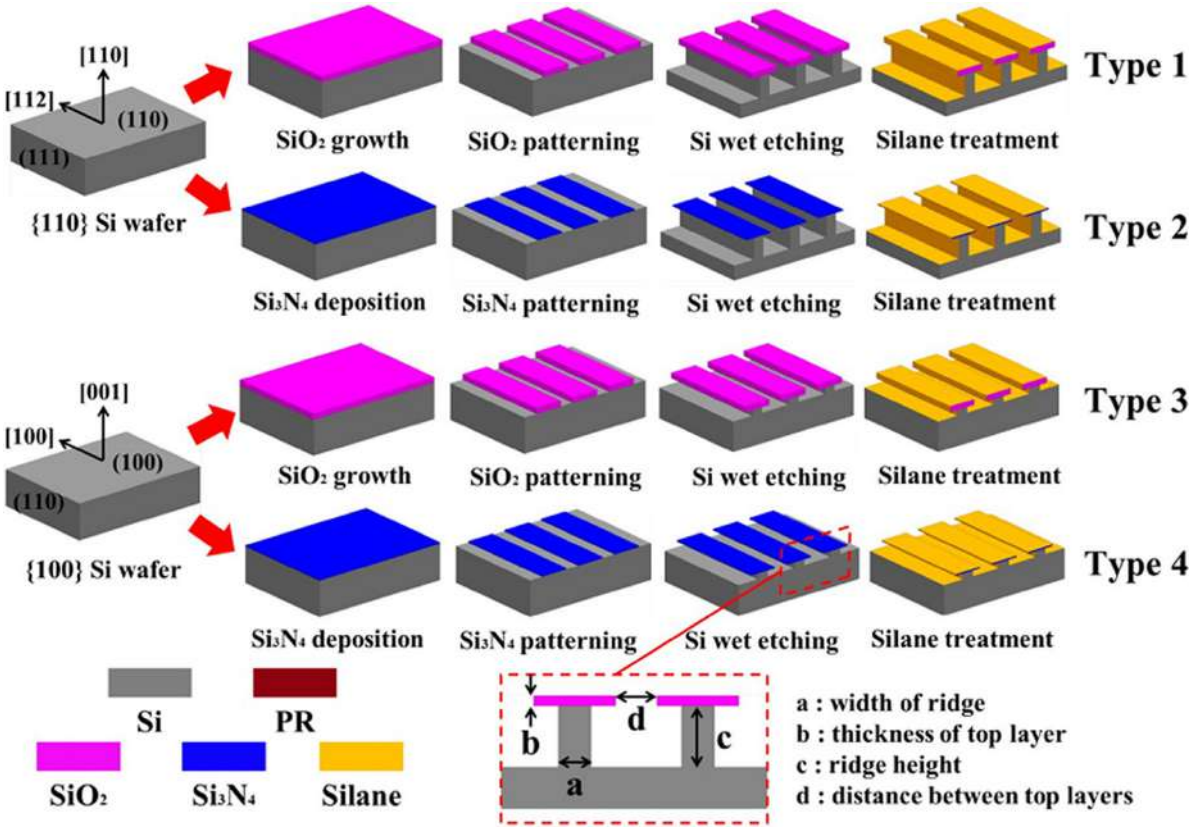

Fig. 20. Schematic view of the fabrication processes for the grooved mushroom structures and geometric parameters [175].

properties, is of great importance. So far many pieces of research have been done on this subject [151,183–185]. Peng and Bhushan [186] fabricated a hierarchical structure via etching method, which exhibited high mechanical stability.

Lee et al. [175] fabricated a superoleophobic surface with the grooved mushroom structure on a silicon wafer via chemical etching method which is a simple and cost-effective method and afterward, they investigated the wetting properties of the surface. Schematic of this process is shown in Fig. 20. In this figure, geometrical parameters that are incorporated on the surface is also being shown. The fabrication process consists of fabricating 4 structures which SiO_2 and Si_3N_4 layers were grown on the silicon wafers substrate via thermal oxidation and low-pressure chemical vapor deposition processes, respectively. After this step, the type 1 and type 2 silicon wafers were etched in tetramethyl ammonioum hydroxide solution, in 85°C. Etching parameters were controlled precisely in order to achieve a structure with controlled geometry. The type 3 and type 4 specimens were etched in Tetramethylammonium hydroxide (TMAH) solution, in 54°C. After the etching step, the etched specimens were treated by molecular vapor deposition of Tridecafluoro-1,1,2,2-tetrahydrooctyltrichlorosilane, for minor interfacial energy.

Song et al. [151] fabricated re-entrant structure on the aluminum substrate via etching method which leads to the creation of superoleophobic property on the surface. The re-entrant structures include rectangular-shape in micro/nanometer scale and step-like Al structures which are achieved via electrochemical etching and Ag grains in nanometer scale are also obtained from immersion in $[Ag(NH_3)_2]^+$ solution. Furthermore, surface energy decreased due to the presence of perfluorooctanic acid containing $-CF_3$ and $-CF_2$ groups. Results from this research showed that the creation of the re-entrant structure and also reduction in the surface energy because of the presence of $-CF_3$ and $-CF_2$ groups, lead to a 160° angle for contact angle of the oil. Fig. 21 shows the SEM images of the electrochemically etched Al surface. As can be seen, electrochemical etching results in the creation of rectangular-shaped and step-like erections in 1–5 micrometer scale. Also, it can be found out that the main phase is Al. The main reason behind the creation of this structure after electrochemical etching is related to the great quantities of grain boundaries and dislocations presence in polycrystalline Al [187].

Seungmuk Ji et al. [179] also fabricated superhydrophobic and superoleophobic structures on the Al surface via an etching process. The formation process includes grinding, acid etching and coating with fluoroalkylsilane in sequence. The wettability of the fabricated coating was characterized using different liquids with various surface energies, such as water, diiodomethane, and hexadecane. The best wetting properties were observed with 10 min etching and it was found out that the nanostructure on Al surface was disappeared with 20 min etching which leads to the reduced wettability

Yu Strong et al. [188] manufactured superhydrophobic and oleophobic surfaces on Zn substrate via chemical etching process and hydrothermal reaction. The fabricated surface consists of micro hexagonal prisms with 4 μm in length, 0–1 μm in the gap and 0.4–1 μm in diameter. Then, the fabricated surface had superhydrophobic and oleophobic properties with a fluoride coating. In this study, the effects of diverse parameters such as etching time and hydrothermal reaction factors, on the coating wettability were examined and the etching time of the 90 s and the hydrothermal temperature of 95°C were found out as the optimum parameters. With these optimum parameters, the contact angle of water was 151.8$\mathring{5}$ and 145.6$\mathring{2}$ for the contact angle of edible peanut oil. Furthermore, the superhydrophobic and oleophobic surface have fabricated via electroless etching of silicon in sodium tetrafluoroborate ($NaBF_4$) aqueous solution [189]. Then, silver particles were deposited on the fabricated surface which changes the overall physical morphology and finally, the obtained surface was coated with two low surface compounds, in order to create superhydrophobic and oleophobic properties. Results from this study showed that the modification with poly(α,β,β-trifluorostyrene) (PTFS) had the best outcome and by using this method, the contact angle of 160$\mathring{0}$ and 110$\mathring{0}$ were obtained for water and hexadecane, respectively. However; creating re-entrant structure by the deposition of silver particles on the nanostructured silicons improved the wetting properties.

4.2.3. Lithography

By using this method, it is feasible to have precise control on the surface construction and surfaces with different patterns and sizes can readily be fabricated via this method. This method has some advantages including convenient creation of the template and using it for multiple times and low cost of it [190,191]. Fabrication of the superoleophobic surfaces using lithography has been the subject of many studies [192–195].

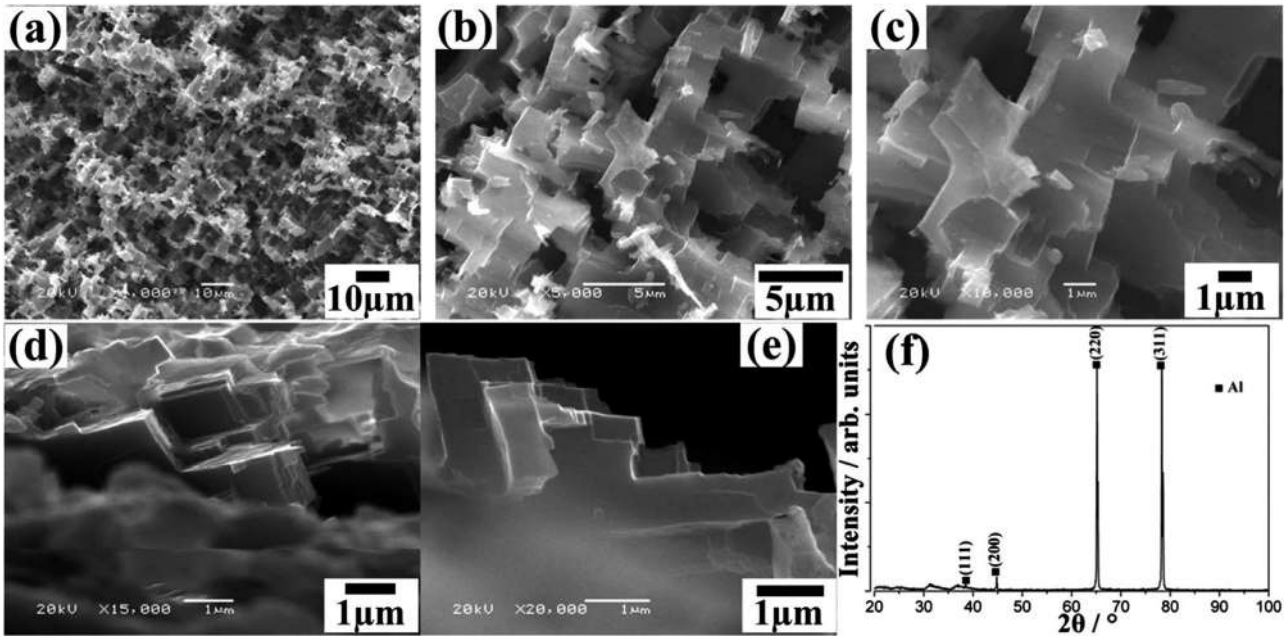

Fig. 21. SEM images and XRD pattern of electrochemically etched Al surfaces: (a–c) top-view SEM images; (d and e) tilt-view SEM images; and (f) XRD pattern [151].

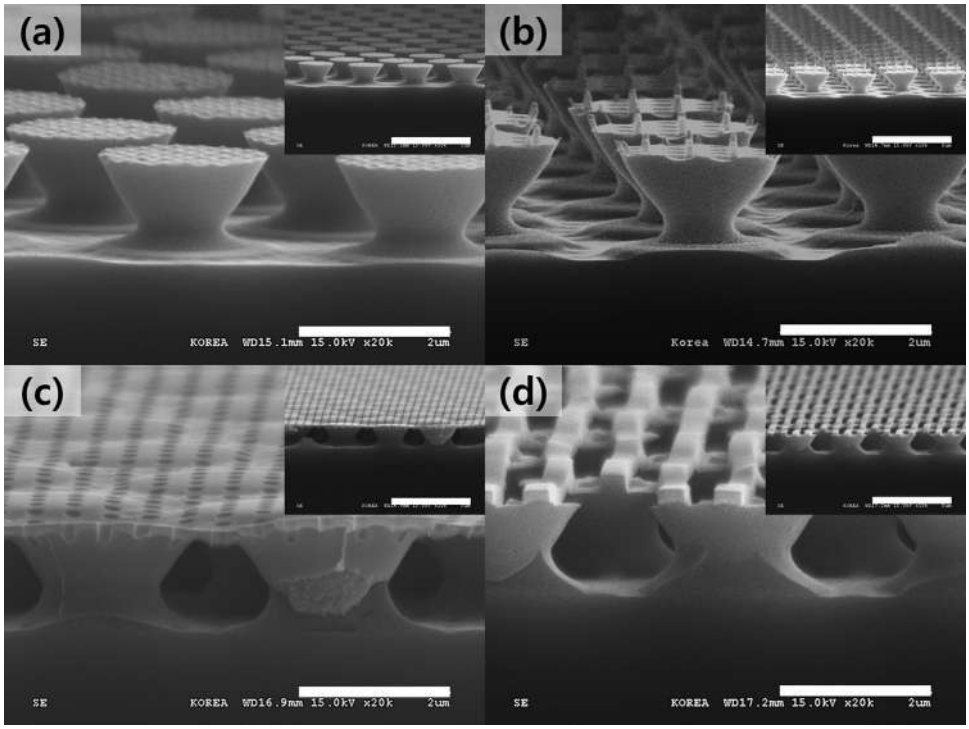

Fig. 22. SEM images of different types of nanopatterns embedded overhang structures: (a) cone-, (b) pillar-, (c) hole-, and (d) lineshaped nanopatterns (scale bar = 2 μm). Inserts are low magnifications, respectively (scale bar = 5 μm) [196].

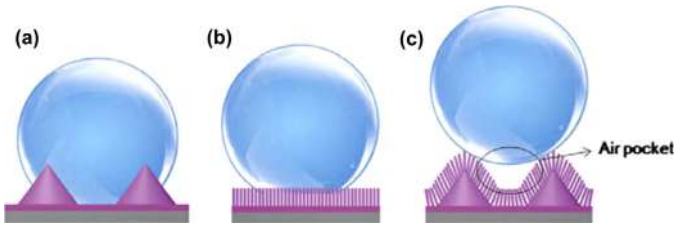

Fig. 23. Surface wetting of (a) the micro-pattern, (b) Nanorods, and (c) the hierarchical structure [200].

In research by Choi et al. [196], the reverse nanoimprint lithography technique was exploited to generate a surface with both oleophobic and superhydrophobic features and an overhang structure. These researchers created four types of nanopatterns on the surface of the overhang structure separately applying the improved version of inverse imprint lithography in order to improve oleophobicity. On the other hand, the mentioned researchers coated the achieved overhang structure with a fluoroalkylsilane monolayer to decrease the surface energy. The oleophobic feature was enhanced due to the presence of various overhang angles caused by the generation of the nanopatterns on the surface. Fig. 22 contains data on various kinds of nanopatterns created on the surface.

Four various kinds of nanopatterns (i.e., cone, hole, line, and pillar) are defined and exhibited in the mentioned figure. In addition, the pillar and cone-shaped nanopatterns are presented in Fig. 22(a) and (b), respectively. According to the results, these nanopatterns had no impacts on the overhang angle and were only present on the overhang structures. However, the features were affected by these nanopatterns through the increase of the solid-liquid interface's area. Meanwhile, the line and hole-shaped nanopatterns exerted an impact and formed new kinds of overhang structures, which could have an impact on the wetting features.

The colloidal method or nanosphere lithography is a favorable and flexible method for the organization of self-assembly particles [197] and there are many studies about the fabrication of superhydrophobic and self-cleaning surfaces by using this method [171,198,199]. The superhydrophobic, oleophobic and superoleophobic surfaces with ordered hierarchical (triple-scale) structure were fabricated on the polymeric substrate of methyl methacrylate (PMMA) via polystyrene (PS) microparticle colloidal lithography method by Ellinas et al. [191]. In order to create amphiphobicity, the fluorocarbon plasma deposition treatment was carried out on the obtained surface. It was observed that improvement of the hydrophobic and oleophobic properties was related to the hierarchical and re-entrant topologies.

Combined with hydrothermal synthesis, the ultraviolet nanoimprint lithography was carried out to apply the ZnO nano-in-micro hierarchical structures in the formation of the superhydrophobic and superoleophobic surfaces in a study by Byeol Jo et al. [200]. Results were indicative of a high level of superhydrophobicity ((contact angle above 160̊) presented by the attained structure. Moreover, the sliding angle and the contact angle hysteresis were below one and two degrees, respectively.

The combination of nanorods and micropatterns led to the creation of air pockets in a structural manner, thereby causing the observed behavior, as shown in Fig. 23. In this figure, the structural combination of nanorods and micropattern resulted in the creation of air pockets between the water droplets and the hierarchical structure, which is related to the hierarchical ZnO structure. Following the generation of air pockets, a composite interface is created between the hierarchical structure and water droplet made of liquid-air fraction and a solid-liquid fraction. The creation of composite interface leads to the changing of the surface wetting condition of the ZnO hierarchical nano-in-micro structure from Wenzel to the Cassie–Baxter state, causing the formation of the superhydrophobicity on the surface [201].

4.2.4. Conductive polymers

The accompanying polymers have particular optoelectronic features that lead to their sensitivity to different stimuli, compared to other elements. In addition, they have fascinating uses in oil/water separation membranes, sensors, and optical devices. Oxidative chemical

polymerization creates the conducting polymer nanostructures in these methods, chemical vapor deposition, plasma deposition and electrodeposition (pre and post approaches).

The substrate surface is covered by metal using the electrodeposition method and the surface morphology of the fabricated coating can be controlled by changing the parameters that affect the electrodeposition method. There are some studies about the fabrication of superoleophobic surfaces via this method [202–206]. Electrodeposition is applicable on both flat and non-flat surfaces, the only requirement is the substrate must be conductive and does not get oxidize simply. For instance, electrodeposition can be carried out on gold, platinum, stainless steel and titanium, however; not on aluminum. Since long fluorinated tails can have destructive effects on the environment [207], nowadays fabrication of the superoleophobic surfaces using short fluorinated tails is challenging. Therefore, most of the times, a combination of fluoropolymers with short tails (conductive polymers) and electrodeposition method is used for manufacturing a superoleophobic surface. The conductive polymers with fluorinated chains or hydrocarbon chains can be replaced for the creation of superoleophobicity [208–213]. Using conductive polymers has advantages such as various possible states of wetting properties and also various electrical and optical properties [214,215]. One of the advantages of this method for fabrication of the superoleophobic surfaces is that it has only one step. Also by using this method, films with controlled surface morphologies and surface roughness can be obtained through adjusting deposition charge, electrochemical parameters and chemical structure of the monomer [216,217]. According to the references, polymerizable core like pyrrole ، thiophene،, 3,4-ethylene dioxythiophene (EDOT) and 3,4 ethylenedioxypyrrole (EDOP) does have a high impact on the superoleophobic features of the polymeric films and it seems that EDOP derivatives have the highest impact [116,218–220]. This effect has been reported by other researchers who used EDOP products for the fabrication of the superoleophobic surfaces.

As mentioned in previous sections, surfaces with specific roughness and morphology which is called re-entrant structure and also fluorinated compounds with long perfluorinated tails are required for the fabrication of superoleophobic surfaces. However; because of the toxicity problems with these long tails [34,221], most of the strategies are toward the fabrication of superoleophobic surfaces using short perfluorinated tails. To this end, Darmanin and Guittard [202] fabricated superoleophobic surfaces using EDOT derivatives and EDOT– NH–F_n monomers. The polymers were deposited at a constant potential via the electrodeposition method and the wettability of the film was described by static and dynamic contact angles. The results showed that reaching superoleophobic properties is possible only with F-butyl tails. It was also concluded that presence of the nanofibers (re-entrant structures) and the amide connectors may lead to the increased stability of Cassie-Baxter state by oil droplets, which results in the possibility of reaching near Cassie-Baxter state with polymers including F-butyl tails.

Recently it has been shown that the superoleophobicity of the poly (3,4-ethylenedioxythiophene) polystyrene sulfonate (PEDOT) polymers can be improved by making a connection between the fluorinated chains and the polymer, with an amide connector. Also, Drame et al. [222] added two fluorinated chains to these polymers, in order to improve the superoleophobicity of these polymers.

The fluorinated tails create a specific morphology in addition to the reduction of surface energy, in order to create superoleophobicity [223,224]. Researchers have shown that the surfaces with various morphologies can be obtained through the electrochemical polymerization of the fluorinated monomers [225,226]. In these studies, various surface morphologies have obtained via this method. The precise effect of the fluorinated tails on the conductive polymers' morphology which is fabricated via electrical deposition, has been investigated by Darmanin and Guittard [227]. For this research, a series of the fluorinated monomers and their hydrocarbon homologs were synthesized and in an identical condition, were deposited on the surface via electrodeposition method. Results from this study showed that the fluorinated monomers have a role in the fabrication of surface morphology with the purpose of creating superoleophobicity. In fact, in an identical condition of polymerization, highly fluorinated pyrroles lead to a spherical microstructure while the surfaces obtained from hydrocarbon pyrrole are almost flat. Also in another study [228], it has been showed that the fluorophobic effect leads to a nanoporous structure due to the use of fluorinated EDOP which causes a superoleophobic property on the surface.

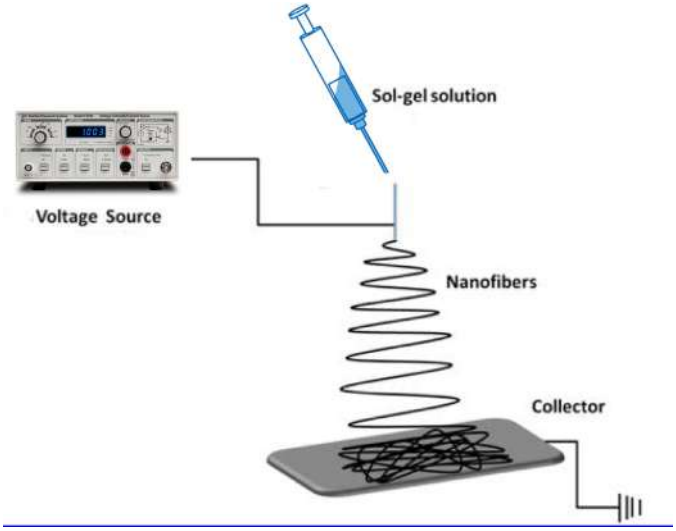

Fig. 24. Schematic diagram of the electrospinning set-up.

4.2.5. *Electrospinning*

Electrospinning is a modest but multipurpose technique for the production of continuous fibers with diameters smaller than nanometers and also with porosities about 30–90 percents from various polymeric materials [229]. A simple set-up used in the electrospinning process is presented in Fig. 24.

This method has been implemented in order to fabricate superhydrophobic surfaces [230,231] and also been carried out to fabricate superoleophobic surfaces [111,232,233]. To assure the improvement of the non-wetting property from liquids with low surface energy, fibers' diameter and the distance between fibers can be controlled by adjusting variables of electrospinning for example solvent, viscosity, surface energy, and electrical conductivity. Also, both of the superoleophobic and superhydrophobic properties of the fibers are able to be improved by subordinate structures like wrinkles, beads or intrananofibers [234,235]. The electrospinning method can be carried out as two steps or a single step process, however; most of the times this process is done in two steps and after the electrospinning of ordinary polymers process, materials which result in the creation of superoleophobicity should be deposited on the surface. The single step process which includes electrospinning of the fluorinated compounds is difficult due to the fact that fluorinated compounds do not dissolve in the electrospinning solutions [236]. Nevertheless, many researchers pursue the direct electrospinning process of fluorinated polymers. Rin Choi et al. [236] fabricated a network of poly (2,2,2-trifluoroethyl methacrylate) (PTFEMA) nanofibers via electrospinning method without further post surface treatments. Results from this study showed that the surface was rich in fluorine. Also, the created superoleophobicity by this method was dependent on the fibers' diameter and the distance between them. Fig. 25 shows the SEM images of the PTFEMA fibers electrospun in solutions with 24, 26, 28 and 30 wt%. Also the fibers' diameter, distribution of fibers and contact angle of hexadecane can be observed in this figure. As can be seen, the fibers' diameter increases with the increase of PTFEMA concentration in the electrolyte and the contact angle of

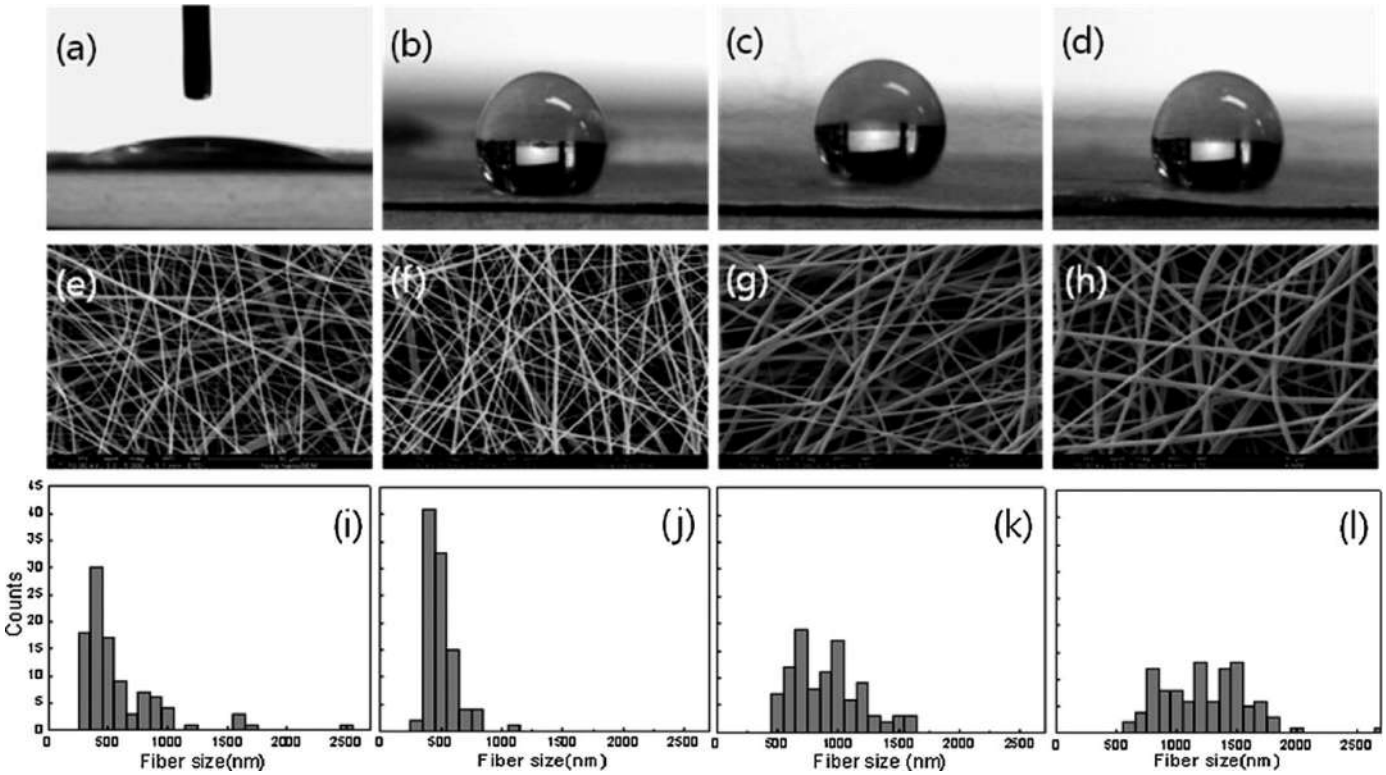

Fig. 25. Hexadecane contact angle images, SEM images, and their distributions of diameters of 100 individual fibers gained randomly in SEM images of PTFEMA fibers electrospun with different polymer solution concentration (a, e, i) 24 wt.-%, (b, f, j) 26 wt.-% (c, g, k) 28 wt.-%, and (d, h, l) 30 wt.-%. The volume of hexadecane is 6 mL 236.

hexadecane in solutions with 26, 28 and 30 wt%, were the highest amount, equal to 150̊. The oleophilicity of the electrospun specimen with 24 wt% attributed to the high variation of the fibers' diameter.

Ganesh et al. [237] used electrospinning method for the deposition of SiO_2 nanofibers, uniformly on the glass. In this process, the SiO_2 nanofibers acted as a template for the fabrication of superamphiphobic surfaces. After the deposition of the SiO_2 nanofibers, porous membranes of silica were applied to the surface via vapor deposition treatment, in order to create superoleophobicity and after the heat treatment, the fabricated coating includes hybrid silica network which this network consists of SiO_2 nanofibers embedded with silica membranes. Results from this study showed that the contact angle of water and hexadecane was approximately 161̊ and 146̊, respectively. Also, researchers believe that these types of coatings can be utilized as a self-cleaning surface in the windows. Also, in another study [238] by this group of researchers, TiO_2 nanostructures were applied to the surface of glass via electrospinning method, in order to obtain superoleophobic and superhydrophobic surfaces. The fabricated surface was hydrophilic at first and then with silane treatment, the surface nature was changed to a superhydrophobic and superoleophobic surface. Results showed an angle of 166̊ for water and 138̊ for hexadecane. Also, the results confirmed high mechanical and thermal stability along with good adhesion to the substrate. Having these properties in mind, these types of coatings are a suitable option for industrial applications.

4.2.6. Layer by layer method (LBL) assembly

In general, the layer by layer method is described as a process that involves consecutive absorption of the species with negative and positive charges via immersing in the solutions. The reaction between the charged species is used in this method and layers will be deposited on the surface with species with opposite charges (polymers, particles, surfactants and …), one after another. This will result in a multilayer coating which layers are electrostatically cross-linked. This technique can be used in various applications due to the fact that components with different charges can be used in each layer. This method is widely used for the fabrication of superhydrophobic surfaces [239,240]. Also, it has been used for the nanoparticles assembly [241,242] and fabrication of superoleophobic surfaces [243]. Cao and Gao [244] fabricated a transparent coating with both superhydrophobic and superoleophobic properties, using silica nanoparticles assembly and also the sacrificial polystyrene nanoparticles. At first, the silica and polystyrene nanoparticles were deposited via the layer by layer assembly technique. Using this method, it is possible to have precise control on the chemical composition, surface morphology and also the coating thickness is controllable in the nano-scale range. Li et al. [245] used this method and the SiO_2 nanoparticles with different sizes in order to fabricate a series of nanoparticle- coatings with the hierarchical raspberry-like structure and dual roughness, on the stainless steel meshes which are used for the water/oil separation. Brown and Bhushan [246] fabricated a surface which possesses both superoleophobic and superhydrophobic properties with high mechanical stability, via combining the layer by layer and fluorosilane vapor deposition methods. Fig. 26 shows a schematic of the steps involved in the fabrication of this coating and also the chemical structure of each of the species. As it is shown, the obtained coating consists of 4 layers which are deposited separately. Each of these layers assists in fabricating a coating with high mechanical stability. Polydiallyldimethylammonium chloride (PDDA) was used as a polymer-based layer due to its high cathodic charge density and good connection with the glass substrate.

4.2.7. Solution-immersion

The solution-immersion is a simple method in order to fabricate superhydrophobic and superoleophobic surfaces and it has also been used for the fabrication of superoleophobic coatings [247,248]. Zhu et al. [249] used a two-step method for fabricating a coating with both superhydrophobic and superoleophobic properties on the copper

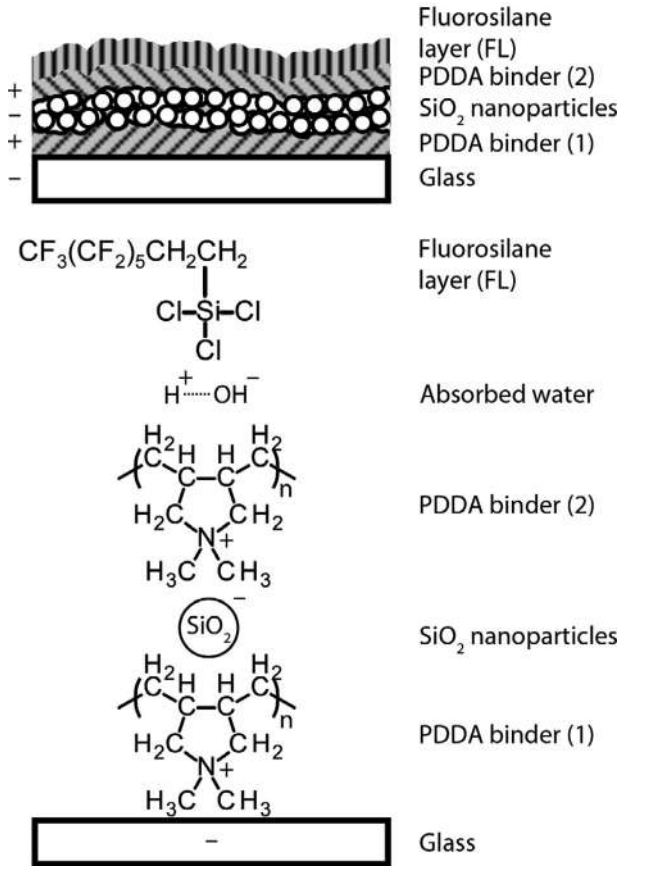

Fig. 26. Schematic of the layer-by-layer composite coating. Each layer is deposited separately. Also shown are the chemical composition and charge of each layer. The fluorosilane (FL) condenses onto the layer-by-layer stack via absorbed water [246].

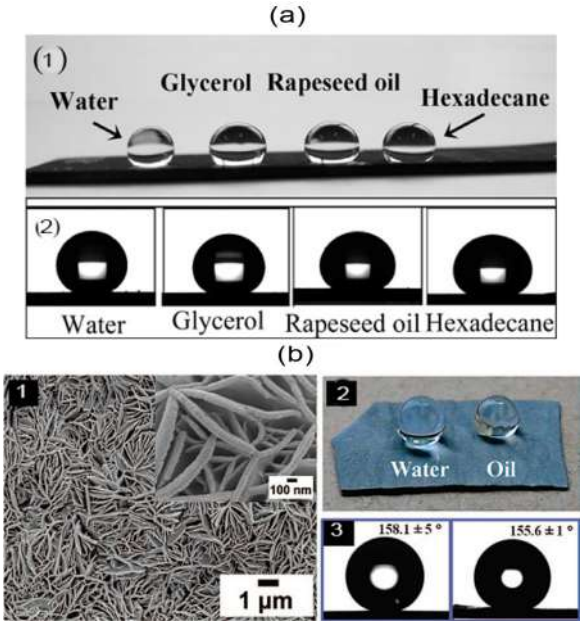

Fig. 27. (a) Optical images of water, glycerol, rapeseed oil, and hexadecane droplets on the superamphiphobic surface (1) and their contact angle profiles (2). (b) (1) Large-area SEM image of the prepared petal-like surface; the inset is a high-resolution SEM image. (2) The camera pictures of water and oil droplets setting on the as-prepared surface. (3) Contact angle profiles of a water droplet (left) and oil droplet (right) on the surface [250].

substrate which the first step included immersion for obtaining a surface with hierarchical morphology and the second step was creating a superamphiphobic surface by perfluorooctanoic acid. After these two steps, the surface became superamphiphobic which this property attributed to the simultaneous effect of the surface chemistry and the specific surface morphology. Fig. 27.a shows the surface wettability by liquids with different surface energies. As can be seen, water, glycerol and rapeseed oil have a spherical shape on the surface and also their sliding angle is smaller than 15°. This behavior has been observed for alkane liquids like hexadecane which has the contact angle of 153̊ and the sliding angle of 2̊3.

Meng et al. [250] fabricated a superhydrophobic/superoleophobic coating with one step via immersing the zinc substrate in an ethanol solution containing perfluoro carboxylic acid, at ambient temperature and for several days. Creating superoleophobicity and superhydrophobicity in this method was due to the electrochemical reaction in the solution. After 10 days of soaking in the solution, the contact angle of water reached 158.1̊ and the contact angle of oil reached 155.6̊ which this fact is shown in Fig. 27.b. Also, the camera pictures of these liquids on the substrate are prepared which are shown in this figure. These pictures display the excellent superoleophobicity and superhydrophobicity and also the surface morphology of the prepared surface can be observed which is peta-like. This microstructure is like the microstructure of lotus leaf.

4.2.8. Hydrothermal

The hydrothermal method is one of the important and effective methods for incorporating roughness on the surface. The fabricated surface can be precisely controlled using this method. One of the flaws of this method is the high price of its equipment and also being hazardous which has limited its practical applications. Furthermore, high pressures and high temperatures are being used in this method. This method has been implemented in order to fabricate superoleophobic surfaces [251,252]. Wang and Guo [253] fabricated the TiO_2 coatings with hierarchical rutile TiO_2 flowers structure using a single step hydrothermal process on a thin fluorine-doped oxide substrate. The obtained coatings exhibited superhydrophobicity in the air and also superoleophobicity in the underwater which leads to the excellent self-cleaning property in the underwater. One of the main properties of the obtained coating was the self-cleaning property due to the presence of TiO_2 which is the cause of probable applications of the coating in the industry. In another study [254] via hydrothermal treatment, *ZnO* nanorods were fabricated on the substrate under ambient condition. The obtained surface exhibited superhydrophobicity in the air and superoleophobicity in the underwater.

4.2.9. Anodizing

Anodizing is one of the surface treatments of metals that a metal surface converts to an oxide by the application of anodic current on the metals surface and their alloys. Sometimes this treatment is used as a metals protection technology [255,256]. Surfaces with controlled morphologies can be achieved using this method. This method has been used for the creation of super oil repellent surfaces [257–261]. Titanium oxide is one of the most important and applied semi-conductors due to the unique properties it has and has been used in many applications [262,263]. There are many methods available for the fabrication of titanium oxide on various substrates [264,265]. Therefore, it is obvious that using the anodizing method on the titanium substrate is an important and useful method for the fabrication of superoleophobic surfaces. The electrochemical anodizing method is a modest, fast and flexible method for the assembly of arrays of TiO_2 nanotubes on a titanium substrate [266,267]. Barthwal et al. [257] used an electrochemical and two-step anodizing method. First titanium oxide nanotubes were grown on the titanium substrate in an aqueous solution then a layer of fluorooctyltrichlorosilane was coated for the creation of surface superoleophobicity. This sequence of treatment is shown in

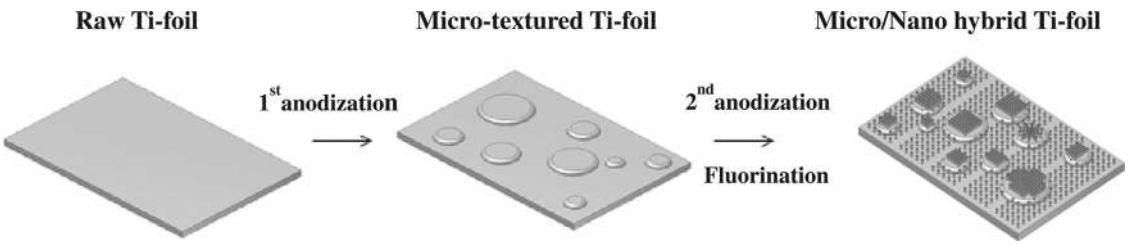

Fig. 28. Schematic diagram of the fabricated micro- and nanostructured Ti foil [259].

Fig. 28. In this study, the wetting properties of the obtained coating were investigated by liquids with different surface energies and the longtime stability was also studied. Researchers believed that the obtained coatings via this method could have many industrial applications.

Furthermore, Li et al. [268] achieved underwater superoleophobicity by growing TiO_2 nanotubes with hierarchical structure via the anodizing method. They fabricated underwater superoleophobic porous membranes on the titanium substrate. The fabricated porous membranes included TiO_2 nanotubes with a hierarchical structure which showed superhydrophobicity in air and superoleophobicity in underwater. This property made it possible to use the obtained membrane in water/oil separation applications. In this condition, water easily penetrates through the membrane which leads to the water/oil separation. Also, the obtained membrane causes water refinement as the water passes through the membrane. In addition, results from the wetting recovery of the porous membranes were related to the wetting recovery at the time of encountering contaminations from organic molecules.

A surface with the hierarchical dual-pore geometry was fabricated via a combined, practical and cost-effective method of chemical etching, then anodizing and pore widening by Nakayama et al. [269] on the aluminum substrate. After coating with fluoroalkyl phosphate, the surface on the aluminum became superoleophobic. Results from this study showed that the dual-pore structure with optimum condition exhibited super-repellency even for liquids with very low surface energy. Li et al. [268] used a similar procedure consist of chemical etching and then anodizing in order to fabricate a superhydrophobic/superoleophobic coating on the aluminum substrate. The fluorination treatment led to the superoleophobicity and superhydrophobicity on the surface. A diagram of the fabrication stages of the Ag NP-loaded hierarchical coating is shown in Fig. 29. Before anodizing treatment, the substrate was immersed in a HCl and $CuCl_2$ solution to have a hierarchical step-like structure. After the anodizing treatment in the oxalic acid solution, in order to create a chemical bond between Ag NPs on the aluminum surface, APS monolayer was implemented on the substrate surface via vapor deposition technique and then Ag NPs were stabilized on the APS monolayer by amino-group bond, throughout the self-assembly procedure and thereafter, by the fluorination treatment of the specimen with species with minor surface energy, a surface with high superhydrophobicity and high superoleophobicity was obtained.

4.2.10. Spray coating

Spray coating is a simple technique for the fabrication of superhydrophobic coatings and recently it has been implemented in order to fabricate superoleophobic surfaces, too [91,110,270,271]. In this method metal perfluoroalkanoates are used as the coating for the fabrication of superoleophobic surfaces via the chemical etching of the metals in perfluoroalkanoates, the perfluoro carboxylic acid solution [250] and then applying the coating process. This method requires much time and also it is limited to the specific substrates. Yang et al. [140] introduced a simple method for the synthesis of copper perfluorooctanoate via a reaction between copper acetate and perfluorooctanoic acid in the water. They showed that via spraying this material, a uniform coating with the high superoleophobic property will be obtained and a solid-liquid-air composite interface will be formed and the contact angle will reach above the 150̊, even for the liquids with low surface energy. The coating superoleophobicity was attributed to the obtained re-entrant morphology and also the super low surface energy which is preventing from the change of Cassie-Baxter state to the Wenzel state. The SEM images of this coating and the contact angles for the liquids with dissimilar surface energies are shown in Fig. 30. As can be observed, the hierarchical structure is clear in the images and also the multiple scales roughnesses and high amount of porosities on the coating surface can be seen. A considerable issue from Fig. 30(b) is the presence of re-entrant morphology on the surface. Also, the droplets on the surface which are shown in the images indicate that they tend to stay in a spherical shape, even in the case of liquids with

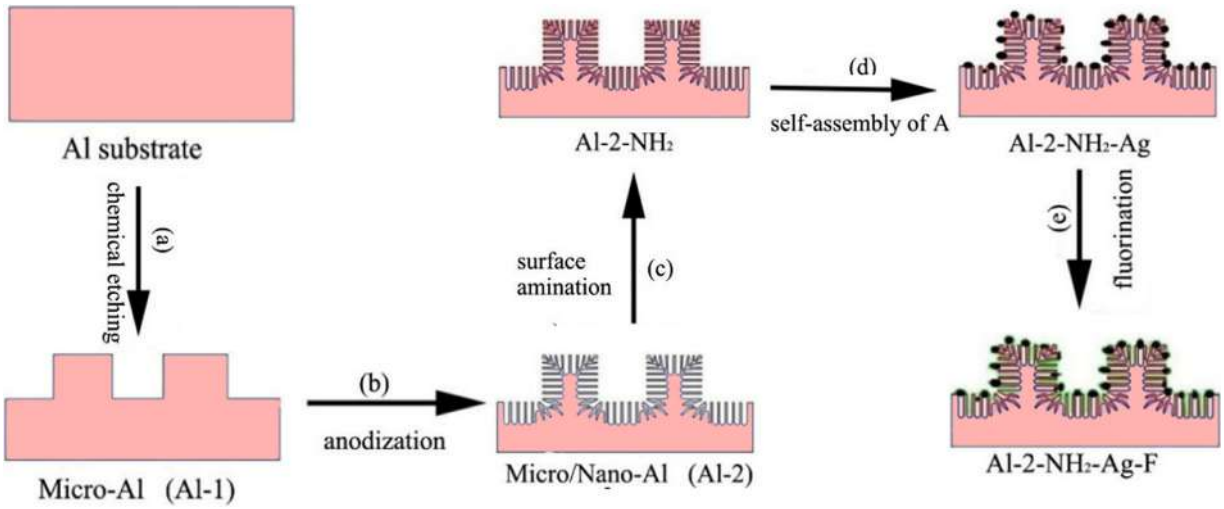

Fig. 29. Schematic illustration of fabricated Ag NP-loaded hierarchical superamphiphobic surface on the Al substrates [268].

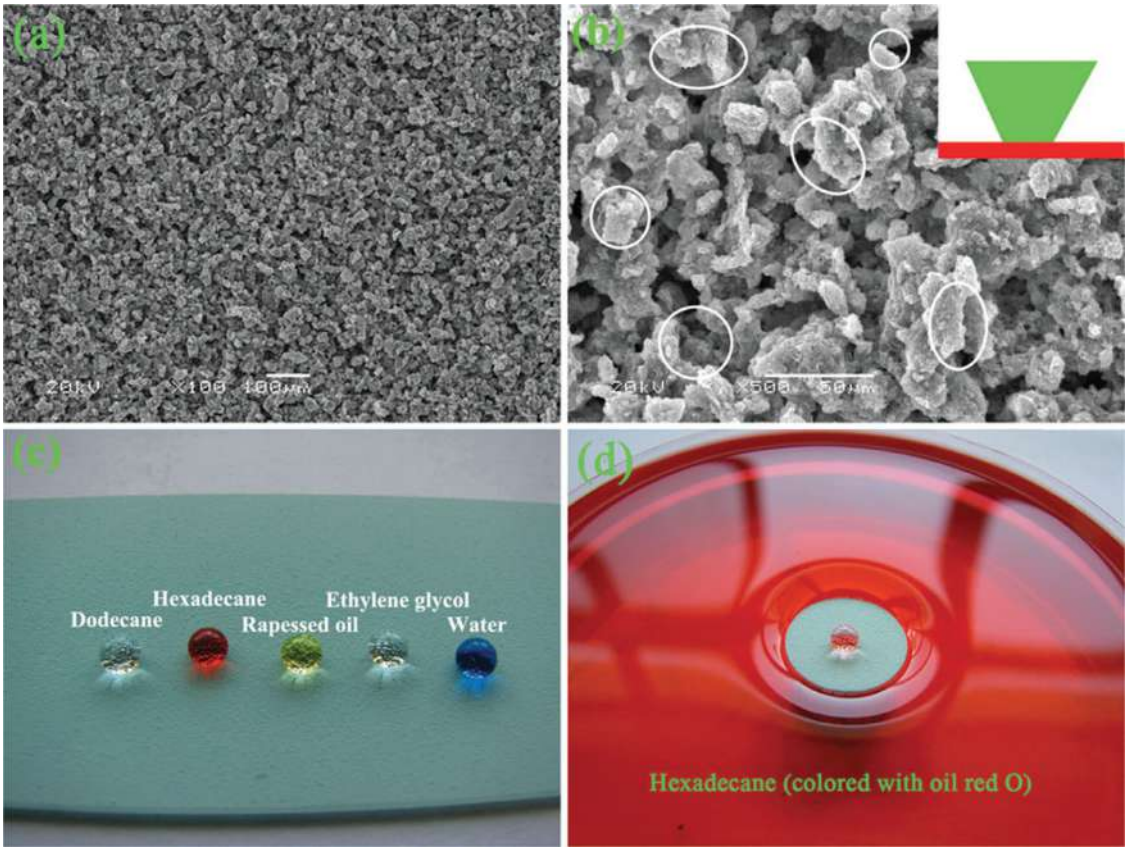

Fig. 30. SEM images of the copper perfluorooctanoate coating at (a) low and (b) high magnification. The inset shows a schematic diagram of re-entrant geometries. (c) Droplets of water, ethylene glycol, rapeseed oil, hexadecane and dodecane on the superoleophobic coating. (d) The high hexadecane repellency of the superoleophobic coating when kept in a petri dish with hexadecane [140] (colored with oil red O). (For interpretation of the references to color in this figure legend, the reader is referred to the web version of this article.)

lowermost surface energy like dodecane and this is due to the obtained surface superoleophobicity. The shiny surface under the droplets is due to the presence of stocked air and also the formation of the solid-liquid-air composite interface.

4.2.11. Other approaches

Fundamental methods for the manufacturing of the superoleophobic coatings and surfaces have mentioned in previous sections. However, recently some other methods for the fabrication of superoleophobic surfaces have been introduced which these include the template method [194,272–274]. In this method, natural or structural synthetic materials can be used as a template for the fabrication of superoleophobic surfaces with a hierarchical structure. The next method is pyrolysis [275,276] and chemical vapor deposition (CVD) [277] which is a chemical technique used for the fabrication of solid materials with high purity and high performance, and have been used for the fabrication of superoleophobic surfaces. Other processes that have been implemented in order to fabricate superoleophobic surfaces include laser processes as a novel method for the fabrication of surfaces with specific topology [278–280]. This is a single-step and environmental-friendly method in which the surface structure can be controlled by manipulating the parameters involved in the process. Casting has also been implemented in order to fabricate superoleophobic surfaces [281]. The summarized results of the recent fabricated superoleophobic surface are given in Table 2.

5. Applications of superoleophobic coatings

As the advancement of the industry and an increasing requirement for the surfaces with special wettability, the necessity of the superoleophobic surfaces has been grown. In this section, the most important applications of the superoleophobic surfaces are presented. The most important application of superoleophobic surfaces is schematically summarized in Fig. 31.

5.1. Fabrication of transparent coatings

A widespread of studies have been focused on the superamphiphobic coatings. Optic surfaces which possess the ability to repel several types of liquids are a suitable candidate for the applications in various technologies such as self-cleaning solar panels, antifreeze windows, anti-wind coatings in the automobile industry and aerospace, and anti-smudge touch screens. If the superamphiphobic surface were to be transparent, their structural size should be smaller than the visible light wavelength. Therefore, all of the longitudinal scales should be 300 nm or less. Almost every researcher in this section used SiO_2 particles due to its unique hydrophobicity on the surface and the capability of passing visible light wavelength through itself. Mazumder et al. [305] reported a surface with high transparency (93.8% visible spectrum transmission, 1% diffraction and 0.5% reflection). The surface was made-up by a mixture of dewetting and reactive-ion etching (RIE) processes (the primary nanopillars) on a glass surface and via combustion chemical vapor deposition (CCVD) (branches of secondary nanoparticles). At the final step, a layer of fluorosilane was applied on the specimens.

Coating transparency is needed by several uses of liquid-repellent surfaces. In this regard, polydimethylsiloxane (PDMS) along with a scalable and easy method of production were applied by Martin et al. [98] to generate transparent superoleophobic surfaces. A superoleophobic binder/nanoparticle coating was formed by adding

Table 2
A summarization of recent fabricated superoleophobic surface.

Matrix	Coating materials	Methods	Surface structure	OCA	Oil	Ref
Stainless steel mesh	PDDA/halloysite nanotubes	LBL assembly	Hierarchical structure	U151.5∘	Chloroform	[131]
Copper Mesh	TiO_2/CuO	Electrochemical anodization and LBL self-assembly	Hierarchical structure	U162°	Dichloromethane	[282]
Copper mesh	$CuWO_4/Cu_2O$	Electrochemical anodization method	Hierarchical cauliflower-like structure	U156°	Dichloromethane	[283]
Copper mesh	Zn/ZnO crystal	Electrodeposition method	Flower-like hierarchical structure	U155.6°	DCE	[201]
Sapphire	–	Femtosecond laser	Micro-line-patterned nanostructures	U153°	1, 2-dichloroethane	[284]
Brass wire mesh	Zinc oxide nanorods	Electrodeposition and hydrothermal reaction	Hierarchical structure	>U150°	Various oils	[285]
Stainless steel mesh	TiO_2	Spray coating	Rough nanostructures	>U150	Various oil	[286]
Steel mesh	Co_3O_4	Hydrothermal method	Needle structure	U154.8°	Gasoline	[287]
Stainless steel mesh	$BiVO_4$	Immersion followed by calcination	Micro/nanostructure	U168°	Diesel	[282]
Stainless steel mesh	TiO_2 nanofibers	Hydrothermal method and Spray coating	Micro and nanostructure	U162°	1,2- dichloroethane	[288]
Copper mesh	TiO_2/CuO	Anodization and LBL self-assembly	Hierarchical nanostructures	162°	Dichloromethane in aqueous media	[289]
Stainless steel mesh	Chitosan	Spray coating	Micro/nano hierarchical structure	159°	Unreported	[282]
Silk textiles	Siloxane + SiO_2 composite	Spray coating	Microscale clusters with nanostructures	159∘	Olive oil	[290]
Aluminum surface	–	Femtosecond laser	Hierarchical rough microstructure	U157°	1,2-dichloroethane	[291]
Titanium	TiO_2	Chemical acid etching and anodization	Hierarchical microhorn/nanopore structures	156.4 °	Hexadecane	[292]
Aluminum	PDES	Two-step chemical etching process + fluorosilane dip coating	Hierarchical micro/nanostructure	157	Ethylene glycol	[293]
Various substrates	ZnO	Ultraviolet nanoimprint lithography with hydrothermal synthesis	Hierarchical structure	159°	Diiodomethane	[294]
Copper mesh	$Cu(OH)_2$ nanowire-haired membranes	Chemical-based oxidation method	Micro/nano-hierarchical structure	U155 °	1, 2-dichloroethane	[295]
2J85 ferromagnetic alloy	–	Hydrofluoric acid etching	Reentrant micro/nanometre-scale rough structures	151°	White oil	[296]
Polyacrylonitrile (PAN) nanofibrous membrane	SiO_2/NFM	Electrospinning and electrospraying methods	Hierarchically structured skin	> U158°	Various oils	[297]
Glass	PFOTES-SiO_2/SiO_2 nanoparticles	Sol-gel method and spray coating	Re-entrant structure	164°	Glycerol	[6]
Zinc plate	Zinc perfluorocarboxylate	Solution-immersion	Petal-like microstructure	155.6°	Unreported	[298]
Si wafer	SiO_2/silane	Wet etching process	Grooved mushroom structure	159°	Hexadecane	[299]
Glass	Fluorinated silica nanoparticle	Sol–gel process and spin-coating process	–	158.6	Diiodomethane	[300]
–	VTMS-VMDMS marshmallow-like gel covered with perfluoro-alkyl groups	Sol-gel process and the thiol–ene click reaction.	Co-continuous macroporous structure	151	n-hexadecane	[166]
Ti alloy	TiO_2	Electrochemical etching	Hierarchical micro/nano structures	U158.9°	Dichloromethane	[301]
Various substrates	Fluorinated ZnO	Ultraviolet nanoimprint lithography with hydrothermal synthesis	Hierarchical structure	>155°	Diiodomethane	[302]
Aluminum foil	PTFEMA fibers	Electrospinning Without Functionalization	Re-entrant structure	154.2	Hexadecane	[303]
Gold plate	$Polyedopc_3f_6$	Electropolymerization	–	152.2	Hexadecane	[303]
Glass	TiO_2 nanostructures	Electrospinning	Rice like structure	138.5°	Hexadecane	[304]

Table 3
The summary of literature about transparent superoleophobic surfaces.

Substrate	Coating technique	Coat	Optical transmittance reduction	Water droplet Surface tension ($mN.m^{-1}$)	CA (°)	CAH (°)	SA (°)	Ref.
A4 paper	Spray coating	Fluorinated SiO_2 nanoparticle suspensions.	43%	72.8	168	< 1	< 1	[307]
Glass	CCVD	Branching nanostructures and nanonodules	< 0.5%		170		< 4	[307]
Master-molded polydimethyl siloxane (PDMS) pillars	Spray coating	1H,1H,2H,2H -heptadecafluorodecyl polyhedral oligomeric silsesquioxane (F-POSS)		10	155			[308]
Steel		Silica – Fluoropolymer Hybrid Nanoparticles	40%		150			[309]
Glass	Spray coating	5 layers of a 20 nm silica nanoparticle, 2 layers of an 80 nm hollow silica nanosphere, and 3 layers of a mesoporous silica nanosheet			171		< 1	[310]
Glass	Spray coating	Carbon nanotube/SiO_2			165		< 1	[311]

fluorination through fluorosilane. As presented with flat PDMS, the polymer is inherently transparent. For the superhydrophobic samples, transparency enhancement through the micropatterning and not the binder/nanoparticle coating leads to the decrease of transparency. However, transparency for the fluorination step is slightly reduced due to the adding of a small thickness level by the fluorination, compared to the binder/nanoparticle layer. Chen et al. [306] has developed transparent, pH-responsive inverse opal film via the oil-water interfacial self-assembly method. As is shown in Fig. 32, the whole procedure is depicted in order to build a transparent small surface.

5.2. Corrosion resistant coatings

Another major property of the superamphiphobic surfaces is their corrosion resistivity. Due to this fact, many studies have been done on the deposition of these coatings onto the metallic surfaces. In recent years, there are several reports about the superamphiphobic surfaces which are applied to iron [312], copper [249,313,314], zinc [315], aluminum [316–319], titanium [320], and other alloys [321–323] and metal oxides [324]. Yuan et al. [312] have successfully deposited superamphiphobic coatings onto the iron by preparing several acidic baths and a perfluorocarboxylic acid bath at the end. No pieces of rust observed in a normal environment after 6 months, since the superamphiphobic had applied onto the iron specimen. Fig. 33(a) indicates the SEM image of cast iron without the coating and (b) is the SEM image of the coated cast iron by acetic acid and H_2O_2.

Hao et al. [325] have made-up CuO hierarchical flower-like structures which looked like to the surface morphology of the lotus greenery on X90 pipeline steel substrate. potentiodynamic polarization measurement designated that the superamphiphobic CuO film clearly enhanced the corrosion resistance of the X90 pipeline steel. This coating has been achieved through two steps consisting of Cu electrodeposition, and fluorinated modifications. A major application of superoleophobic surfaces is underwater oil trapping or water/oil separation which is discussed next sections. Su et al. [326] have developed an Ag nanoparticles coating using HF immersion for etching and then specimens were immersed in STA solution. Anti-corrosion feature may depend on the mechanical steady stainless steel mesh, the hierarchical structure coated via Ag nanoparticles and the superhydrophobicity.

5.3. Self-cleaning surfaces

The self-cleaning surfaces first discovered with the investigation of blue lotus microstructure in 1970, which in spite of a smooth appearance, has nano- or micro-scale roughness. The self-cleaning phenomenon depends on the contact angle, therefore the self-cleaning surfaces are divided into two class, superhydrophilic and superhydrophobic. The superoleophobic surfaces can be classified along with the superhydrophobic surfaces.

Brown et al. [246] fabricated a transparent self-cleaning surface using a film with fluorinated compounds and copolymers. In this study, the settlement of water-oil on the surface was enhanced by controlling the surface roughness and also the self-cleaning ability was shown by the oil and water droplets and calculating the receding contact angle of the hexadecanes.

Xiong et al. fabricated a series of polymers via consecutive anodic polymerization [332,333] and the method of atomic transfer radical polymerization (ATRP) [334–336]. They also used PIPSMA blocks to enhance the coating by sol-gel method and PFOEMA copolymers for the preparation of surfaces with low tension. These two copolymers have been utilized for the fabrication of various amphiphobic coatings, either singular [333] or in combination with silicate nanoparticles. The obtained coatings could maintain their properties after 50 cycles of machine wash.

Xiong et al. [337] fabricated a superamphiphobic coating on the glass and cotton fabric via spray-deposition method and

Table 4
Summary of results of literature about the application of superoleophobic surface in corrosion resistance.

Substrate	Coating technique	Corrosion behavior enhancement	Water droplet Surface tension ($mN.m^{-1}$)	OCA (°)	SA (°)	Ref.
Zn	Chemical methods	Improved		152	<10	[327]
Co	Deposition	97%	72.1	166	<5	[328]
TiO2	Epoxy	Improved		155		[329]
Al	Spray coating	Improved		173	<1	[330]
X90 Stainless Steel	Electrodeposition	95%		152	14	[325]
Stainless Steel	Solution-casting method	Improved		150	<10	[331]
Metal or glass slide	Solution-casting method	Improved		167		[325]

photopolymerization of resins including SiO_2 nanoparticles and perfluorinated thiols. The obtained coating exhibited adequate thermal and chemical resistance. Another study on spray coating was done by Muthiah et al. [338] in order to fabricate a superamphiphobic and mechanically-durable surface on the glass. The obtained surface showed anti-smudge properties, too. The spray coating was composed of SiO_2 nanoparticles and fluoropolymers. The anti-smudge property was measured by cleaning the coating which has artificially contaminated, by employing an oil-impregnated cloth. Recently, another group of researchers have developed chitosan (CS)/poly(vinyl alcohol) (PVA) coatings cross-linked with glutaraldehyde (GA) [339]. The most important aspect of this coating is it's underwater self-cleaning and durability. It was realized that the procedure of immersing the CS/PVA coatings into NaOH solution was vital to improve rough structure on the coating surface. Peng et al. [186], has fabricated superoleophobic aluminum developing nanoretcula nanostructures on aluminum surface. The superoleophobicity was achieved by trapping of air inside hierarchical micro/nanostructure. As is shown in Fig. 34, after the rinsing process, there were still a few particles lasting on the nanostructured surface, although the microstructured and hierarchical surfaces became totally clean. These results prove that the microstructured and hierarchical surfaces provide more effectiveness contaminant elimination capacity in comparison with the nanostructured surface.

The summary of the results of literature about the application of superoleophobic surface in fabrication self-cleaning surface is shown in Table 5.

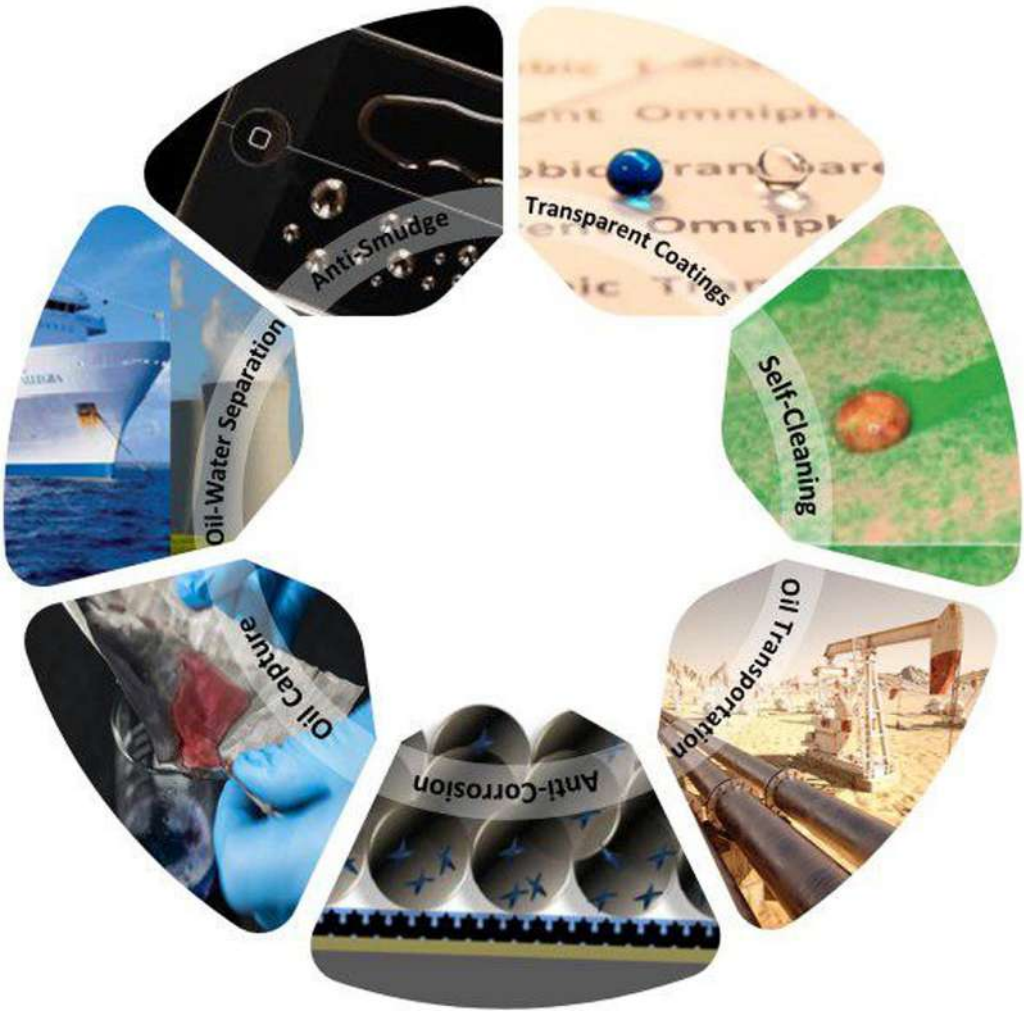

Fig. 31. Schematic of various application of superoleophobic surface.

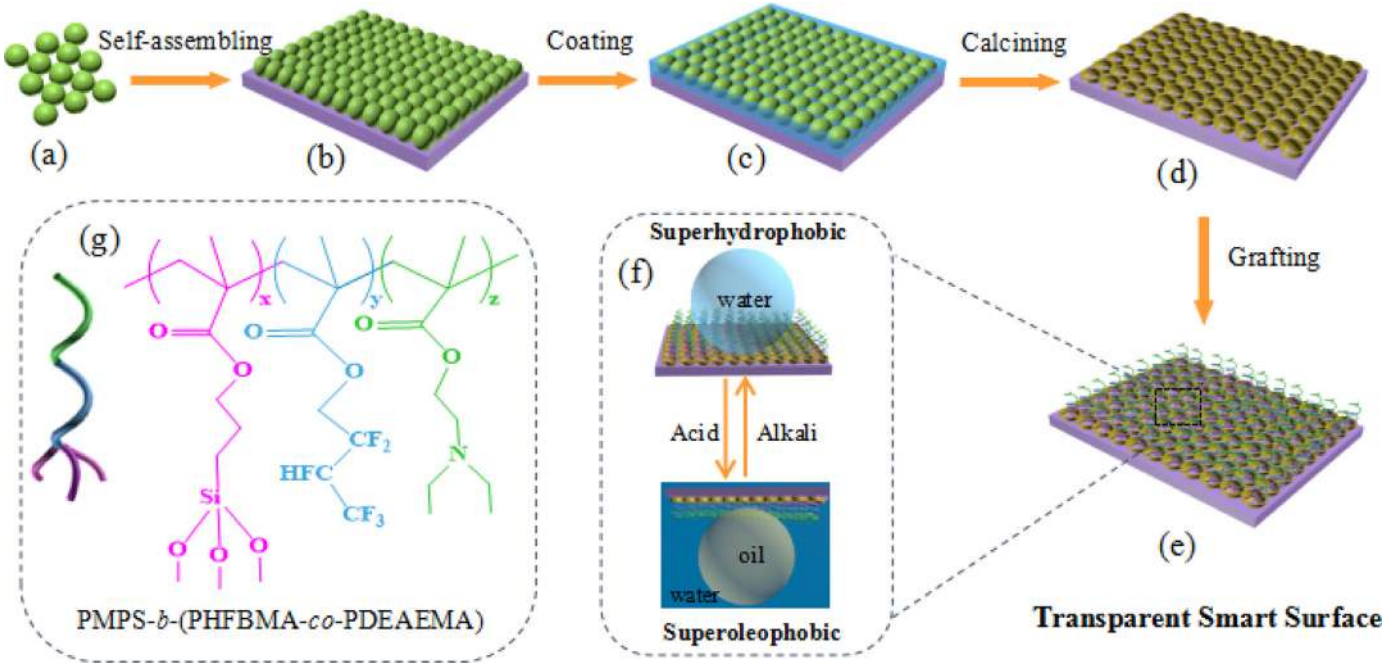

Fig. 32. The preparation and property of the transparent smart surface. (a) PS spheres; (b) PS spheres self-assembled on the surface of the substrate to form a monolayer; (c) the colloidal monolayer was backfilled with MANUSCRIPT the solution of TEOS; (d) the organic colloids was calcined to obtain an inverse opal film composed of silica; (e) the surface was modified by the copolymer PMPS- b -P(HFBMA- co -DEAEMA) to form the transparent smart surface; (f) the reversible transition between superhydrophobicity and underwater superoleophobicity of the transparent smart surface; (g) the molecular structure of the copolymer PMPS- b -P(HFBMA- co -DEAEMA) [306].

5.4. Separation/filtration of gas, oil, and non-oil aerosols

The porous superamphiphobic particles have many applications in the filtration fields. The first group of filtration is for gaseous particles. The main challenge in this matter is to reach the high transmission rate along with the prevention of embrittlement and clogging the filter pores. Wei et al. [340] have developed a novel method enhancing the filtration effectiveness for separation of minor oil mists from the air without speciously increasing the air flow resistance. Through a chemical procedure using a perfluoroalkyl acrylic copolymer, they have successfully increased the filtration effectiveness for minor oil mists from 96.40% to 99.44%, while the pressure drop is increased only by 6% but the downstream oil mist content is decreased by 85%.

The second class of filtration was introduced by Wang et al. [341]. In this performance, filtration of the oil and non-oil aerosol particles is carried out by employing a nanofibrous membrane synthesized from electrospun polyacrylonitrile/PU nanofibres and fluorinated PU.

Separation of oil and water by the superamphiphobic filters is introduced in the third class. Currently, an intelligent coating has been generated by Xu et al. [342] with the application of the combination of heptadecafluorononanoic acid containing TiO_2 sol and silica nanoparticles applying the dip-coating method. Separation of oil and water is made possible when the coating owns the superhydrophilic and superamphiphobic features through the exposure of the attained coating upon ammonia. Moreover, the coating can be exploited for several compounds, including PU sponges and polyester fabrics. The pre-wetting technique that can eliminate water from the light water-oil combination and suspensions by gravity in a discriminatory manner was exploited by Ge et al. [297] to generate a water-oil separator which has multiple functions. Applying SiO_2 nanoparticles, a paper cloth was spray coated to generate the superamphiphobic separator. Currently, gaseous oil method or discriminatory clarification of liquid, gas and water has been developed by a number of researchers [343]. Generally, the approach is exploited to assess the wettability of three-dimensional graphene foams. As is shown in Fig. 35, three separate surfaces has been developed with a different condition to allow gas, water or oil to pass.

5.5. Oil transportation

There have been some reports that the smart superamphiphobic coatings are able to manipulate oil droplets with the degree of adhesion or external stimulation. These surfaces have applications in localized chemical reactions, drug delivery, ultra-small laboratory chips and etc. Huang et al. [344] fabricated superamphiphobic surfaces with TiO_2 nanoparticles via a combination of anodizing and self-assembly technique along with the surface fluorination at the end. The micro-pattern process of the surface was carried out by covering the surface with water-proof alcohol-based ink. Finally, the adhesion of the covered and uncovered surfaces with ink was greatly different and a few images of the droplet manipulation, sensitizing, and site-selective cell immobilization was displayed. Zhou et al. deposited perfluorosilane monolayers using ultraviolet (UV) light and found that it leads to the enhanced wetting properties however; this method requires special types of equipment and strong power supply. Fig. 36 shows a comparison between two methods of the patterned superamphiphobic surface preparation.

Kang et al. [345] fabricated anisotropic micro-grooves with directional oil sliding property which is inspired from rice leaf. With patterns of prism and rectangle which are fabricated via UV-assisted micro molding procedure using a combination of photoinitiator and acrylate functionalized prepolymer consisting of Al_2O_3 nanoparticles. The surfaces with arrays of overhang lines were capable of oil anisotropic sliding on the surfaces according to the measured contact angle (CA) and sliding angle (SA $<$ 20) for the mineral oil droplets and photoresist. Zhang et al. [150] have developed an antigravity oil gathering and transportation underwater driven mostly by the surface energy release of oil droplets. this underwater antigravity superoleophobic “pump” can unceasingly carry oil from water/oil phase to air/oil phase, which can meet the necessities for the large-area oil gathering in an oil spill. Also Xu et al. [342] fabricated dual superoleophobic polyimide films

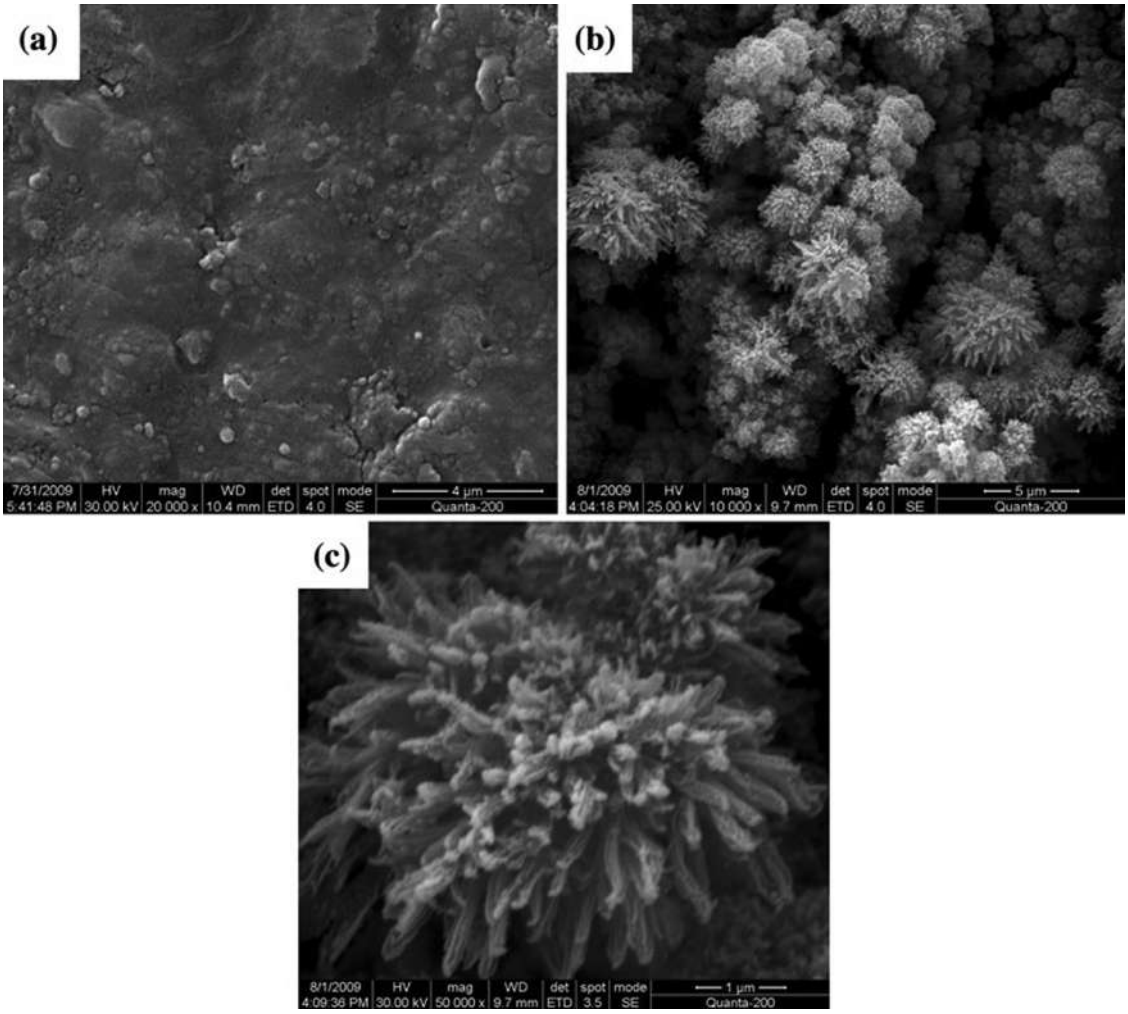

Fig. 33. SEM images of (a) untreated common cast iron substrate surface, and (b) the acetic acid/H2O2-treated common iron substrate surface; (c) is the higher magnification than (b) [312].

and a stainless steel mesh using a simple one-step hydrothermal approach. The most important aspect of this study is the simplicity of the method which led to fabrication of dual superoleophobic materials in various oil—water system.

Another technique to achieve oleophobicity is through using a liquid-liquid interface instead of the complex solid-liquid interface which has been described previously. In these case, usually, there is a need for a perfluorinated lubricant in which all of the classic lubricants has the hydrophobic property and other liquids repellency except oil. The chemistry of the fluorine which has been spoken about would lead to the oleophobicity. When a porous or patterned surface in micro-scale is used, it is possible to increase the surface adhesion to its maximum capacity, if the designing has been done accurately. In the end, by keeping the lubricant inside the pores, the lifetime of the surface could be increased. The chemical similarity of the lubricant and the material could also improve its adhesion. In contrast to the superoleophobic surface, the lubricant surface is very smooth and the oleophobicity of the surface is not related to the surface pattern, but it's dependent on the forces among lubricant and oil. Commonly these have smaller static CA and similar dynamic to the superoleophobic surfaces. Therefore, the oil droplets on these surfaces which will form angles smaller than $\overset{\circ}{5}$, will be sliding.

The concept of oil-lubricated pores was first described by Wong et al. [346] which was called "Slippery Liquid-Infused Porous Surfaces" (SLIPS) that were inspired by pitcher plants which imprison prey with the peristome [347]. Table 6 includes development, advances and SLIPS surfaces applications that show significance and applicability of them.

The main scheme is to fashion a large-area surface texture by means of micro- and/or nanoscale structures that can be merged with a totally wetting nonvolatile lubricating liquid which is also hydrophobic to water, therefore, avoiding the lubricant from being moved. Having a great surface area of this textured surface leads to the captivation of the lubricant into surface pores and to spread into and be held by the surface while also creating an unchanging thin film through the surface. In this condition, a water droplet stays on the lubricant film, consequently, completely eliminating direct contact amid the droplet and the solid surface and the associated contact angle hysteresis which l leads to contact line pinning [356]. It should be noted that the efficiency of liquid-repellent property of is not instigated from the nano/microstructures but the thin film of lubricating liquid on the top of the nano/microstructured layer, the chemically consistent and physically flat lubricant film on the surface outcomes in a low CAH and SA. This allows water and organic droplets to simply move on the surface even with the CA much lesser than 150° SLIPS then shows both slippery and omniphobic features.

5.6. Oil capture

The leakage of oil into the sea or into deeper sections can result in serious ecological problems [357]. Specific methods and technique must be used for the separation of the oil that will be spilled into the sea

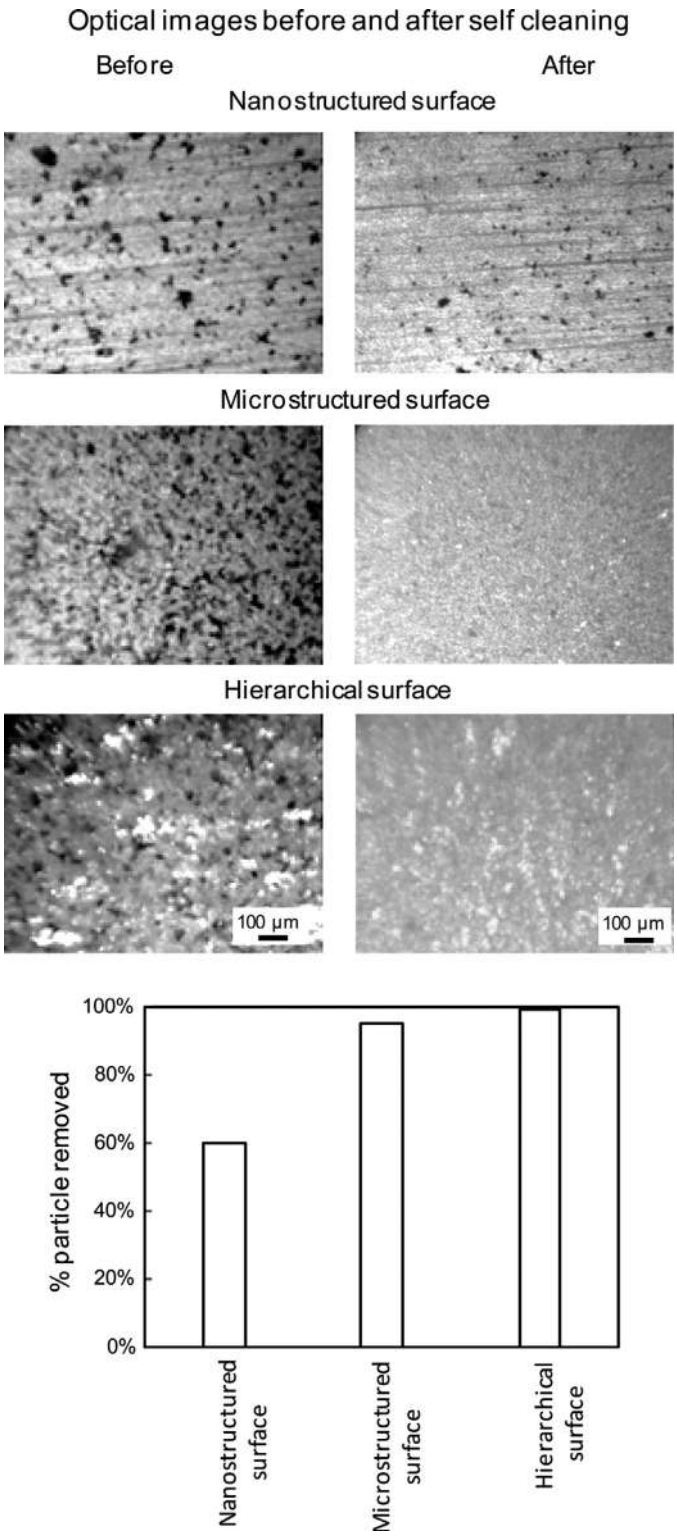

Fig. 34. Optical microscope images of the samples, including the nanostructured, microstructured, and hierarchical surfaces before and after self-cleaning experiments. silicon carbide (SiC) nanoparticles were removed partially from the nanostructured surface, while the microstructured and hierarchical surfaces become totally clean after the experiments. Particle analysis software was used to quantify particle removal [186].

[358]. In general, there is a need for an eco-friendly, oil or other liquids absorbent in high amounts, ultra-lightweight, stable and durable mechanism [359]. Recently there have been many studies on the oil capture and oil transportation through an aqueous environment [1,335,357,358,360–372]. Chen et al. [373] successfully fabricated oil-repellent surface inspiring from the robust anchoring ability and easy availability of plant polyphenols. By altering tannic acid concentration in solution and also pH and temperature, they were able to fabricate diverse superoleophobic surfaces. Fig. 37 show various oil-repellent surfaces with different CA values which based on their application can be used in different environments to decrease oil pollutions Using a controllable oil-adhesion within the range of ultralow-ultrahigh, another group of researchers has generated a “mechanical hand” according to the glass surface that has a superoleophobic pattern [374]. A non-structured flat center circle domain with oleophobicity and intermittently organized designed micro/nano dual-scale rough domain with superoleophobicity are among the parts of the surfaces. We can tune the surface morphologies and relevant adhesions through changing the area ratio of the two, more specifically known as the center circle's diameter. This device can be applied to perform oil rapid capture, transportation, and fusion. Specifically, the mechanical hand can be exploited in the manufacturing of bioreactors, in-situ detectors, and microfluidic devices.

6. Perspectives on eco-friendly approaches

Green or Sustainable Chemistry is an idea that discusses the formation of chemical products and procedures that decrease or remove the usage and fabrication of unsafe substances. They have used entirely compounds and chemical procedures that do not have undesirable costs for the environment. It is grounded on a few principles that can be implemented to primarily produce or reproduce molecules, compounds, reactions, and procedures that are more harmless for human healthiness and the environment [375].

Even though strong researches have been prepared in the advancement of liquid-repellent surfaces, current surfaces display limited repellency to oils and are not totally or in some cases at all environment-friendly. Produced surfaces are continually accompanying with biological and environmental risks due to their poisonousness and non-biocompatibility of fluorochemicals. A perfect oil-repellent layer should have steady oleophobicity to various types of oils, have a duty to be able to be deposited in a guileless process on materials irrespective to their scope, form, or structure. And the chemicals implemented in the creation of the oil-repellent layer must be eco-friendly [376]. Overall, the improved omniphobicity of a surface are instructed because of the attendance of fluorine atoms. This usually is demonstrated when a substance’s C-H bonds are replaced by C-F bonds. The expansion and design are converting from the usage of chemical structures including Fluorine atoms to eco-friendlier substances and molecules. These hazards are dual: first, there is danger linked with the synthetic procedures in the production of suitable fluorochemicals where the compounds mixed and derivatives of these procedures are not reflected ’green,’ and second, the deterioration of such compounds (as well as artificial Perfluorooctanoic acid [PFOA or Perfluorooctane sulfonic acid [PFOS]) on final output, which may let the compounds to discover their path into the wide-ranging inhabitants by means of following bioaccumulation trails (contamination of water storages, polluting the food chain, etc.).

Almost every one of the methods that have been presented for the manufacture of oleophobic surfaces so far requires fluorinated materials. The perfluorinated compounds which contain eight or more carbons in their structure have caused some concerns about health issues and bioaccumulation in humans, biopersistence, remaining toxicity, even by partitioning, and nutrition issues [74,335,377]. In addition, even after the decomposition of these materials which take a long time, some the by-products would still be toxic like perfluorooctanoic acid [378–380] and perfluorooctanesulphonate [381]. alongside the long-chain fluorinated complexes issue, there are other worries as well in relation to the mentioned methods. Most of them require poisonous and flammable solvents and/or corrosive acids which can endanger the

Table 5
Summary of results of literature about the application of superoleophobic surface in fabrication self-cleaning surface.

Substrate	Coating technique	Coat	WCA (°)	UOCA (°)	Ref.
Stainless steel mesh	LbL	Sodium silicate and TiO_2 nanoparticles	20	165	[337]
Stainless steel mesh	dip coating	Copolymer-fluorosurfactant	<10	80	[338]
TiO2	LbL	Polyelectrolyte binder/SiO_2 nanoparticles/fluorosurfactant/ Polydiallyldimethylammonium chloride	<5	155	[326]
Fluorine-doped tin oxide	one-step hydrothermal method	Hierarchical rutile TiO_2 flowers	64	155	[327]
Stainless steel mesh	LbL	Poly (diallyldimethylammonium chloride)/halloysite nanotubes	68	145	[339]
Stainless steel mesh	LbL	Ultralong copper microwires/TiO_2 nanowires	<1	93	[340]
Stainless steel mesh	one-step solution-based coating method	Methyltrimethoxysilane	80	163	[341]

health of those who come in contact with them. Despite these issues, the eco-friendly methods for fabricating patterned surfaces, using long-chain fluorocarbon molecules, are still challenging and unsolved.

In this section of the review, the progress, challenges, and perspectives of the alternative methods for the fabrication in which have less risk of the used materials and the methods to achieve oleophobic properties on the surface are presented. These processes require using risk-free and non-flammable solvents, short-chain fluorinated complexes (C6 or less) or alternative materials free of fluorine atoms.

6.1. Shorter-chained fluorinated

Suggested to have the equal positive physicochemical properties deprived of the complications relating to toxicity in humans and wildlife, the shorter-chained C6-based greaseproofing agents have been currently applied by the industry as a replacement for C8-PFCs. Current studies have proposed the complete and quick excretion of C6-PFCs and their lack of accumulation in biological fluids [34]. Fabrication of superomniphobic surfaces that cause no harm to the environment has been carried out by short-chained fluorinated compounds, reported in other studies. In research by Milionis et al. [382], hydrophobic nanosilica and biodegradable thermoplastic starch composites were applied to fabricate superhydrophobic surfaces While not applied to oleophobicity, it is possible to attain roughness of the surface by different hydrophobicity and measures through the use of an easy coating done by spraying. In this research, an extra layer of the diluted C6 fluorinated chemical compound was sprayed, which resulted in the achieving of RA of 15° and a CA of 166° with oil. A short-chained fluorinated silane sol-gel mixture encompassing tetramethoxysilane (TMOS) and 3,3,3-trifluoropropyltrimethoxysilane was exploited by Park et al. [383] to create a transparent and flat surface with active oleophobicity for various alkane liquids. According to the mentioned scholars,

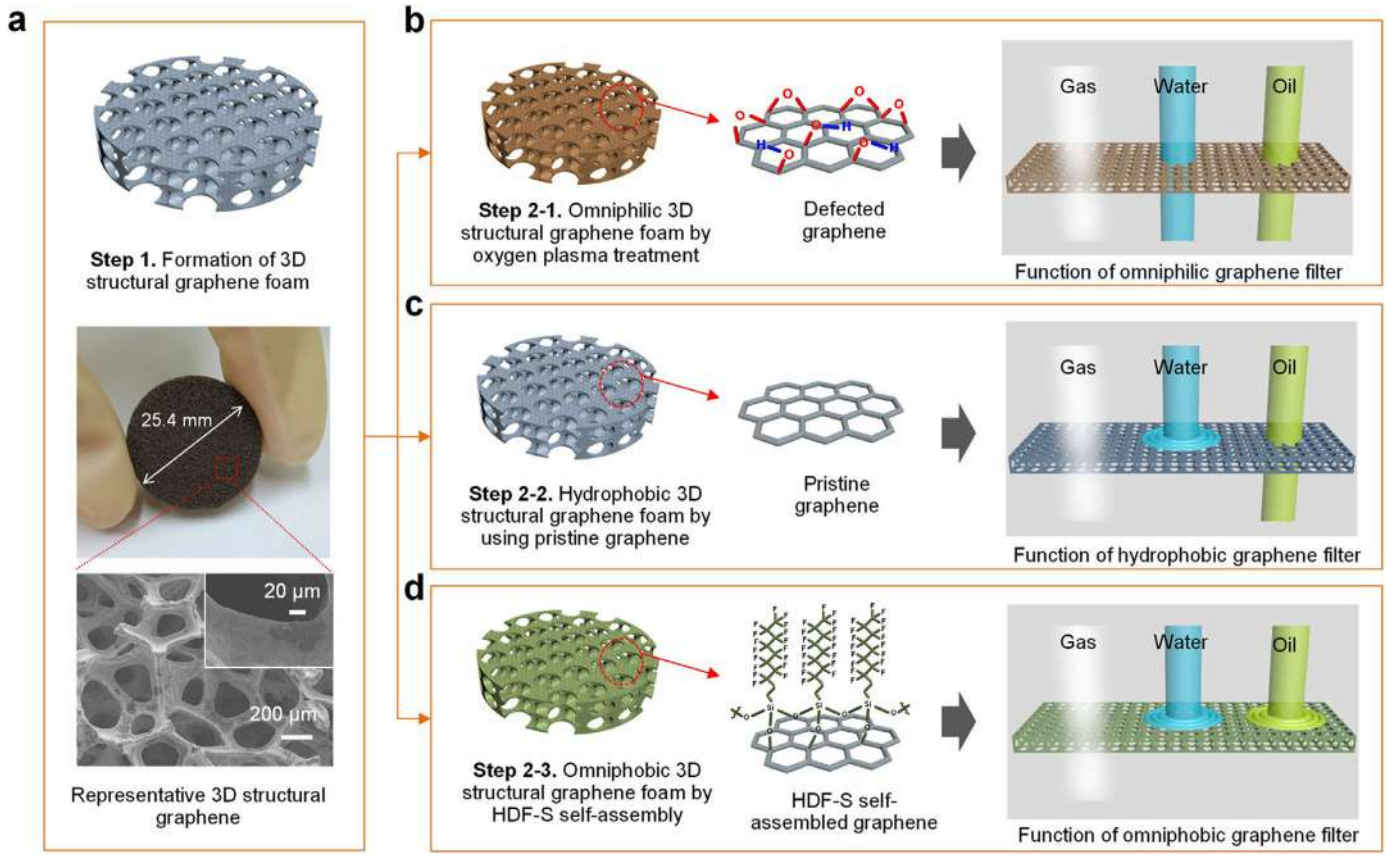

Fig. 35. (a) Photograph of a 3D structural graphene foam 25.4 mm in diameter. FE-SEM image of the graphene foam with an average pore diameter of 150–200 μm. The inset shows a higher magnification image of the surface of a single graphene wire, in which the graphene laminated on the fracture surface is clearly observed. (b–d) Schematic illustration of three different types of graphene by using surface treatment and their selective filtering properties [343].

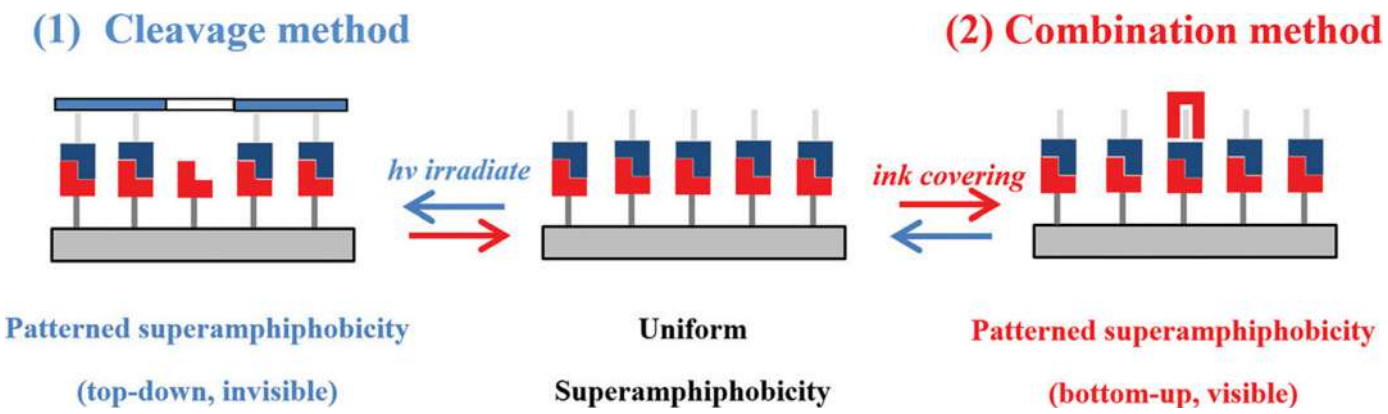

Fig. 36. Schematic illustrations of two contrary patterned superamphiphobicity process by the mechanisms of a top-down "cleavage method" (left) and a bottom-up "combination method" (right) [344].

application of TMOS exerts significant impacts on the formation of a homogeneous/continuous film and enhancement of dynamic wettability for different alkane liquids. To reduce the biodegenerative impacts of long and linear perfluorocarbon chains, El-Maiss et al. [384] studied the possibility of using branched perfluorocarbon chains instead of the mentioned type of perfluorocarbon chains.

In order to prepare superoleophobic nanocomposites through the application of fluoroalkyl end-capped vinyltrimethoxysilane oligomer/calcium silicide nanocomposites by the technique of sol-gel, Saito et al. [385] corresponded calcium silicide particles with fluorinated oligomer reaction under alkaline conditions. According to the results, a pyrolytic product was generated by mixing these nanoparticles with calcium fluoride by calcining at 800°C. This shows that a new environmental cyclical type-fluorine recycle system can be created due to the capacity of these composites.

6.2. Other substitution

Saifaldeen et al. [380] fabricated aluminum with a textured surface without using any type of chemical and toxic materials. The surface was prepared via machine-driven sanding (micro-roughness) and boiling water method (nano-roughness). At the final chemical treatment, fluorinated silane was used for the fabrication of nano-textured surface which led to a superamphiphobic surface along with the two methods that have mentioned. This group of researchers carried out the boiling water treatment onto a copper layer. Relaying on the time of being exposed to boiling water, achieving a variety of topographies was possible starting from cubic-like *CuO* to leaf-like *CuO* nanoparticles.

In the last part, there are some studies which prove that the oleophobicity can be reached even without using the fluorine-containing compounds. Urata et al. [386] fabricated a hybrid film on the surface via a simple process of sol-gel centered on cohydrolysis and co-condensation of a combination of a series of alkyltriethoxysilanes with a various number of carbon atoms in its chain, from 3 to 18. Unexpectedly, once carbon atom numbers of an alkyl chain were 10 or less, the obtained hybrid film was very even, greatly translucent and showed insignificant CAH formed with several alkane droplets (hexadecane, dodecane, and decane), even their static CA was small (20–40). In these hybrid surfaces, the alkane droplets could readily move without pinning, in small deviation angle (< 5). Alternatively, as the number of carbon atoms increases above 12, both the transparency and the probe mobility will decrease. The TMOS molecules play a crucial part in the creation of continuous films (as a binder) and also act as an amplifier of the long-chain alkyl flexibility (as a molecular spacer), which will lead to a smooth and liquid-like surface. This group of researchers found out the reason behind the mobility amplification of the alkane droplets, was its relationship with the dielectric constant. Rohrbach et al. [387] fabricated hydrated hydrophobic, oleophobic cellulose-based filters which are utilized in the water-oil separation. In this process, the filter was coated by a layer of nanofibrillated cellulose hydrogel via the dipping-drying method and the hydrophilic behavior of the hydrogel layer was benefited. This mechanism would lead to the formation of a filter with a hydrated layer absorbing. A threefold interface formed of a hydrogel layer, water and oil will enhance the oleophobicity. The hydrogel roughness will cause water to get trapped in microscopic valleys. Considerable difference of the surface energy between water and oil will prevent oil permeation into the filter. Both water and oil permeation through the filter are possible without the coating. By hydrating this coating, the oleophobicity will be achieved without using the traditional functional groups. The hydrophobic/

Table 6
Development, advances and SLIPS surfaces applications.

Authors	SLIPS surfaces advancements
Wong (2011) [346]	Slippery Liquid-Infused Porous Surfaces (SLIPS) introduction which was inspired by pitcher plants
P.Kim (2013) [348]	It was learned that the boehmite nanostructures are the most real parameter on the liquid-repellency property which are derived from the aluminum or alumina coating fabricated via sol-gel
Zhang (2014) [349]	By controlling the evaporation process, it is possible to achieve a variety of adhesion degrees (oleophobic and slippery, adhesive and superoleophobic and lotus leaf-like superoleophobicity).
Daniel (2014) [350]	the liquid-repellency was successfully controlled by adjusting the lubricant temperature and viscosity.
Yeo (2014)	Fabrication of flexible, transparent SLIPS.
Sunny (2014) [351]	Preparation of nano-scale SLIPS using LBL method using positively charged polyelectrolytes and negatively charged SiO_2 nanoparticles
You (2014) [352]	Development of the device which can control the movement of droplets with low surface energy on areas of the omniphobic SLIPS. In contrast to the old PDMS-based microfluidic devices, due to its compatibility with organic solvents, this device is capable of performing organic reactions.
Yang (2015) [353]	proved that the SLIPS fabricated on the low alloy steel can afford an effective self-standing layer to protect the steel substrate.
Zhang j. (2017) [354]	Fabrication of a SLIPS coat on Mg alloy with anti-icing performance
Kuan-KaiTseng (2018) [355]	Fabrication of the highly-transparent slippery surfaces with omniphobicity developed from porous superhydrophilic nanoparticulate thin films through hydrophobization and liquid lubricant infusion.

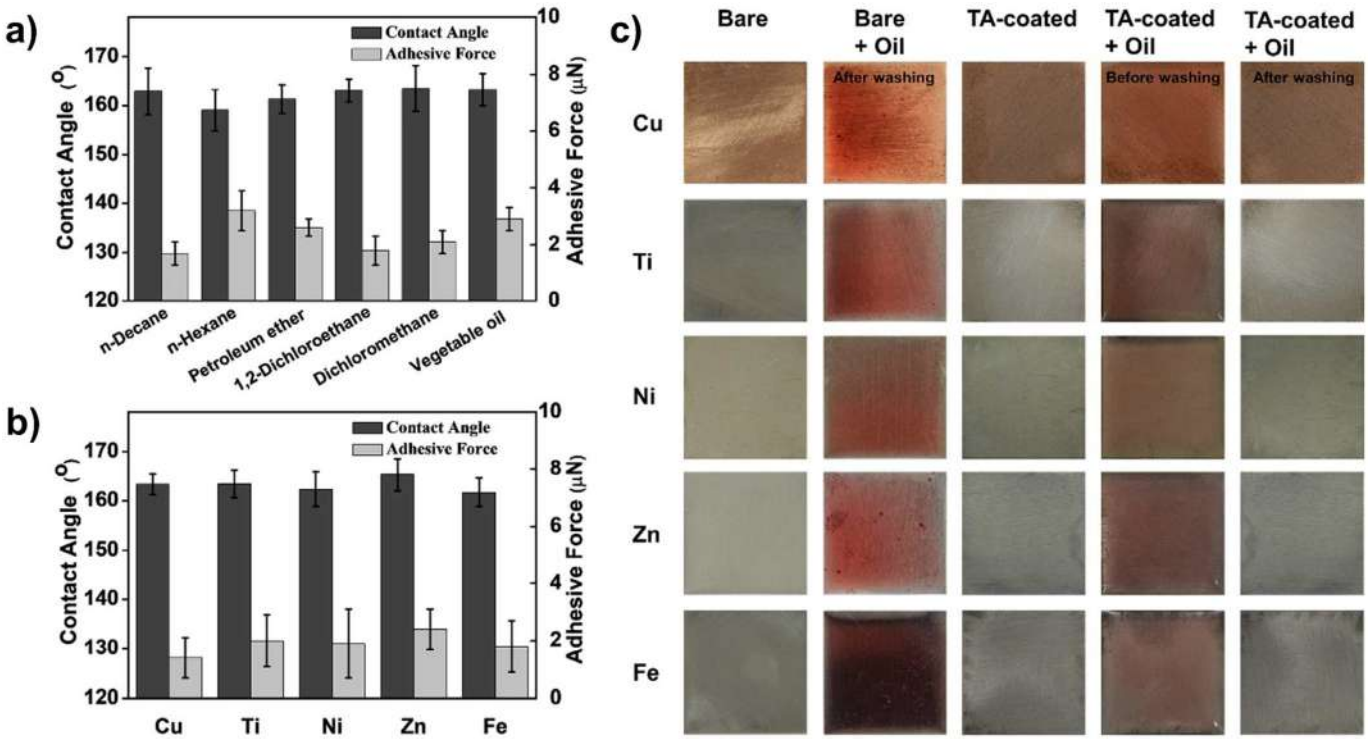

Fig. 37. A general strategy to fabricate underwater superoleophobic surfaces with ultra-low oil adhesion for different oils and metal sheets. The underwater superoleophobicity and ultra-low oil adhesion of (a) different oils and (b) various TA-coated metal sheets. (c) Digital images show that there is no residual oil (silicon oil dyed by oil red O, viscosity = 14,000 CST) stained on the TA-coated sheets after washing by water compared with the bare sheets, revealing the excellent anti-oil adhesion property [373]. (For interpretation of the references to color in this figure legend, the reader is referred to the web version of this article.)

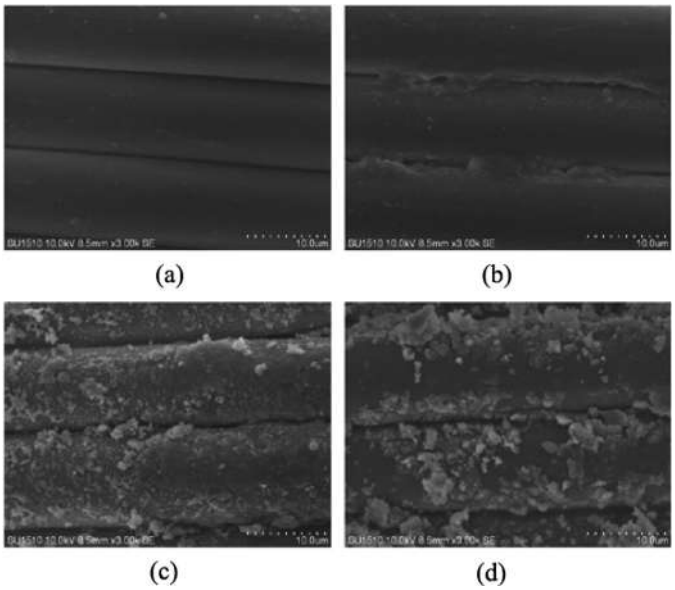

Fig. 38. Surface morphology of nylon fabric: (a) untreated, (b) BTCA treated, (c) BTCA–TBT treated, and (d) BTCA–TBT–OA treated. (note: BTCA 2%; TBT treatment: TBT: acetic acid = 1:0.6 in mole, TBT:H2O = 1:8 in mole, TBT : ethanol = 1:90 in mass, reaction time 2 h; OA treatment: OA 4%, NH4OH 1%, fabric was cured for 5 min at 110°C) [388].

oleophobic behavior is achieved by incorporating differences in characteristics and structures of the cellulose in both microscopic and nanoscopic scale, without using any detrimental chemical materials. In another research by Du et al. [388], they fabricated omniphobic surfaces via treatments including tetrabutyltitanate (TBT) and octadecylamine (OA) which have increased the surface roughness and reduced the interfacial energy. It was also observed that by increasing possible reactive sites and with 1,2,3,4-Butanetetracarboxylic (BTCA) acid, the hydrophobicity will be enhanced. As shown in Fig. 38, there are considerable differences in the surface morphology of BTCA- and TBT-treated and untreated samples [389].

Underwater superoleophobic films for oil/water segregation have made excessive development. However, there are still a few trials in this modest manufacturing of low-cost and eco-friendly membranes with underwater superoleophobicity. Wang and Wang [390] a facile $NaClO_2$ treatment which can fabricate an eco-friendly superoleophobic surface. The advanced textile can be implemented as a gravity-driven oil/water separation filter with high efficiency (>92.8%). Moreover, Hou et al. [391] have fabricated a unique stainless topology using PDDA/halloysite nanotubes which can perform a good oil/water separation in underwater conditions. The hierarchical arrangement and roughness of the PDDA/HNTs coating surface were organized by regulating the amount of layer deposition.

7. Conclusion

In this paper, we tried to build a comprehensive review of recent progress and fundamentals of the superoleophobic surfaces' requirement for fabrication, examination, evaluation, fabrication methods, and application. Due to the lower surface energy of oil, it is tough to manufacture superoleophobic surface in comparison with the superhydrophobic surfaces. According to these complex requirements, only a few surfaces have been reported with the superoleophobic property. Thus, recent progress in designing, fabrication, and maintaining on superominophobic surfaces were investigated and thoroughly reviewed. According to the results of recent researches, number of progresses in fabricating superoleophobic surfaces such as sol-gel, etching, lithography, electrodeposition of conductive polymers, electrospinning, LBL assembly, solution-immersion, hydrothermal, anodizing, and spray coating alongside to the contact angle of each method were reviewed.

Due to the special characteristic of the superoleophobic surfaces, these surfaces have been found numerous applications such as fabrication of transparent coatings, application in fabricating corrosion resistant coating, application in fabricating of self-cleaning surfaces, SLIPS, oil/water separation-filtration, oil transportation, and oil capture were studied in details in this paper. Also in this review paper, perspectives on eco-friendly approaches to fabricate superoleophobic surface was reviewed. The expansion trend of superoleophobicity may encounter a tense development in the direction of the design, awareness, and usage of more complex and intelligent superoleophobic surfaces. The prospect of superoleophobic surfaces is optimistic and exhilarating due to the excessive marketing, promising horizons and increasing the number of researchers and engineers dedicated to attaining superoleophobicity. In today's world, more and more companies are moving towards omniphibic and superomniphibic surfaces because of the vast range of applications which helpd them to explore brand new opportunities.

References

[1] F. Zhang, W.B. Zhang, Z. Shi, D. Wang, J. Jin, L. Jiang, Nanowire-haired inorganic membranes with superhydrophilicity and underwater ultralow adhesive superoleophobicity for high-efficiency oil/water separation, Adv. Mater. 25 (2013) 4192–4198.

[2] C. Z, L. H, L. H, D. Y, F. K, L. C, Y. J, Z. N, S. K, Regulating underwater oil adhesion on superoleophobic copper films through assembling n-Alkanoic acids, ACS Appl. Mater. Interfaces 16 (2015).

[3] T. Darmanin, F. Guittard, Superhydrophobic and superoleophobic properties in nature, Mater. Today 15 (2015).

[4] Z. Guo, W. Liu, Biomimic from the superhydrophobic plant leaves in nature: binary structure and unitary structure, Plant Sci. 172 (2007) 1103–1112.

[5] J. Zeng, B. Wang, Y. Zhang, H. Zhu, Z. Guo, Strong amphiphobic porous films with oily-self-cleaning property beyond nature, Chem. Lett. 43 (2014) 1566–1568.

[6] Z. Wang, M. Elimelech, S. Lin, Environmental applications of interfacial materials with special wettability, Environ. Sci. Technol. 50 (2016) 2132–2150.

[7] R. Renner, The long and the short of perfluorinated replacements, Environ. Sci. Technol. 40 (2006) 12–13.

[8] A. Calvimontes, The measurement of the surface energy of solids using a laboratory drop tower, NPJ Microgravity 25 (2017), https://doi.org/10.1038/s41526-017-0031-y.

[9] N. Durand, D. Mariot, B. Améduri, B. Boutevin, F. Ganachaud, Tailored covalent grafting of hexafluoropropylene oxide oligomers onto silica nanoparticles: toward thermally stable, hydrophobic, and oleophobic nanocomposites, Langmuir 27 (2011) 4057–4067.

[10] Y. Yuan, T.R. Lee, Surface Science Techniques, Springer, 2013, pp. 3–34.

[11] T. Young, An essay on the cohesion of fluids, Philos. Trans. Royal Soc. Lond. 95 (1805) 65–87.

[12] R.J. Good, A thermodynamic derivation of wenzel's modification of young's equation for contact Angles; together with a theory of hysteresis1, J. Am. Chem. Soc. 74 (1952) 5041–5042.

[13] N. Zhao, Q. Xie, L. Weng, S. Wang, X. Zhang, J. Xu, Superhydrophobic surface from vapor-induced phase separation of copolymer micellar solution, Macromolecules 38 (2005) 8996–8999.

[14] R.N. Wenzel, Resistance of solid surfaces to wetting by water, Ind. Eng. Chem. 28 (1936) 988–994.

[15] A. Marmur, Wetting on hydrophobic rough surfaces: to be heterogeneous or not to be, Langmuir 19 (2003) 8343–8348.

[16] R. Blossey, Self-cleaning surfaces—virtual realities, Nat. Mater. 2 (2003) 301–306.

[17] A. Cassie, S. Baxter, Wettability of porous surfaces, Trans. Faraday Soc. 40 (1944) 546–551.

[18] H.Y. Erbil, C.E. Cansoy, Range of applicability of the Wenzel and Cassie− Baxter equations for superhydrophobic surfaces†, Langmuir 25 (2009) 14135–14145.

[19] T. Koishi, K. Yasuoka, S. Fujikawa, T. Ebisuzaki, X.C. Zeng, Coexistence and transition between Cassie and Wenzel state on pillared hydrophobic surface, Proc.Natl. Acad. Sci. 106 (2009) 8435–8440.

[20] M. Lundgren, N.L. Allan, T. Cosgrove, Modeling of wetting: a study of nanowetting at rough and heterogeneous surfaces, Langmuir 23 (2007) 1187–1194.

[21] Y.C. Jung, B. Bhushan, Dynamic effects induced transition of droplets on biomimetic superhydrophobic surfaces, Langmuir 25 (2009) 9208–9218.

[22] R.J. Vrancken, H. Kusumaatmaja, K. Hermans, A.M. Prenen, O. Pierre-Louis, C.W. Bastiaansen, D.J. Broer, Fully reversible transition from Wenzel to Cassie−Baxter states on corrugated superhydrophobic surfaces, Langmuir 26 (2009) 3335–3341.

[23] M. Reyssat, J. Yeomans, D. Quéré, Impalement of fakir drops, EPL (Europhys. Lett.) 81 (2007) 26006.

[24] W. Barthlott, C. Neinhuis, Purity of the sacred lotus, or escape from contamination in biological surfaces, Plant 202 (1997) 1–8.

[25] C. Neinhuis, W. Barthlott, Characterization and distribution of water-repellent, self-cleaning plant surfaces, Ann. Bot. 79 (1997) 667–677.

[26] K. Koch, B. Bhushan, W. Barthlott, Diversity of structure, morphology and wetting of plant surfaces, Soft Matter 4 (2008) 1943–1963.

[27] K. Koch, B. Bhushan, W. Barthlott, Multifunctional surface structures of plants: an inspiration for biomimetics, Prog. Mater Sci 54 (2009) 137–178.

[28] R. Rakitov, S.N. Gorb, Brochosomal coats turn leafhopper (Insecta, Hemiptera, Cicadellidae) integument to superhydrophobic state, Proc. Royal Soc. Lond. B 280 (2013) 20122391.

[29] G.S.W. Mingxia Sun, Yongmei Zheng, Jolanta A. Watson, Aiping Liang, Wetting properties on nanostructured surfaces of cicada wings, J. Exper. Biol. (2009).

[30] H. Bellanger, T. Darmanin, E. Taffin de Givenchy, F. Guittard, Chemical and physical pathways for the preparation of superoleophobic surfaces and related wetting theories, Chem. Rev. 114 (2014) 2694–2716.

[31] H. Zhao, K.-.C. Park, K.-.Y. Law, Effect of surface texturing on superoleophobicity, contact angle hysteresis, and "robustness", Langmuir 28 (2012) 14925–14934.

[32] T. Li, J. He, Y. Zhang, L. Yao, T. Ren, B. Jin, In situ formation of artificial moth-eye structure by spontaneous nano-phase separation, Nature (2018), https://doi.org/10.1038/s41598-018-19414-x.

[33] W. Wetekamp, in Intelligent data acquisition and advanced computing systems, (2011).

[34] M. Houde, J.W. Martin, R.J. Letcher, K.R. Solomon, D.C. Muir, Biological monitoring of polyfluoroalkyl substances: a review, Environ. Sci. Technol. 40 (2006) 3463–3473.

[35] N. Isu, Human and environment-friendly materials for dwelling spaces, JOURNAL-SCCJ 40 (2006) 187.

[36] M.E. Hay, Marine chemical ecology: what's known and what's next, J. Exp. Mar. Biol. Ecol. 200 (1996) 103–134.

[37] B. Dean, B. Bhushan, Shark-skin surfaces for fluid-drag reduction in turbulent flow: a review, Philosophical Transactions of the Royal Society of London A: Mathematical, Physical and Engineering Sciences 368 (2010) 4775–4806.

[38] W.C. Bigelow, D.L. Pickett, W.A. Zisman, Oleophobic monolayers (Films adsorbed from solution in non-polar liquids), J Colloid Sci (1946) 513–538.

[39] J. Leja, G.W. Poling, Proceedings of the 5th Mineral Processing Congress, London, 1960.

[40] R.W. Smithwich, Contact-angle studies of microscopic mercury droplets on glass. *J. Colloid Interface. Sci.*. 123, 482–485.

[41] B.S. Yilbas, A. Ibrahim, H. Ali, M. Khaled, T. Laouib, Hydrophobic and optical characteristics of graphene and graphene oxide films transferred onto functionalized silica particles deposited glass surface, Appl. Surf. Sci. 442 (2018).

[42] G.S. Lai, W.J. Laua, S. Goh, A.F. Ismail, Y.H. Tan, C.Y. Chong, R. Krause-Rehberg, S. Awadc, Tailor-made thin film nanocomposite membrane incorporated with graphene oxide using novel interfacial polymerization technique for enhanced water separation, Chem.l Eng. J. 344 (2018) 524–534.

[43] A.F. Taggart, T.C. Taylor, Transactions of the American Institute of Mining and Metallurgical Engineers 87 American Institute of Mining, Metallurgical, and Petroleum Engineers, 1930.

[44] X. Sun, Y. Yao, D. Liu, Y. Zhou, Investigations of CO_2-water wettability of coal: NMR relaxation method, Int. J. Coal Geol. 188 (2018) 38–50.

[45] F.M. Fowkes, W.D. Harkins, The state of monolayers adsorbed at the interface solid—aqueous solution, J. Am. Chem. Soc. 62 (1940) 3377–3386.

[46] S. GT, C. DE, A refractive tilting-plate technique for measurement of dynamic contact angles, J. Coll. Interf. Sci. 286 (2005) 310–318.

[47] M. Remer, G. Sobieraj, K. Gumowski, J. Rokicki, Dynamic contact of droplet with superhydrophobic surface in conditions favour icing, J. Phys.: conf. ser. 530 (2014).

[48] C.-.T. Hsieh, F.-.L. Wu, W.-.Y. Chen, Super water-and oil-repellencies from silica-based nanocoatings, Surface Coatings Technol. 203 (2009) 3377–3384.

[49] S.F. Kistler, Hydrodynamics of wetting, Surfactant Sci. 49 (1993) 311.

[50] P.H. Steen, Capillarity and interfacial phenomena, Wetting Spreading Res. Trends Fluid Mech. (1996) 286–295.

[51] B. Taylor, Concerning the ascent of water between two glass plates, Philos. Trans. Royal Soc. 538 (1930) 1712.

[52] F. Hauksbee, An experiment touching the ascent of water between two glass plates in an hyperbolick figure, Philos. Trans. R. Soc. London 27 (1712) 539.

[53] G. Mason, N. Morrow, Capillary behavior of a perfectly wetting liquid in irregular triangular tubes, J. Colloid Interface Sci. 142 (1991) 262–274.

[54] P. Concus, R. Finn, On The Behavior of a Capillary Surface in a Wedge, Proceedings of the National Academy of Sciences, 63 (1969), pp. 292–299.

[55] A.M. Schwartz, The dynamics of contact angle phenomena, Adv. Colloid and Interface Sci. 4 (1975) 349–374.

[56] J.B.R.W.D. Bascom, Microvoids in glass-resin Composites. Their origin and effect on composite strength, Ind. Eng. Chem. Prod. Res. Dev. (1968) 172–178.

[57] F. Restagno, C. Poulard, C. Cohen, L. Vagharchakian, L. Léger, Contact angle and contact angle hysteresis measurements using the capillary bridge technique, Langmuir 28 (2009) 11188–11196.

[58] N.R. Tawde, K.G. Parvatikar, Unstable pendant drops in relation to drop-weight method of surface tension, Indian J. Phys. 19 (1958) 147–148.

[59] B.E. Blaisdell, The Physical Properties of Fluid Interfaces of Large Radius of Curvature. I. Integration of LaPlace's Equation for the Equilibrium Meridian of a Fluid Drop of Axial Symmetry in a Gravitational Field. Numerical Integration and Tables for Sessile Drops of Moderately Large Size, J. Mater. Phys. 19 (1940), https://doi.org/10.1002/sapm1940191186.

[60] S. Fordham, On the calculation of surface tension from measurements of pendant drops, Proceedings of the Royal Society of London, 194a 1948, https://doi.org/10.1098/rspa.1948.0063.

[61] J.K. Spelt, Y. Rotenberg, D.R. Absolom, A.W. Neumann, Sessile-drop contact angle measurements using axisymmetric drop shape analysis, Colloids Surfaces 23 (1987) 127–137.

[62] S.H. Anastasiadis, J.-.K. Chen, J.T. Koberstein, A.F. Siegel, J.E. Sohn, J.A. Emerson,

The determination of interfacial tension by video image processing of pendant fluid drops, J. Colloid Interface Sci. 119 (1987) 55–66.
[63] P. Cheng, D. Li, L. Boruvka, Y. Rotenberg, A.W. Neumann, Automation of axisymmetric drop shape analysis for measurements of interfacial tensions and contact angles, Colloids Surfaces 43 (1990) 151–167.
[64] Y. Rotenberg, L. Boruvka, A.W. Neumann, Determination of surface tension and contact angle from the shapes of axisymmetric fluid interfaces, J. Colloid Interface Sci. 93 (1983) 169–183.
[65] A. Kalantarian, R. David, A.W. Neumann, Methodology for high accuracy contact angle measurement, Langmuir 25 (2009) 14146–14154.
[66] R. OI, N. AW, Axisymmetric drop shape Analysis: computational methods for the measurement of interfacial properties from the shape and dimensions of pendant and sessile drops, J. Colloid Interface Sci. 196 (1997) 136–147.
[67] E. Moy, P. Cheng, Z. Policova, S. Treppo, D. Kwok, D.P. Mack, P.M. Sherman, A.W. Neuman, Measurement of contact angles from the maximum diameter of non-wetting drops by means of a modified axisymmetric drop shape analysis, Colloids Surfaces 58 (1991) 215–227.
[68] R.O. Duda, and P.E. Hart, *Pattern classification and scene analysis*, New York (1973).
[69] F.K. Skinner, Y. Rotenberg, A.W. Neumann, Contact angle measurements from the contact diameter of sessile drops by means of a modified axisymmetric drop shape analysis, J. Colloid Interface Sci. 130 (1989) 25–34.
[70] M.G. Cabezas, A. Bateni, J.M. Montanero, A.W. Neumann, A new method of image processing in the analysis of axisymmetric drop shapes, Colloids Surfaces A 255 (2005) 193–200.
[71] K.A. Matis, E.N. Peleka, Alternative flotation techniques for wastewater treatment: focus on electroflotation, Sep. Sci. Technol. 45 (2010).
[72] B. Bhushan, Springer Handbook of Nanotechnology, Springer, 2010.
[73] A.M. -Vilas, A.B. Reyes, and M.L.G. Martın, Ultrasmall liquid droplets on solid Surfaces: production,Imaging, and relevance for current wetting research. 136–1390 (2009).
[74] US EPA. 2010/2015 PFOA stewardship program. http://www.epa.gov/oppt/pfoa/pubs/stewardship/index.html. Accessed 2 Aug 2014.
[75] G.E. Charles, S.G. Mason, The coalescence of liquid drops with flat liquid/liquid interfaces, J. Colloid Sci. 15 (1960) 236–267.
[76] G.A. Bach, D.L. Koch, A. Gopinath, Coalescence and bouncing of small aerosol droplets, J. Fluid Mech. 518 (2004) 157–185.
[77] C. Josserand, S.T. Thoroddsen, Drop Impact on a Solid Surface, Ann. Rev. Fluid Mech. 48 (2016) 365–391.
[78] Y. Couder, E. Fort, C.-.H. Gautier, A. Boudaoud, From bouncing to floating: noncoalescence of drops on a fluid bath, Phys. Rev. Lett. 94 (2005) 17.
[79] S. Chandra, C.T. Avedisian, On the collision of a droplet with a solid surface, Proc. R. Soc. A 432 (1991) 13–41.
[80] X. Chen, S. Mandre, An experimental study of the coalescence between a drop and an interface in Newtonian and polymeric liquids, AIP Phys. Fluids 18 (2006), https://doi.org/10.1063/1.2349586.
[81] H.C. Pumphrey, P.A. Elmore, The entrainment of bubbles by drop impacts, J. Fluid Mech. 220 (1990) 539–567.
[82] V. Mehdi-Nejad, J. Mostaghimi, S. Chandra, Air bubble entrapment under an impacting droplet, AIP Phys. Fluids 15 (2002).
[83] S. Mandre, M. Mani, M.P. Brenner, Precursors to splashing of liquid droplets on a solid surface, Phys. Rev. Lett. 102 (2009).
[84] J.M. Kolinski, L. Mahadevan, and S.M. Rubinstein, Drops can bounce from perfectly hydrophilic surfaces. 9. (2014).
[85] J.d. Ruiter, F. Mugele, D.V.D. Endea, Air cushioning in droplet impact. I. Dynamics of thin films studied by dual wavelength reflection interference microscopy, Phys. Fluids 27 (2015) 121–124.
[86] J.d. Ruiter, R. Lagraauw, H.T.M.V.D. Ende, F.G. Mugele, Wettability-independent bouncing on flat surfaces mediated by thin air films, Nat. Phys 11 (2015) 48–53.
[87] J. Zimmermann, F.A. Reifler, G. Fortunato, L.C. Gerhardt, S. Seeger, A Simple, one-step approach to durable and robust superhydrophobic textiles, Adv. Funct. Mater. 18 (2008).
[88] X. Y, L. Y, H. DW, W. CP, Mechanically robust superhydrophobicity on hierarchically structured Si surfaces, Nanotechnology 21 (2010).
[89] M. Sakai, T. Yanagisawa, A. Nakajim, Effect of surface structure on the sustainability of an air layer on superhydrophobic coatings in a water-ethanol mixture, Langmuir 25 (2009) 6–13.
[90] T. Verho, C. Bower, P. Andrew, S. Franssila, Olli Ikkala, R.H.A. Ras, Mechanically durable superhydrophobic surfaces, Adv. Mater. 23 (2010) 673–678.
[91] A. Steele, I. Bayer, E. Loth, Inherently superoleophobic nanocomposite coatings by spray atomization, Nano Lett. 9 (2008) 501–505.
[92] C. Aulin, S.H. Yun, L. Wågberg, T. Lindström, Design of highly oleophobic cellulose surfaces from structured silicon templates, ACS Appl. Mate.r Interfaces 1 (2009) 2443–2452.
[93] T.-.S. Lin, C.-.F. Wu, C.-.T. Hsieh, Enhancement of water-repellent performance on functional coating by using the Taguchi method, Surface Coatings Technol. 200 (2006) 5253–5258.
[94] Z. Xue, M. Liu, L. Jiang, Recent developments in polymeric superoleophobic surfaces, J. Poly. Sci. Part B 50 (2012) 1209–1224.
[95] A. Hirao, K. Sugiyama, H. Yokoyama, Precise synthesis and surface structures of architectural per-and semifluorinated polymers with well-defined structures, Prog. Polym. Sci. 32 (2007) 1393–1438.
[96] Z. Chu, S. Seeger, Superamphiphobic surfaces, Chem. Soc. Rev. 43 (2014) 2784–2798.
[97] F.C. Birjandi, J. Sargolzaei, Super-non-wettable surfaces: a review, Colloids Surfaces A 448 (2014) 93–106.
[98] J.W. Martin, M.M. Smithwick, B.M. Braune, P.F. Hoekstra, D.C. Muir, S.A. Mabury, Identification of long-chain perfluorinated acids in biota from the Canadian Arctic, Environ. Sci. Technol. 38 (2004) 373–380.
[99] A. Bondi, van der Waals volumes and radii, J. Phys. Chem. 68 (1964) 441–451.
[100] M. Meng, S. Deng, Z. Du, B. Wang, Effect of hydro-oleophobic perfluorocarbon chain on interfacial behavior and mechanism of perfluorooctane sulfonate in oil-water mixture, Sci. Rep. 16 (2017) 44694.
[101] T. Nishino, M. Meguro, K. Nakamae, M. Matsushita, Y. Ueda, The lowest surface free energy based on-CF3 alignment, Langmuir 15 (1999) 4321–4323.
[102] A.F. Thünemann, K.H. Lochhaas, Surface and solid-state properties of a fluorinated polyelectrolyte-surfactant complex, Langmuir 15 (1999) 4867–4874.
[103] A.F. Thünemann, Nano-structured materials with low surface energies formed by polyelectrolytes and fluorinated amphiphiles (PEFA), Polym. Int. 49 (2000) 636–644.
[104] M. Antonietti, S. Henke, A. Thünemann, Highly ordered materials with ultra-low surface energies: polyelectrolyte–surfactant, complexes with fluorinated surfactants, Adv. Mater. 8 (1996) 41–45.
[105] E. Goddard, Polymer—surfactant interaction part II. Polymer and surfactant of opposite charge, Colloids surfaces 19 (1986) 301–329.
[106] K. Hayakawa, J.C. Kwak, Surfactant-polyelectrolyte interactions. 1. Binding of dodecyltrimethylammonium ions by sodium dextransulfate and sodium poly (styrenesulfonate) in aqueous solution in the presence of sodium chloride, J Phys Chem 86 (1982) 3866–3870.
[107] K. Hayakawa, J.C. Kwak, Study of surfactant-polyelectrolyte interactions. 2. Effect of multivalent counterions on the binding of dodecyltrimethylammonium ions by sodium dextran sulfate and sodium poly (styrene sulfonate) in aqueous solution, J. Phys. Chem. 87 (1983) 506–509.
[108] K. Lochhaas, A. Thünemann, M. Antonietti, Polyelectrolyte-surfactant complexes with fluorinated surfactants: a new type of material for coatings, Surface Coatings Int. 82 (1999) 451–455.
[109] L. Li, Y. Wang, C. Gallaschun, T. Risch, J. Sun, Why can a nanometer-thick polymer coated surface be more wettable to water than to oil? J. Mater. Chem. 22 (2012) 16719–16722.
[110] J. Yang, Z. Zhang, X. Xu, X. Zhu, X. Men, X. Zhou, Superhydrophilic–superoleophobic coatings, J. Mater. Chem. 22 (2012) 2834–2837.
[111] U. Cengiz, M.Z. Avci, H.Y. Erbil, A.S. Sarac, Superhydrophobic terpolymer nanofibers containing perfluoroethyl alkyl methacrylate by electrospinning, Appl. Surf. Sci. 258 (2012) 5815–5821.
[112] Y. Katano, H. Tomono, T. Nakajima, Surface property of polymer films with fluoroalkyl side chains, Macromolecules 27 (1994) 2342–2344.
[113] R. Van de Grampel, W. Ming, A. Gildenpfennig, W. Van Gennip, J. Laven, J. Niemantsverdriet, H. Brongersma, G. de With, R. Van der Linde, The outermost atomic layer of thin films of fluorinated polymethacrylates, Langmuir 20 (2004) 6344–6351.
[114] Q. Wang, Q. Zhang, X. Zhan, F. Chen, Structure and surface properties of polyacrylates with short fluorocarbon side chain: role of the main chain and spacer group, J. Polymer Sci. Part A 48 (2010) 2584–2593.
[115] U. Cengiz, N.A. Gengec, H.Y. Erbil, Surface characterization of flat and rough films of perfluoromethacrylate-methylmethacrylate statistical copolymers synthesized in CO2-expanded monomers, Colloid Polym. Sci. 291 (2013) 641–652.
[116] T. Darmanin, F. Guittard, One methylene unit to control super oil-repellency properties of conducting polymers, Chem. Commun. (2009) 2210–2211, https://doi.org/10.1039/B822791H.
[117] I.J. Park, S.-.B. Lee, C.K. Choi, Surface properties of the fluorine-containing graft copolymer of poly ((perfluoroalkyl) ethyl methacrylate)-g-poly (methyl methacrylate), Macromolecules 31 (1998) 7555–7558.
[118] U. Cengiz, H.Y. Erbil, The lifetime of floating liquid marbles: the influence of particle size and effective surface tension, Soft Matter 9 (2013) 8980–8991.
[119] X. Xu, F. Guo, J. Yang, X. Zhu, Q. Xue, Superamphiphobic self-assembled monolayer of thiol on the structured Zn surface, Colloid. Surface. 396 (2012) 90–95.
[120] C.E. Cansoy, U. Cengiz, The effect of perfluoroalkyl and hydrocarbon liquid chain lengths on oleophobic behaviors of copolymer surfaces, Colloids Surfaces A 441 (2014) 695–700.
[121] S.T. Iacono, S.M. Budy, J.M. Mabry, D.W. Smith, Synthesis, characterization, and properties of chain terminated polyhedral oligomeric silsesquioxane-functionalized perfluorocyclobutyl aryl ether copolymers, Polymer (Guildf) 48 (2007) 4637–4645.
[122] J.M. Mabry, A. Vij, S.T. Iacono, B.D. Viers, Innentitelbild: fluorinated polyhedral oligomeric silsesquioxanes (F-POSS)(Angew. Chem. 22/2008), Angewandte Chemie 120 (2008) 4094.
[123] S.S. Chhatre, J.O. Guardado, B.M. Moore, T.S. Haddad, J.M. Mabry, G.H. McKinley, R.E. Cohen, Fluoroalkylated silicon-containing surfaces− estimation of solid-surface energy, ACS Appl. Mater. Interfaces 2 (2010) 3544–3554.
[124] S.C. Kettwich, S.N. Pierson, A.J. Peloquin, J.M. Mabry, S.T. Iacono, Anomalous macromolecular assembly of partially fluorinated polyhedral oligomeric silsesquioxanes, New J. Chem. 36 (2012) 941–946.
[125] J.M. Mabry, A. Vij, S.T. Iacono, B.D. Viers, Fluorinated polyhedral oligomeric silsesquioxanes (F-POSS), Angewandte Chemie 120 (2008) 4205–4208.
[126] S. Srinivasan, S.S. Chhatre, J.M. Mabry, R.E. Cohen, G.H. McKinley, Solution spraying of poly (methyl methacrylate) blends to fabricate microtextured, superoleophobic surfaces, Polymer (Guildf) 52 (2011) 3209–3218.
[127] W. Choi, A. Tuteja, S. Chhatre, J.M. Mabry, R.E. Cohen, G.H. McKinley, Fabrics with tunable oleophobicity, Adv. Mater. 21 (2009) 2190–2195.
[128] A. Tuteja, W. Choi, J.M. Mabry, G.H. McKinley, R.E. Cohen, Robust omniphobic surfaces, Proceedings of the National Academy of Sciences, 105 2008, pp. 18200–18205.

[129] A. Tuteja, W. Choi, G.H. McKinley, R.E. Cohen, M.F. Rubner, Design parameters for superhydrophobicity and superoleophobicity, MRS Bulletin 33 (2008) 752–758.
[130] S.M. Ramirez, Y.J. Diaz, R. Campos, R.L. Stone, T.S. Haddad, J.M. Mabry, Incompletely condensed fluoroalkyl silsesquioxanes and derivatives: precursors for low surface energy materials, J. Am. Chem. Soc. 133 (2011) 20084–20087.
[131] Kun Hou, Yicheng Zeng, Cailong Zhou, Jiahui Chen, Xiufang Wen, Shouping Xu, Jiang Cheng, Yingguang Lin, Pihui Pi, Durable underwater superoleophobic PDDA/halloysite nanotubes decorated stainless steel mesh for efficient oil–water separation, Appl. Surf. Sci. 416 (2017) 332–344.
[132] N. Herzer, C. Haensch, S. Hoeppener, U.S. Schubert, Orthogonal functionalization of silicon substrates using self-assembled monolayers, Langmuir 26 (2010) 8358–8365.
[133] D. Mahadik, A.V. Rao, A.P. Rao, P. Wagh, S. Ingale, S.C. Gupta, Effect of concentration of trimethylchlorosilane (TMCS) and hexamethyldisilazane (HMDZ) silylating agents on surface free energy of silica aerogels, J. Colloid Interface Sci. 356 (2011) 298–302.
[134] D. Janssen, R. De Palma, S. Verlaak, P. Heremans, W. Dehaen, Static solvent contact angle measurements, surface free energy and wettability determination of various self-assembled monolayers on silicon dioxide, Thin Solid Films 515 (2006) 1433–1438.
[135] K. Malaga, U. Mueller, Relevance of hydrophobic and oleophobic properties of antigraffiti systems on their cleaning efficiency on concrete and stone surfaces, J. Mater. Civil Eng. 25 (2012) 755–762.
[136] W. Wang, J. Salazar, H. Vahabi, A. Joshi-Imre, W.E. Voit, A.K. Kota, Metamorphic superomniphobic surfaces, Adv. Mater. 29 (2017).
[137] R. Seemann, M. Brinkmann, E.J. Kramer, F.F. Lange, R. Lipowsky, Wetting morphologies at microstructured surfaces, Proceedings of the National Academy of Sciences of the United States of America, 102 2005, pp. 1848–1852.
[138] T. Onda, S. Shibuichi, N. Satoh, K. Tsujii, Super-water-repellent fractal surfaces, Langmuir 12 (1996) 2125–2127.
[139] C. Extrand, Model for contact angles and hysteresis on rough and ultraphobic surfaces, Langmuir 18 (2002) 7991–7999.
[140] J. Yang, Z. Zhang, X. Men, X. Xu, X. Zhu, A simple approach to fabricate superoleophobic coatings, New J. Chem. 35 (2011) 576–580.
[141] T. Darmanin, F. Guittard, S. Amigoni, E.T. de Givenchy, X. Noblin, R. Kofman, F. Celestini, Superoleophobic behavior of fluorinated conductive polymer films combining electropolymerization and lithography, Soft Matter 7 (2011) 1053–1057.
[142] S. Herminghaus, Roughness-induced non-wetting, EPL (Europhys. Lett.) 52 (2000) 165.
[143] Fabrication of non-aging superhydrophobic surfaces by packing flower-like hematite particles, Proceedings of the APS March Meeting Abstracts, 2008.
[144] L. Cao, H.-.H. Hu, D. Gao, Design and fabrication of micro-textures for inducing a superhydrophobic behavior on hydrophilic materials, Langmuir 23 (2007) 4310–4314.
[145] R.T. Rajendra Kumar, K.B. Mogensen, P. Bøggild, Simple approach to superamphiphobic overhanging silicon nanostructures, J. Phys. Chem. C 114 (2010) 2936–2940.
[146] A. Tuteja, W. Choi, M. Ma, J.M. Mabry, S.A. Mazzella, G.C. Rutledge, G.H. McKinley, R.E. Cohen, Designing superoleophobic surfaces, Science 318 (2007) 1618–1622.
[147] M. Xu, Inventor, method for manufacturing re-entrant microstructure. (2016).
[148] A. Ahuja, J. Taylor, V. Lifton, A. Sidorenko, T. Salamon, E. Lobaton, P. Kolodner, T. Krupenkin, Nanonails: a simple geometrical approach to electrically tunable superlyophobic surfaces, Langmuir 24 (2008) 9–14.
[149] H. Zhao, K.-Y. Law, V. Sambhy, Fabrication, surface properties, and origin of superoleophobicity for a model textured surface, Langmuir 27 (2011) 5927–5935.
[150] Y. Zhang, M. Cao, Y. Peng, X. Jin, D. Tian, K. Liu, L. Jiang, Bioinspired continuous and spontaneous antigravity oil collection and transportation, Adv. Mater. 28 (2018).
[151] J. Song, S. Huang, K. Hu, Y. Lu, X. Liu, W. Xu, Fabrication of superoleophobic surfaces on al substrates, J. Mater. Chem. A 1 (2013) 14783–14789.
[152] M. Nosonovsky, Multiscale roughness and stability of superhydrophobic biomimetic interfaces, Langmuir 23 (2007) 3157–3161.
[153] M. Ma, R.M. Hill, G.C. Rutledge, A review of recent results on superhydrophobic materials based on micro-and nanofibers, J. Adhes. Sci. Technol. 22 (2008) 1799–1817.
[154] J.-.L. Liu, X.-.Q. Feng, G. Wang, S.-.W. Yu, Mechanisms of superhydrophobicity on hydrophilic substrates, J. Phys. 19 (2007) 356002.
[155] D.H. Reneker, A.L. Yarin, H. Fong, S. Koombhongse, Bending instability of electrically charged liquid jets of polymer solutions in electrospinning, J. Appl. Phys. 87 (2000) 4531–4547.
[156] M. Ma, R.M. Hill, J.L. Lowery, S.V. Fridrikh, G.C. Rutledge, Electrospun poly (styrene-block-dimethylsiloxane) block copolymer fibers exhibiting superhydrophobicity, Langmuir 21 (2005) 5549–5554.
[157] M. Ma, M. Gupta, Z. Li, L. Zhai, K.K. Gleason, R.E. Cohen, M.F. Rubner, G.C. Rutledge, Decorated electrospun fibers exhibiting superhydrophobicity, Adv. Mater. 19 (2007) 255–259.
[158] F. Xia, L. Jiang, Bio-inspired, smart, multiscale interfacial materials, Adv. Mater. 20 (2008) 2842–2858.
[159] S. Kim, E. Cheung, M. Sitti, Wet self-cleaning of biologically inspired elastomer mushroom shaped microfibrillar adhesives, Langmuir 25 (2009) 7196–7199.
[160] J. Lee, R.S. Fearing, Contact self-cleaning of synthetic gecko adhesive from polymer microfibers, Langmuir 24 (2008) 10587–10591.
[161] S.M. Kang, S.M. Kim, H.N. Kim, M.K. Kwak, D.H. Tahk, K.Y. Suh, Robust superomniphobic surfaces with mushroom-like micropillar arrays, Soft Matter 8 (2012) 8563–8568.
[162] A.M. Mohamed, A.M. Abdullah, N.A. Younan, Corrosion behavior of superhydrophobic surfaces: a review, Arabian J. Chem. 8 (2015) 749–765.
[163] B. Mahltig, H. Böttcher, Modified silica sol coatings for water-repellent textiles, J. Solgel. Sci. Technol. 27 (2003) 43–52.
[164] S. Pilotek, H.K. Schmidt, Wettability of microstructured hydrophobic sol-gel coatings, J. Solgel. Sci. Technol. 26 (2003) 789–792.
[165] Y.-.C. Sheen, W.-.H. Chang, W.-.C. Chen, Y.-.H. Chang, Y.-.C. Huang, F.-.C. Chang, Non-fluorinated superamphiphobic surfaces through sol–gel processing of methyltriethoxysilane and tetraethoxysilane, Mater. Chem. Phys. 114 (2009) 63–68.
[166] G. Hayase, K. Kanamori, G. Hasegawa, A. Maeno, H. Kaji, K. Nakanishi, A superamphiphobic macroporous silicone monolith with Marshmallow-like flexibility, Angewandte Chemie Inte. Edn. 52 (2013) 10788–10791.
[167] C.-.T. Hsieh, F.-.L. Wu, W.-.Y. Chen, Contact angle hysteresis and work of adhesion of oil droplets on nanosphere stacking layers, J.Phys. Chem. C 113 (2009) 13683–13688.
[168] Y. Goto, H. Takashima, K. Takishita, H. Sawada, Creation of coating surfaces possessing superhydrophobic and superoleophobic characteristics with fluoroalkyl end-capped vinyltrimethoxysilane oligomeric nanocomposites having biphenylene segments, J. Colloid Interface Sci. 362 (2011) 375–381.
[169] Y.C. Sheen, Y.C. Huang, C.S. Liao, H.Y. Chou, F.C. Chang, New approach to fabricate an extremely super-amphiphobic surface based on fluorinated silica nanoparticles, J. Polymer Sci. Part B 46 (2008) 1984–1990.
[170] M. Hikita, K. Tanaka, T. Nakamura, T. Kajiyama, A. Takahara, Super-liquid-repellent surfaces prepared by colloidal silica nanoparticles covered with fluoroalkyl groups, Langmuir 21 (2005) 7299–7302.
[171] C.-.T. Hsieh, Y.-.S. Cheng, S.-.M. Hsu, J.-.Y. Lin, Water and oil repellency of flexible silica-coated polymeric substrates, Appl. Surf. Sci. 256 (2010) 4867–4872.
[172] E. Sumino, T. Saito, T. Noguchi, H. Sawada, Facile creation of superoleophobic and superhydrophilic surface by using perfluoropolyether dicarboxylic acid/silica nanocomposites, Polym. Adv. Technol. 26 (2015) 345–352.
[173] B. Xia, H. Liu, Y. Fan, W. Zhu, C. Geng, Preparation of robust CuO/TiO2 superamphiphobic steel surface through chemical deposition and Sol–Gel methods, Adv. Eng. Mater. 121 (2016).
[174] X. Wu, Q. Fu, D. Kumar, J.W.C. Ho, P. Kanhere, H. Zhou, Z. Chen, Mechanically robust superhydrophobic and superoleophobic coatings derived by sol–gel method, Mater. Des. 89 (2016) 1302–1309.
[175] D.-.K. Lee, E.-.H. Lee, Y.H. Cho, A superoleophobic surface with anisotropic flow of hexadecane droplets, Microsystem Technologies (2016) 1–7.
[176] S. Huang, J. Song, Y. Lu, F. Chen, H. Zheng, x. Yang, X. Liu, J. Sun, C.J. Carmalt, I.P. Parkin, Underwater spontaneous pumpless transportation of nonpolar organic liquids on extreme wettability patterns, ACS Appl. Mater. Interfaces (2016).
[177] G. Ren, Z. Zhang, X. Zhu, B. Ge, K. Wang, X. Xu, X. Men, X. Zhou, A facile method for imparting superoleophobicity to polymer substrates, Appl. Phys. A 114 (2014) 1129–1133.
[178] J. Ou, W. Hu, S. Liu, M. Xue, F. Wang, W. Li, Superoleophobic textured copper surfaces fabricated by chemical etching/oxidation and surface fluorination, ACS Appl. Mater. Interfaces 5 (2013) 10035–10041.
[179] S. Ji, P.A. Ramadhianti, T.-.B. Nguyen, W.-d. Kim, H. Lim, Simple fabrication approach for superhydrophobic and superoleophobic Al surface, Microelectron. Eng. 111 (2013) 404–408.
[180] K. Ellinas, S.P. Pujari, D.A. Dragatogiannis, C.A. Charitidis, A. Tserepi, H. Zuilhof, E. Gogolides, Plasma micro-nanotextured, scratch, water and hexadecane resistant, superhydrophobic, and superamphiphobic polymeric surfaces with perfluorinated monolayers, ACS Appl. Mater. Interfaces 6 (2014) 6510–6524.
[181] L. Wang, Y. Sun, Y. Gao, D. Guo, Preparation of durable underwater superoleophobic Ti6Al4V surfaces by electrochemical etching, Surface Eng. (2015) 1–10.
[182] L. Iglesias-Rubianes, S. Garcia-Vergara, P. Skeldon, G. Thompson, J. Ferguson, M. Beneke, Cyclic oxidation processes during anodizing of Al–Cu alloys, Electrochim. Acta 52 (2007) 7148–7157.
[183] M. He, X. Zhou, X. Zeng, D. Cui, Q. Zhang, J. Chen, H. Li, J. Wang, Z. Cao, Y. Song, Hierarchically structured porous aluminum surfaces for high-efficient removal of condensed water, Soft. Matter. 8 (2012) 6680–6683.
[184] Z. Guo, F. Zhou, J. Hao, W. Liu, Stable biomimetic super-hydrophobic engineering materials, J. Am. Chem. Soc. 127 (2005) 15670–15671.
[185] F. Zhang, L. Zhao, H. Chen, S. Xu, D.G. Evans, X. Duan, Corrosion resistance of superhydrophobic layered double hydroxide films on aluminum, Angewandte Chemie Int. Edin 47 (2008) 2466–2469.
[186] S. Peng, B. Bhushan, Mechanically durable superoleophobic aluminum surfaces with microstep and nanoreticula hierarchical structure for self-cleaning and antismudge properties, J. Colloid Interface Sci. 461 (2016) 273–284.
[187] W. Xu, J. Song, J. Sun, Q. Dou, X. Fan, Fabrication of superhydrophobic surfaces on aluminum substrates using NaNO3 electrolytes, J. Mater. Sci. 46 (2011) 5925–5930.
[188] H. Li, S. Yu, X. Han, E. Liu, Y. Zhao, Fabrication of superhydrophobic and oleophobic surface on zinc substrate by a simple method, ColloidsSurfaces A 469 (2015) 271–278.
[189] T.P.N. Nguyen, R. Dufour, V. Thomy, V. Senez, R. Boukherroub, Y. Coffinier, Fabrication of superhydrophobic and highly oleophobic silicon-based surfaces via electroless etching method, Appl. Surf. Sci. 295 (2014) 38–43.
[190] M. Im, H. Im, J.-.H. Lee, J.-.B. Yoon, Y.-.K. Choi, A robust superhydrophobic and superoleophobic surface with inverse-trapezoidal microstructures on a large transparent flexible substrate, Soft. Matter 6 (2010) 1401–1404.
[191] K. Ellinas, A. Tserepi, E. Gogolides, From superamphiphobic to amphiphilic

polymeric surfaces with ordered hierarchical roughness fabricated with colloidal lithography and plasma nanotexturing, Langmuir 27 (2011) 3960–3969.
[192] S.E. Lee, H.-J. Kim, S.-H. Lee, D.-G. Choi, Superamphiphobic surface by nanotransfer molding and isotropic etching, Langmuir 29 (2013) 8070–8075.
[193] X. Liu, W. Wu, X. Wang, Z. Luo, Y. Liang, F. Zhou, A replication strategy for complex micro/nanostructures with superhydrophobicity and superoleophobicity and high contrast adhesion, Soft Matter 5 (2009) 3097–3105.
[194] X. Deng, L. Mammen, H.J. Butt, D. Vollmer, Candle soot as a template for a transparent robust superamphiphobic coating, Science 335 (2012) 67–70.
[195] W. Liu, X. Liu, J. Fangteng, S. Wang, L. Fang, H. Shen, S. Xiang, H. Sun, B. Yang, Bioinspired polyethylene terephthalate nanocone arrays with underwater superoleophobicity and anti-bioadhesion properties, Nanoscale 6 (2014) 13845–13853.
[196] H.-J. Choi, S. Choo, J.-H. Shin, K.-I. Kim, H. Lee, Fabrication of superhydrophobic and oleophobic surfaces with overhang structure by reverse nanoimprint lithography, J. Phys. Chem. C 117 (2013) 24354–24359.
[197] J.C. Hulteen, R.P. Van Duyne, Nanosphere lithography: a materials general fabrication process for periodic particle array surfaces, J. Vacuum Sci. Technol. A 13 (1995) 1553–1558.
[198] H. Yang, P. Jiang, Self-cleaning diffractive macroporous films by doctor blade coating, Langmuir 26 (2010) 12598–12604.
[199] J. Wang, Y. Zhang, T. Zhao, Y. Song, L. Jiang, Recent research progress in wettability of colloidal crystals, Sci. China Chem. 53 (2010) 318–326.
[200] H.-B. Jo, J. Choi, K.-J. Byeon, H.-J. Choi, H. Lee, Superhydrophobic and superoleophobic surfaces using ZnO nano-in-micro hierarchical structures, Microelectron. Eng. 116 (2014) 51–57.
[201] Q. You, G. Ran, C. Wang, Y. Zhao, Q. Song, A novel superhydrophilic–underwater superoleophobic Zn-ZnO electrodeposited copper mesh for efficient oil/water separation, Sep. Purif. Technol. 193 (2018) 21–28.
[202] T. Darmanin, F. Guittard, Superoleophobic surfaces with short fluorinated chains? Soft Matter 9 (2013) 5982–5990.
[203] H. Bellanger, T. Darmanin, E.T. De Givenchy, F. Guittard, Influence of intrinsic oleophobicity and surface structuration on the superoleophobic properties of PEDOP films bearing two fluorinated tails, J. Mater. Chem. A 1 (2013) 2896–2903.
[204] T. Darmanin, F. Guittard, Molecular design of conductive polymers to modulate superoleophobic properties, J. Am. Chem. Soc. 131 (2009) 7928–7933.
[205] J. Xi, L. Feng, L. Jiang, A general approach for fabrication of superhydrophobic and superamphiphobic surfaces, Appl. Phys. Lett. 92 (2008) 053102.
[206] T. Darmanin, J. Tarrade, E. Celia, F.D.R. Guittard, Superoleophobic meshes with high adhesion by electrodeposition of conducting polymer containing short perfluorobutyl chains, J. Phys. Chem. C 118 (2014) 2052–2057.
[207] J.P. Giesy, K. Kannan, Global distribution of perfluorooctane sulfonate in wildlife, Environ. Sci. Technol. 35 (2001) 1339–1342.
[208] F. Zhang, W.B. Zhang, Z. Shi, D. Wang, J. Jin, L. Jiang, Nanowire-haired inorganic membranes with superhydrophilicity and underwater ultralow adhesive superoleophobicity for high-efficiency oil/water separation, Adv. Mater. 25 (2013) 4192–4198.
[209] Q. Wen, J. Di, L. Jiang, J. Yu, R. Xu, Zeolite-coated mesh film for efficient oil–water separation, Chem. Sci. 4 (2013) 591–595.
[210] S.-C. Luo, S.S. Liour, H.-h. Yu, Perfluoro-functionalized PEDOT films with controlled morphology as superhydrophobic coatings and biointerfaces with enhanced cell adhesion, Chem. Commun. 46 (2010) 4731–4733.
[211] S.-C. Luo, J. Sekine, B. Zhu, H. Zhao, A. Nakao, H.-h. Yu, Polydioxythiophene nanodots, nonowires, nano-networks, and tubular structures: the effect of functional groups and temperature in template-free electropolymerization, ACS Nano 6 (2012) 3018–3026.
[212] S. Taleb, T. Darmanin, F. Guittard, Superhydrophobic conducting polymers with switchable water and oil repellency by voltage and ion exchange, RSC Adv 4 (2014) 3550–3555.
[213] T. Darmanin, F. Guittard, Highly hydrophobic films with various adhesion by electrodeposition of poly (3, 4-bis (alkoxy) thiophene) s, Soft Matter 9 (2013) 1500–1505.
[214] T.K. Das, S. Prusty, Review on conducting polymers and their applications, Polym. Plast. Technol. Eng. 51 (2012) 1487–1500.
[215] C. Li, H. Bai, G. Shi, Conducting polymer nanomaterials: electrosynthesis and applications, Chem. Soc. Rev. 38 (2009) 2397–2409.
[216] L. Xu, Z. Chen, W. Chen, A. Mulchandani, Y. Yan, Electrochemical synthesis of perfluorinated ion doped conducting polyaniline films consisting of helical fibers and their reversible switching between superhydrophobicity and superhydrophilicity, Macromol. Rapid. Commun. 29 (2008) 832–838.
[217] J.H. Chang, I.W. Hunter, A superhydrophobic to superhydrophilic in situ wettability switch of microstructured polypyrrole surfaces, Macromol. Rapid Commun. 32 (2011) 718–723.
[218] H. Bellanger, T. Darmanin, F. Guittard, Surface structuration (micro and/or nano) governed by the fluorinated tail lengths toward superoleophobic surfaces, Langmuir 28 (2011) 186–192.
[219] J. Tarrade, T. Darmanin, E.T. De Givenchy, F. Guittard, Super liquid-repellent properties of electrodeposited hydrocarbon and fluorocarbon copolymers, RSC Adv. 3 (2013) 10848–10853.
[220] O. Dunand, T. Darmanin, F. Guittard, Superhydrophobic conducting polymers based on hydrocarbon poly (3, 4-Ethylenedioxyselenophene), Chem. Phys. Chem. 14 (2013) 2947–2953.
[221] J.M. Conder, R.A. Hoke, W. De Wolf, M.H. Russell, R.C. Buck, Are PFCAs bioaccumulative? A critical review and comparison with regulatory criteria and persistent lipophilic compounds, Environ. Sci. Technol. 42 (2008) 995–1003.
[222] A. Dramé, T. Darmanin, S.Y. Dieng, E.T. De Givenchy, F. Guittard, Superhydrophobic and oleophobic surfaces containing wrinkles and nanoparticles of PEDOT with two short fluorinated chains, RSC Adv. 4 (2014) 10935–10943.
[223] T. Darmanin, M. Nicolas, F. Guittard, Electrodeposited polymer films with both superhydrophobicity and superoleophilicity, Phys. Chem. Chem. Phys. 10 (2008) 4322–4326.
[224] T. Darmanin, M. Nicolas, F. Guittard, Synthesis and properties of perfluorinated conjugated polymers based on polyethylenedioxythiophene, polypyrrole, and polyfluorene. Toward surfaces with special wettabilities, Langmuir 24 (2008) 9739–9746.
[225] M. Nicolas, F. Guittard, S. Géribaldi, Synthesis of stable super water-and oil-repellent polythiophene films, Angewandte Chemie Int. Edn. 45 (2006) 2251–2254.
[226] M. Nicolas, F. Guittard, S. Géribaldi, Stable superhydrophobic and lipophobic conjugated polymers films, Langmuir 22 (2006) 3081–3088.
[227] T. Darmanin, F. Guittard, Fluorophobic effect for building up the surface morphology of electrodeposited substituted conductive polymers, Langmuir 25 (2009) 5463–5466.
[228] T. Darmanin, F. Guittard, One-pot method for build-up nanoporous super oil-repellent films, J. Colloid Interface Sci. 335 (2009) 146–149.
[229] S. Ramakrishna, K. Fujihara, W.-E. Teo, T.-C. Lim, Z. Ma, An Introduction to Electrospinning and Nanofibers, World Scientific, 2005.
[230] M. Wan, A template-free method towards conducting polymer nanostructures, Adv. Mater. 20 (2008) 2926–2932.
[231] H. Tang, H. Wang, J. He, Superhydrophobic titania membranes of different adhesive forces fabricated by electrospinning, J. Phys. Chem. C 113 (2009) 14220–14224.
[232] B. Sharma, R. Verma, C. Baur, J. Bykova, J.M. Mabry, D.W. Smith, Ultra low dielectric, self-cleansing and highly oleophobic POSS-PFCP aryl ether polymer composites, J. Mater. Chem. C 1 (2013) 7222–7227.
[233] S. Pan, A.K. Kota, J.M. Mabry, A. Tuteja, Superomniphobic surfaces for effective chemical shielding, J. Am. Chem. Soc. 135 (2012) 578–581.
[234] W. Cui, X. Li, S. Zhou, J. Weng, Degradation patterns and surface wettability of electrospun fibrous mats, Polym. Degrad. Stab. 93 (2008) 731–738.
[235] M. Guo, B. Ding, X. Li, X. Wang, J. Yu, M. Wang, Amphiphobic nanofibrous silica mats with flexible and high-heat-resistant properties, J. Phys. Chem. C 114 (2009) 916–921.
[236] G.R. Choi, J. Park, J.W. Ha, W.D. Kim, H. Lim, Superamphiphobic web of PTFEMA fibers via simple electrospinning without functionalization, Macromol. Mater. Eng. 295 (2010) 995–1002.
[237] V.A. Ganesh, S.S. Dinachali, H.K. Raut, T.M. Walsh, A.S. Nair, S. Ramakrishna, Electrospun SiO 2 nanofibers as a template to fabricate a robust and transparent superamphiphobic coating, RSC Adv. 3 (2013) 3819–3824.
[238] V.A. Ganesh, S.S. Dinachali, A.S. Nair, S. Ramakrishna, Robust superamphiphobic film from electrospun TiO2 nanostructures, ACS Appl. Mater. Interfaces 5 (2013) 1527–1532.
[239] L. Zhai, F.C. Cebeci, R.E. Cohen, M.F. Rubner, Stable superhydrophobic coatings from polyelectrolyte multilayers, Nano Lett. 4 (2004) 1349–1353.
[240] L. Zhang, H. Chen, J. Sun, J. Shen, Layer-by-layer deposition of poly (diallyldimethylammonium chloride) and sodium silicate multilayers on silica-sphere-coated substrate-facile method to prepare a superhydrophobic surface, Chem. Mater. 19 (2007) 948–953.
[241] Y. Zhao, Z. Xu, X. Wang, T. Lin, Photoreactive azido-containing silica nanoparticle/polycation multilayers: durable superhydrophobic coating on cotton fabrics, Langmuir 28 (2012) 6328–6335.
[242] T. Wang, T.T. Isimjan, J. Chen, S. Rohani, Transparent nanostructured coatings with UV-shielding and superhydrophobicity properties, Nanotechnology 22 (2011) 265708.
[243] J. Yang, Z. Zhang, X. Men, X. Xu, X. Zhu, X. Zhou, Q. Xue, Rapid and reversible switching between superoleophobicity and superoleophilicity in response to counterion exchange, J. Colloid Interface Sci. 366 (2012) 191–195.
[244] L. Cao, D. Gao, Transparent superhydrophobic and highly oleophobic coatings, Faraday Discuss. 146 (2010) 57–65.
[245] X. Li, D. Hu, K. Huang, C. Yang, Hierarchical rough surfaces formed by LBL self-assembly for oil–water separation, J. Mater. Chem. 2 (2014) 11830–11838.
[246] P.S. Brown, B. Bhushan, Mechanically durable, superomniphobic coatings prepared by layer-by-layer technique for self-cleaning and anti-smudge, J. Colloid Interface Sci. 456 (2015) 210–218.
[247] B. Leng, Z. Shao, G. de With, W. Ming, Superoleophobic cotton textiles, Langmuir 25 (2009) 2456–2460.
[248] Y. Wang, F. Lin, Y. Dong, Z. Liu, W. Li, Y. Huang, A multifunctional polymeric nanofilm with robust chemical performances for special wettability, Nanoscale 8 (2016) 5153–5161.
[249] X. Zhu, Z. Zhang, X. Xu, X. Men, J. Yang, X. Zhou, Q. Xue, Facile fabrication of a superamphiphobic surface on the copper substrate, J. Colloid Interface Sci. 367 (2012) 443–449.
[250] H. Meng, S. Wang, J. Xi, Z. Tang, L. Jiang, Facile means of preparing superamphiphobic surfaces on common engineering metals, J. Phys. Chem. C 112 (2008) 11454–11458.
[251] J. Zeng, Z. Guo, Superhydrophilic and underwater superoleophobic MFI zeolite-coated film for oil/water separation, Colloids Surfaces A 444 (2014) 283–288.
[252] L. Gao, S. Xiao, W. Gan, X. Zhan, J. Li, Durable superamphiphobic wood surfaces from Cu 2 o film modified with fluorinated alkyl silane, RSC Adv 5 (2015) 98203–98208.
[253] H. Wang, Z. Guo, Design of underwater superoleophobic TiO2 coatings with additional photo-induced self-cleaning properties by one-step route bio-inspired from fish scales, Appl. Phys. Lett. 104 (2014) 183703.
[254] I. Palamà, S. D'Amone, M. Biasiucci, G. Gigli, B. Cortese, Bioinspired design of a photoresponsive superhydrophobic/oleophilic surface with underwater

superoleophobic efficacy, J. Mater. Chem. A 2 (2014) 17666–17675.
[255] G. Wood, J. O'sullivan, The anodizing of aluminium in sulphate solutions, Electrochim. Acta 15 (1970) 1865–1876.
[256] Y. Mizutani, S. Kim, R. Ichino, M. Okido, Anodizing of mg alloys in alkaline solutions, Surface Coatings Technol. 169 (2003) 143–146.
[257] S. Barthwal, Y.S. Kim, S.-H. Lim, Fabrication of amphiphobic surface by using titanium anodization for large-area three-dimensional substrates, J. Colloid Interface Sci. 400 (2013) 123–129.
[258] S. Nishimoto, Y. Sawai, Y. Kameshima, M. Miyake, Underwater superoleophobicity of TiO 2 nanotube arrays, Chem. Lett. 43 (2014) 518–520.
[259] R. Weng, H. Zhang, X. Liu, The nanostructured super-oleophobic liquid-floated rotor gyroscope, Microelectron Eng. 119 (2014) 183–187.
[260] X. Liu, X. Wang, Y. Liang, S.E. Bell, W. Liu, F. Zhou, Superoleophobicity under vacuum, Appl. Phys. Lett. 98 (2011) 194102.
[261] W. Wu, X. W, D. Wang, et al., Alumina nanowire forests via unconventional anodization and super-repellency plus low adhesion to diverse liquids, Chem. Commun. (2009) 1043–1045.
[262] J. Zhao, X. Wang, R. Chen, L. Li, Fabrication of titanium oxide nanotube arrays by anodic oxidation, Solid State Commun. 134 (2005) 705–710.
[263] S. Kaneco, Y. Chen, P. Westerhoff, J.C. Crittenden, Fabrication of uniform size titanium oxide nanotubes: impact of current density and solution conditions, Scr. Mater. 56 (2007) 373–376.
[264] F. Li, X. Li, Photocatalytic properties of gold/gold ion-modified titanium dioxide for wastewater treatment, Appl. Catalysis A. 228 (2002) 15–27.
[265] L. Sirghi, M. Nakamura, Y. Hatanaka, O. Takai, Atomic force microscopy study of the hydrophilicity of TiO2 thin films obtained by radio frequency magnetron sputtering and plasma enhanced chemical vapor depositions, Langmuir 17 (2001) 8199–8203.
[266] M. Liu, S. Wang, Z. Wei, Y. Song, L. Jiang, Bioinspired design of a superoleophobic and low adhesive water/solid interface, Adv. Mater. 21 (2009) 665–669.
[267] A. Kar, Y.R. Smith, V. Subramanian, Improved photocatalytic degradation of textile dye using titanium dioxide nanotubes formed over titanium wires, Environ. Sci. Technol. 43 (2009) 3260–3265.
[268] L. Li, Z. Liu, Q. Zhang, C. Meng, T. Zhang, J. Zhai, Underwater superoleophobic porous membrane based on hierarchical TiO 2 nanotubes: multifunctional integration of oil–water separation, flow-through photocatalysis and self-cleaning, J. Mater. Chem. A 3 (2015) 1279–1286.
[269] K. Nakayama, E. Tsuji, Y. Aoki, H. Habazaki, Fabrication of superoleophobic hierarchical surfaces for low-surface-tension liquids, RSC Adv. 4 (2014) 30927–30933.
[270] B. Li, J. Zhang, Z. Gao, Q. Wei, Semitransparent superoleophobic coatings with low sliding angles for hot liquids based on silica nanotubes, J. Mater. Chem. A 4 (2016) 953–960.
[271] L. Xiong, L.L. Kendrick, H. Heusser, J.C. Webb, B.J. Sparks, J.T. Goetz, W. Guo, C.M. Stafford, M.D. Blanton, S. Nazarenko, Spray-deposition and photopolymerization of organic–inorganic thiol–ene resins for fabrication of superamphiphobic surfaces, ACS Appl. Mater. Interfaces 6 (2014) 10763–10774.
[272] L. Lin, M. Liu, L. Chen, P. Chen, J. Ma, D. Han, L. Jiang, Bio-inspired hierarchical macromolecule–nanoclay hydrogels for robust underwater superoleophobicity, Adv. Mater. 22 (2010) 4826–4830.
[273] S.F. Toosi, S. Moradi, M. Ebrahimi, S.G. Hatzikiriakos, Microfabrication of polymeric surfaces with extreme wettability using hot embossing, Appl. Surf. Sci. 378 (2016) 426–434.
[274] J.S. Arora, J.C. Cremaldi, M.K. Holleran, T. Ponnusamy, J. He, N.S. Pesika, V.T. John, Hydrogel inverse replicas of breath figures exhibit superoleophobicity due to patterned surface roughness, Langmuir (2016).
[275] Y. Li, X. Zhu, B. Ge, X. Men, P. Li, Z. Zhang, Versatile fabrication of magnetic carbon fiber aerogel applied for bidirectional oil-water separation, Appl. Phys. A 120 (2015).
[276] H. Li, X. Wang, Y. Song, Y. Liu, Q. Li, L. Jiang, D. Zhu, Super-"amphiphobic" aligned carbon nanotube films, Angewandte Chemie Int. Edn. 40 (2001) 1743–1746.
[277] S. Coulson, I. Woodward, J. Badyal, S. Brewer, C. Willis, Super-repellent composite fluoropolymer surfaces, J. Phys. Chem. B 104 (2000) 8836–8840.
[278] J. Yong, F. Chen, Q. Yang, D. Zhang, U. Farooq, G. Du, X. Hou, Bioinspired underwater superoleophobic surface with ultralow oil-adhesion achieved by femtosecond laser microfabrication, J. Mater. Chem. A 2 (2014) 8790–8795.
[279] J. Yong, F. Chen, Q. Yang, G. Du, C. Shan, H. Bian, U. Farooq, X. Hou, Bioinspired transparent underwater superoleophobic and anti-oil surfaces, J. Mater. Chem. A 3 (2015) 9379–9384.
[280] J. Yong, F. Chen, Q. Yang, U. Farooq, H. Bian, G. Du, X. Hou, Femtosecond laser controlling underwater oil-adhesion of glass surface, Appl. Phys. A 119 (2015) 837–844.
[281] Q. Xie, J. Xu, L. Feng, L. Jiang, W. Tang, X. Luo, C.C. Han, Facile creation of a super-amphiphobic coating surface with bionic microstructure, Adv. Mater. 16 (2004) 302–305.
[282] Z. Chen, C. Zhou, J. Lin, Z. Zhu, J. Feng, L. Fang, J. Cheng, ZrO2-coated stainless steel mesh with underwater superoleophobicity by electrophoretic deposition for durable oil/water separation, J. Solgel. Sci. Technol. 85 (2017) 22–30.
[283] C. Zhou, J. Cheng, K. Hou, Z. Zhu, Yanfen Zheng, Preparation of CuWO4@Cu2O film on copper mesh by anodization for oil/water separation and aqueous pollutant degradation, Chemical Engineering Journal 307 (2017) 803–811.
[284] D. Chu, K. Yin, X. Dong, Z. Luo, J.-A. Duan, Femtosecond laser fabrication of robust underwater superoleophobic and anti-oil surface on sapphire, API Advences 7 (2017), https://doi.org/10.1063/1.5009609.
[285] X. Zhao, Z. Cheng, G. Luan, R. Li, Y. Zhang, S. Zhao, J. Cao, A zinc oxide nanorods coated brass wire mesh with superhydrophilicity and underwater superoleophobicity prepared by electrochemical deposition combined with hydrothermal reaction, Mater. Lett. 207 (2017) 72–75.
[286] M.A. Gondal, M.S. Sadullah, T.F. Qahtan, M.A. Dastageer, U. Baig, G.H. McKinley, Fabrication and wettability study of WO3 coated photocatalytic membrane for oil-water Separation: a comparative study with ZnO coated membrane, Nature 7 (2017), https://doi.org/10.1038/s41598-017-01959-y.
[287] Y. Chen, N. Wang, F. Guo, L. Hou, Jingchong Liu, J. Liu, Y. Xu, Y. Zhaoa, L. Jianga, A Co3O4 nano-needle mesh for highly efficient, high-flux emulsion separation, J. Mater. Chem. A 4 (2016) 12014–12019.
[288] U.B. Gunatilake, J. Bandara, Efficient removal of oil from oil contaminated water by superhydrophilic and underwater superoleophobic nano/micro structured TiO2 nanofibers coated mesh, Chemosphere 171 (2017) 134–141.
[289] S. Yuan, C. Chen, A. Raza, Ruixue Song, Tie-Jun Zhang, S.O. Pehkonen, and Bin Liang, Nanostructured TiO2/CuO dual-coated copper meshes with superhydrophilic, underwater superoleophobic and self-cleaning properties for highly efficient oil/water separation. *Chem. Eng. J.*. 328, 497–510.
[290] D. Aslanidou, L. Karapanagiotis, C. Panayiotou, Superhydrophobic, superoleophobic coatings for the protection of silk textiles, Progress Organic Coatings 97 (2016) 44–52.
[291] J. Zhang, F. Chen, Q. Yang, J. Yong, J. Huo, Y.F. Hou, A widely applicable method to fabricate underwater superoleophobic surfaces with low oil-adhesion on different metals by a femtosecond laser, Appl. Phys. A 123 (2017) 594.
[292] J.W. Lee, W.b. Hwang, Simple fabrication of superoleophobic titanium surfaces via hierarchical microhorn/nanoporous structure growth by chemical acid etching and anodization, J. Alloys Compd. 728 (2017) 966–970.
[293] G.B. Darband, M. Aliofkhazraei, S. Khorsand, S. Sokhanvar, A. Kabolia, Science and engineering of superhydrophobic surfaces: review of corrosion resistance, chemical and mechanical stability, Arabian J. Chem. (2018), https://doi.org/10.1016/j.arabjc.2018.01.013.
[294] H.-.B. Jo, J. Choi, K.-.J. Byeon, H.-.J. Choi, and HeonLeea, superhydrophobic and superoleophobic surfaces using ZnO nano-in-micro hierarchical structures, Microelectron. Eng. 116 (2014) 51–57.
[295] F. Zhang, W.B. Zhang, Z. Shi, D. Wang, J. Jin, L. Jiang, Nanowire-haired inorganic membranes with superhydrophilicity and underwater ultralow adhesive superoleophobicity for high-efficiency oil/water separation, Adv. Mater. 25 (2013) 4192–4198.
[296] L. Yin, H. Zhang, R. Weng, Z. Wu, X. Liu, Fabrication and drag reduction of the superoleophobic surface on a rotational gyroscope, Surface Eng. 34 (2018) 165–171.
[297] J. Ge, J. Zhang, Fei Wang, Z. Li, J. Yub, B. Ding, Superhydrophilic and underwater superoleophobic nanofibrous membrane with hierarchical structured skin for effective oil-in-water emulsion separation, J. Mater. Chem. A 5 (2017) 497–502.
[298] J. Yong, F. Chen, Q. Yang, J. Huo, X. Hou, Superoleophobic surfaces, Chem. Soc. Rev. 46 (2017) 4168–4217.
[299] D.-.K. Lee, E.-.H. Lee, Y.H. Cho, A superoleophobic surface with anisotropic flow of hexadecane droplets, Microsyst. Technol. 23 (2017) 421–427.
[300] Y.C. S., Y.C. H., C.S. L., H.Y. C., F.C. Chang, New approach to fabricate an extremely super-amphiphobic surface based on fluorinated silica nanoparticles, Polymer Sci. B (2008) 1984–1990.
[301] D.K. Youngsam Yoon, Jeong-Bong Lee, Hierarchical micro/nano structures for super-hydrophobic surfaces and super-lyophobic surface against liquid metal, Micro Nano Syst. Lett. (2014), https://doi.org/10.1186/s40486-014-0003-x.
[302] A. Fernández Estévez, Functional surfaces by means of nanoimprint lithography techniques, Universitat Autònoma de Barcelona. Departament de Física, 2016.
[303] Y. Guo, D. Tang, E. Zhao, Zaiqian Yu, H. Lv, X. Lia, Controlled synthesis of amphiphilic graft copolymer for superhydrophobic electrospun fibres with effective surface fluorine enrichment: the role of electric field and solvent, RSC Adv. 5 (2015) 82789–82799.
[304] Z. Geng, J. He, An effective method to significantly enhance the robustness and adhesion-to-substrate of high transmittance superamphiphobic silica thin films, J. Mater. Chem. A 2 (2014) 16601–16607.
[305] P. Mazumder, Y. Jiang, D. Baker, A. Carrilero, D. Tulli, D. Infante, A.T. Hunt, V. Pruneri, Superomniphobic, transparent, and antireflection surfaces based on hierarchical nanostructures, Nano Lett. 14 (2014) 4677–4681.
[306] K. Chen, J. Jia, Y. Zhao, K. Lv, C. Wanga, Transparent smart surface with pH-induced wettability transition between superhydrophobicity and underwater superoleophobicity, Mater. Des. 135 (2017) 69–76.
[307] J. Li, L. Yan, Q. Ouyang, F. Zha, Z. Jing, X. Li, Z. Lei, Facile fabrication of translucent superamphiphobic coating on paper to prevent liquid pollution, Chem. Eng. J. 246 (2014) 238–243.
[308] D.H.L.K. Golovin, J.M. Mabry, A. Tuteja, Transparent, flexible, superomniphobic surfaces with ultra-low contact angle hysteresis, Angew. Chem. 52 (2013) 13245–13249.
[309] S.G. Lee, D.S. Ham, D.Y. Lee, H. Bong, K. Cho, Transparent superhydrophobic/translucent superamphiphobic coatings based on silica-fluoropolymer hybrid nanoparticles, Langmuir 29 (2013) 15051–15057.
[310] Z. Geng, J. He, L. Xu, L. Yao, Rational design and elaborate construction of surface nano-structures toward highly antireflective superamphiphobic coatings, J. Mater. Chem. A 1 (2013) 8721–8724.
[311] X. Zhu, Z. Zhang, G. Ren, X. Men, B. Ge, X. Zhou, Designing transparent superamphiphobic coatings directed by carbon nanotubes, J. Colloid Interface Sci. 421 (2014) 141–145.
[312] Z. Yuan, J. Xiao, C. Wang, J. Zeng, S. Xing, J. Liu, Preparation of a superamphiphobic surface on a common cast iron substrate, J. Coatings Technol. Res. 8 (2011) 773–777.

[313] T.C. Rangel, A.F. Michels, F. Horowitz, D.E. Weibel, Superomniphobic and easily repairable coatings on copper substrates based on simple immersion or spray processes, Langmuir 31 (2015) 3465–3472.
[314] B. Ge, Z. Zhang, X. Men, X. Zhu, X. Zhou, Sprayed superamphiphobic coatings on copper substrate with enhanced corrosive resistance, Appl. Surf. Sci. 293 (2014) 271–274.
[315] X. Xu, Z. Zhang, F. Guo, J. Yang, X. Zhu, X. Zhou, Q. Xue, Superamphiphobic self-assembled monolayer of thiol on the structured Zn surface, Colloids Surfaces A 396 (2012) 90–95.
[316] S. Peng, X. Yang, D. Tian, W. Deng, Chemically stable and mechanically durable superamphiphobic aluminum surface with a micro/nanoscale binary structure, ACS Appl. Mater. Interfaces 6 (2014) 15188–15197.
[317] A. Starostin, V. Valtsifer, V. Strelnikov, E. Bormashenko, R. Grynyov, Y. Bormashenko, A. Gladkikh, Robust technique allowing the manufacture of superoleophobic (omniphobic) metallic surfaces, Adv. Eng. Mater. 16 (2014) 1127–1132.
[318] X. Jin, X. Zhang, Y. Peng, M. Cao, H. Liu, X. Pei, K. Liu, L. Jiang, Multifunctional engineering aluminum surfaces for self-propelled anti-condensation, Adv. Eng. Mater. 17 (2015) 961–968.
[319] S. Barthwal, Y.S. Kim, S.H. Lim, Mechanically robust superamphiphobic aluminum surface with nanopore-embedded microtexture, Langmuir 29 (2013) 11966–11974.
[320] S. Barthwal, Y.S. Kim, S.H. Lim, Fabrication of amphiphobic surface by using titanium anodization for large-area three-dimensional substrates, J. Colloid Interface Sci. 400 (2013) 123–129.
[321] Y. Sun, L. Wang, Y. Gao, D. Guo, Preparation of stable superamphiphobic surfaces on Ti-6Al-4V substrates by one-step anodization, Appl. Surf. Sci. 324 (2015) 825–830.
[322] H. Li, S. Yu, E. Liu, Y. Zhao, Fabrication and characterization of bionic amphiphobic functional surface on X70 pipeline steel, Microsyst. Technol. 21 (2014) 2003–2010.
[323] H. Yu, X. Tian, H. Luo, X. Ma, Hierarchically textured surfaces of versatile alloys for superamphiphobicity, Mater. Lett. 138 (2015) 184–187.
[324] X. Wang, X. Liu, F. Zhou, W. Liu, Self-healing superamphiphobicity, Chem. Commun. 47 (2011) 2324–2326.
[325] L. Hao, Y. Sirong, Han Xiangxiang, Fabrication of CuO hierarchical flower-like structures with biomimetic superamphiphobic, self-cleaning and corrosion resistance properties, Chem. Eng. J. 283 (2016) 1443–1454.
[326] M. Su, Y. Liu, Y. Zhang, Z. Wang, Y. Li, P. He, Robust and underwater superoleophobic coating with excellent corrosion and biofouling resistance in harsh environments, Appl. Surf. Sci. 436 (2017) 152–161.
[327] L. Hao, S. Yu, X. Han, S. Zhang, Design of submicron structures with superhydrophobic and oleophobic properties on zinc substrate, Mater. Des. 85 (2015) 653–660.
[328] Z. Zhang, X. Zhu, J. Yang, X. Xu, X. Men, X. Zhou, Facile fabrication of superoleophobic surfaces with enhanced corrosion resistance and easy repairability, Appl. Phys. A 108 (2012) 601–606.
[329] K. Liu, M. Cao, A. Fujishima, L. Jiang, Bio-inspired titanium dioxide materials with special wettability and their applications, Chem. Rev. 114 (2014) 10044–10094.
[330] H. Wang, D. Gao, Y. Meng, H. Wang, E. Wang, Y. Zhu, Corrosion-resistance, robust and wear-durable highly amphiphobic polymer based composite coating via a simple spraying approach, ProgressOrgan. Coatings 82 (2015) 74–80.
[331] Z. Du, P. Ding, X. Tai, H. Yang, The facile preparation of ag coated superhydrophobic/superoleophilic mesh for efficient oil/water separation with excellent corrosion resistance, Langmuir 34 (2018) 6922–6929.
[332] G.J.L.D. Xiong, L.Z. Hong, E.J.S. Duncan, Superamphiphobic diblock copolymer coatings, Chem. Mater. 23 (2011) 4357–4366.
[333] G.J.L.D. Xiong, E.J.S. Duncan, Diblock-copolymer-coated water- and oilrepellent cotton fabrics, Langmuir 28 (2012) 6911–6918.
[334] H. Wang, H. Zhou, A. Gestos, Robust superamphiphobic coatings based on silica particles bearing bifunctional random copolymers, ACS Appl. Mater Interfaces. 5 (2013) 10221–10226.
[335] US Environmental Protection Agency, Long-Chain Perfluorinated Chemicals (PFCs) Action Plan, https://www.epa.gov/assessing-and-managing-chemicals-under-tsca/long-chain-perfluorinated-chemicals-pfcs-action-plan, 2009 (accessed 25 July 2019).
[336] W. Jiang, C.M. Grozea, Z. Shi, G. Liu, Fluorinated raspberry-like polymer particles for superamphiphobic coatings, ACS Appl. Mater. Interfaces 6 (2014) 2629–2638.
[337] L. Xiong, L.L. Kendrick, H. Heusser, J.C. Webb, B.J. Sparks, J.T. Goetz, W. Guo, C.M. Stafford, M.D. Blanton, S. Nazarenko, D.L. Patton, Spray-deposition and photopolymerization of organic-inorganic thiol-ene resins for fabrication of superamphiphobic surfaces, ACS Appl. Mater. Interfaces 6 (2014) 10763–10774.
[338] P. Muthiah, B. Bhushan, K. Yun, H. Kondo, Dual-layered-coated mechanically-durable superomniphobic surfaces with anti-smudge properties, J. Colloid Interface Sci. 409 (2013) 227–236.
[339] Q. Wang, Y. Fu, X. Yan, Y. Chang, L. Ren, J. Zhou, Preparation and characterization of underwater superoleophobic chitosan/poly(vinyl alcohol) coatings for self-cleaning and oil/water separation, Appl. Surf. Sci. 412 (2017) 10–18.
[340] X. Wei, F. Chen, H. Wang, H. Zhou, Z. Ji, T. Lin, Efficient removal of aerosol oil-mists using superoleophobic filters, J. Mater. Chem. A 6 (2018) 871–877.
[341] N. Wang, Z. Zhu, J. Sheng, S.S. Al-Deyab, J. Yu, B. Ding, Superamphiphobic nanofibrous membranes for effective filtration of fine particles, J. Colloid Interface Sci. 428 (2014) 41–48.
[342] C.L. Xu, Y.Z. Wang, Novel dual superlyophobic materials in water–oil systems: under oil magneto-fluid transportation and oil–water separation, J. Mater. Chem. A 6 (2018) 2935–2941.
[343] J. Bong, T. Lim, K. Seo, C.A. Kwon, J.H. Park, S.K. Kwak, S. Ju, Dynamic graphene filters for selective gas-water-oil separation, Nature 5 (2015) 14321.
[344] J.Y. Huang, Y.K. Lai, F. Pan, L. Yang, H. Wang, K.Q. Zhang, H. Fuchs, L.F. Chi, Multifunctional superamphiphobic TiO2 nanostructure surfaces with facile wettability and adhesion engineering, Small 10 (2014) 4865–4873.
[345] S.M. Kang, C. Lee, H.N. Kim, B.J. Lee, J.E. Lee, M.K. Kwak, K.Y. Suh, Directional oil sliding surfaces with hierarchical anisotropic groove microstructures, Adv. Mater. 25 (2013) 5756–5761.
[346] T.S. Wong, S.H. Kang, S.K.Y. Tang, E.J. Smythe, B.D. Hatton, A. Grinthal, J. Aizenberg, Bioinspired self-repairing slippery surfaces with pressure-stable omniphobicity, Nature 477 (2011) 443–447.
[347] H.F. Bohn, W. Federle, Insect aquaplaning: nepenthes pitcher plants capture prey with the peristome, a fully wettable water-lubricated anisotropic surface, Proceedings of the National Academy of Sciences of the United States of America, 101 2004, pp. 14138–14143.
[348] P. Kim, M.J. Kreder, J. Alvarenga, J. Aizenberg, Hierarchical or not? Effect of the length scale and hierarchy of the surface roughness on omniphobicity of lubricant-infused substrates, Nano Lett. 13 (2013) 1793–1799.
[349] J. Zhang, L. Wu, B. Li, L. Li, S. Seeger, A. Wang, Evaporation-induced transition from nepenthes pitcher-inspired slippery surfaces to lotus leaf-inspired superoleophobic surfaces, Langmuir 30 (2014) 14292–14299.
[350] D. Daniel, M.N. Mankin, R.A. Belisle, T.S. Wong, J. Aizenberg, Lubricant-infused micro/nano-structured surfaces with tunable dynamic omniphobicity at high temperatures, Appl. Phys. Lett. 102 (2013).
[351] S. Sunny, N. Vogel, C. Howell, T.L. Vu, J. Aizenberg, Lubricant-infused nanoparticulate coatings assembled by layer-by-layer deposition, Adv. Funct. Mater. 12 (2014) 6658–6667.
[352] I. You, T.G. Lee, Y.S. Nam, H. Lee, Fabrication of a micro-omnifluidic device by omniphilic/omniphobic patterning on nanostructured surfaces, ACS Nano 8 (2014) 9016–9024.
[353] S. Yang, R. Qiu, H. Song, P. Wang, Z. Shi, Y. Wang, Slippery liquid-infused porous surface based on perfluorinated lubricant/iron tetradecanoate: preparation and corrosion protection application, Appl. Surf. Sci. 328 (2015) 491–500.
[354] J. Zhang, C. Gu, Jiangping, Robust slippery coating with superior corrosion resistance and anti-icing performance for AZ31B mg alloy protection, Appl. Mater. Interfaces 9 (2017) 11247–11257.
[355] K.-.K. Tseng, W.-.H. Lu, C.-.W. Han, Y.-.M. Yang, Highly-transparent slippery liquid-infused porous surfaces made with silica nanoparticulate thin films, Thin Solid Films 653 (2018) 67–72.
[356] N.R.G. Jim, (Jingting) Luo, Slippery liquid-infused porous surfaces and droplet transportation by surface acoustic waves, Phys. Rev. Appl. 7 (2017) 14–17.
[357] J.B.C. Jackson, J.D. Cubit, B.D. Keller, V. Batista, K. Burns, H.M. Caffey, R.L. Caldwell, S.D. Garrity, C.D. Getter, C. Gonzalez, H.M. Guzman, K.W. Kaufmann, A.H. Knap, S.C. Levings, M.J. Marshall, R. Steger, R.C. Thompson, E. Weil, Ecological effects of a major oil spill on panamanian coastal marine communities, Science 243 (1989) 37–44.
[358] S. Biswas, S.K. Chaudhari, S. Mukherji, Microbial uptake of diesel oil sorbed on soil and oil spill clean-up sorbents, J. Chem. Technol. Biotechnol. 80 (2005) 587–593.
[359] S. Nagappan, J.J. Park, S.S. Park, W.K. Lee, C.S. Ha, Bio-inspired, multi-purpose and instant superhydrophobic-superoleophilic lotus leaf powder hybrid micro-nanocomposites for selective oil spill capture, J. Mater. Chem. A 1 (2013) 6761–6769.
[360] X. Zhu, Z. Zhang, G. Ren, J. Yang, K. Wang, X. Xu, X. Men, X. Zhou, A novel superhydrophobic bulk material, J. Mater. Chem. 22 (2012) 20146–20148.
[361] Z. Niu, J. Chen, H.H. Hng, J. Ma, X. Chen, A leavening strategy to prepare reduced graphene oxide foams, Adv. Mater. 24 (2012) 4144–4150.
[362] Y. Zhao, C. Hu, Y. Hu, H. Cheng, G. Shi, L. Qu, A versatile, ultralight, nitrogen-doped graphene framework, Angewandte Chemie - Int. Edn. 51 (2012) 11371–11375.
[363] X. Gui, J. Wei, K. Wang, A. Cao, H. Zhu, Y. Jia, Q. Shu, D. Wu, Carbon nanotube sponges, Adva. Mater. 22 (2010) 617–621.
[364] M. Cheng, Y. Gao, X. Guo, Z. Shi, J.F. Chen, F. Shi, A functionally integrated device for effective and facile oil spill cleanup, Langmuir 27 (2011) 7371–7375.
[365] Y. Huang, M. Liu, J. Wang, J. Zhou, L. Wang, Y. Song, L. Jiang, Controllable underwater oil-adhesion-interface films assembled from nonspherical particles, Adv. Funct. Mater. 21 (2011) 4436–4441.
[366] D.D. Nguyen, N.H. Tai, S.B. Lee, W.S. Kuo, Superhydrophobic and superoleophilic properties of graphene-based sponges fabricated using a facile dip coating method, Energy Environ. Sci. 5 (2012) 7908–7912.
[367] J. Zhao, W. Ren, H.M. Cheng, Graphene sponge for efficient and repeatable adsorption and desorption of water contaminations, J. Mater. Chem. 22 (2012) 20197–20202.
[368] A.K. Kota, G. Kwon, A. Tuteja, The design and applications of superomniphobic surfaces, NPG Asia Mater. 6 (2014).
[369] A.K. Kota, G. Kwon, W. Choi, J.M. Mabry, A. Tuteja, Hygro-responsive membranes for effective oilwater separation, Nat. Commun. 3 (2012) 102.
[370] C.R. Crick, J.A. Gibbins, I.P. Parkin, Superhydrophobic polymer-coated copper-mesh; membranes for highly efficient oil-water separation, J. Mater. Chem. A 1 (2013) 5943–5948.
[371] X. Zhang, Z. Li, K. Liu, L. Jiang, Bioinspired multifunctional foam with self-cleaning and oil/water separation, Adv. Funct. Mater. 23 (2013) 2881–2886.
[372] Y. Zhu, F. Zhang, D. Wang, X.F. Pei, W. Zhang, J. Jin, A novel zwitterionic polyelectrolyte grafted PVDF membrane for thoroughly separating oil from water with ultrahigh efficiency, J. Mater. Chem. A 1 (2013) 5758–5765.
[373] Y. Chen, J. Meng, Z. Zhu, F. Zhang, L. Wang, Z. Gu, S. Wang, Bio-inspired

underwater super oil-repellent coatings for anti-oil pollution, Langmuir 34 (2018) 6063–6069.
[374] J. Huo, Q. Yang, F. Chen, J. Yong, Y. Fang, J. Zhang, L. Liu, X. Hou, Underwater transparent miniature “Mechanical Hand” based on femtosecond laser-induced controllable oil-adhesive patterned glass for oil droplet manipulation, Langmuir 33 (2017) 3659–3665.
[375] A.D. Anita, Ivanković review of 12 principles of green chemistry in practice, Int. J. Sustain. Green Energy 6 (2017) 39–48.
[376] Li-Ping Xu, D.H. Xiuwen Wu, A green route for substrate-independent oil-repellent coatings, Sci. Rep. 6 (2016) 38016, https://doi.org/10.1038/srep38016.
[377] US food and drug administration, Update on Perfluorinated Grease-proofing Agents. https://www.fda.gov/food/inventory-effective-food-contact-substance-fcs-notifications/update-perfluorinated-grease-proofing-agents, 2019.
[378] C. Lau, J.R. Thibodeaux, R.G. Hanson, M.G. Narotsky, J.M. Rogers, A.B. Lindstrom, M.J. Strynar, Effects of perfluorooctanoic acid exposure during pregnancy in the mouse, Toxicol. Sci. 90 (2006) 510–518.
[379] N. Kudo, Y. Kawashima, Toxicity and toxicokinetics of perfluorooctanoic acid in humans and animals, J. Toxicol. Sci. 28 (2003) 49–57.
[380] Z.S. Saifaldeen, K.R. Khedir, M.F. Cansizoglu, T. Demirkan, T. Karabacak, Superamphiphobic aluminum alloy surfaces with micro and nanoscale hierarchical roughness produced by a simple and environmentally friendly technique, J. Mater. Sci. 49 (2014) 1839–1853.
[381] M. Houde, G. Czub, J.M. Small, S. Backus, X. Wang, M. Alaee, D.C.G. Muir, Fractionation and bioaccumulation of perfluorooctane sulfonate (PFOS) isomers in a lake ontario food web, Environ. Sci. Technol. 42 (2008) 9397–9403.
[382] A. Milionis, R. Ruffilli, I.S. Bayer, Superhydrophobic nanocomposites from biodegradable thermoplastic starch composites (Mater-Bi®), hydrophobic nano-silica and lycopodium spores, RSC Adv. 4 (2014) 34395–34404.
[383] J. Park, C. Urata, B. Masheder, D.F. Cheng, A. Hozumi, Long perfluoroalkyl chains are not required for dynamically oleophobic surfaces, Green Chem. 15 (2013) 100–104.
[384] J. El-Maiss, T. Darmanin, F. Guittard, Branched versus linear perfluorocarbon chains in the formation of superhydrophobic electrodeposited films with low bioaccumulative potential, J. Mater. Sci. 49 (2014) 7760–7769.
[385] T. Saito, Y. Tsushima, H. Sawada, Facile creation of superoleophobic and superhydrophilic surface by using fluoroalkyl end-capped vinyltrimethoxysilane oligomer/calcium silicide nanocomposites—development of these nanocomposites to environmental cyclical type-fluorine recycle through formation of calcium fluoride, Colloid Polym. Sci. 293 (2014) 65–73.
[386] C. Urata, D.F. Cheng, M. Yagihashi, A. Hozumi, A statically oleophilic but dynamically oleophobic smooth nonperflouorinated surface, Angew. Chem. (2012) 3010–3013.
[387] K. Rohrbach, Y. Li, H. Zhu, Z. Liu, J. Dai, J. Andreasen, L. Hu, A cellulose based hydrophilic, oleophobic hydrated filter for water/oil separation, Chem. Commun. 50 (2014) 13296–13299.
[388] L.Z. Jinmei Du, Jing Dong, Ying Li, Changhai Xu, Weidong Gao, Preparation of hydrophobic nylon fabric, J. Eng. Fiber Fabr 11 (2016) 31–37.
[389] J.W. Schultze, M. Lohrengel, Stability, reactivity and breakdown of passive films. Problems of recent and future research, Electrochim. Acta 45 (2000) 2499–2513.
[390] J. Wang, H. Wang, Easily enlarged and coating-free underwater superoleophobic fabric for oil/water and emulsion separation via a facile NaClO2 treatment, Sep. Purif. Technol. 195 (2018) 358–366.
[391] K. Hou, Y. Zeng, C. Zhou, J. Chen, X. Wen, S. Xu, J. ng, Y. Lin, P. Pi, Durable underwater superoleophobic PDDA/halloysite nanotubes decorated stainless steel mesh for efficient oil–water separation, Appl. Surf. Sci. 416 (2017) 344–352.